GAS LASER DISCHARGE NOISE

AND ITS EFFECT ON THE LASER OUTPUT

Thesis by

James Yoh

In Partial Fulfillment of the Requirements

For the Degree of

Doctor of Philosophy

California Institute of Technology

Pasadena, California

1969

(Submitted April 28, 1969)

ACKNOWLEDGEMENTS

ABSTRACT

A large portion of the noise in the light output of a laser oscillator is associated with the noise in the laser discharge. The effect of the discharge noise on the laser output has been studied. The discharge noise has been explained through an ac equivalent circuit of the laser discharge tube.

The discharge noise corresponds to time-varying spatial fluctuations in the electron density, the inverted population density and the dielectric permittivity of the laser medium from their equilibrium values. These fluctuations cause a shift in the resonant frequencies of the laser cavity. When the fluctuation in the dielectric permittivity of the laser medium is a longitudinally traveling wave (corresponding to the case in which moving striations exist in the positive column of the laser discharge), the laser output is frequency modulated.

The discharge noise has been analyzed by representing the laser discharge by an equivalent circuit. An appropriate ac equivalent circuit of a laser discharge tube has been obtained by considering the frequency spectrum of the current response of the discharge tube to an ac voltage modulation. It consist of a series ρLC circuit, which represents the discharge region, in parallel with a capacitance C', which comes mainly from the stray wiring. The equivalent inductance and capacitance of the discharge region have been calculated from the values of the resonant frequencies measured on discharge currents, gas pressures and lengths of the positive column. The experimental data provide for a

set of typical values and dependencies on the discharge parameters for the equivalent inductance and capacitance of a discharge under laser operating conditions. It has been concluded from the experimental data that the equivalent inductance originates mainly from the positive column while the equivalent capacitance is due to the discharge region other than the positive column.

The ac equivalent circuit of the laser discharge has been shown analytically and experimentally to be applicable to analyzing the internal discharge noise. Experimental measurements have been made on the frequency of moving striations in a laser discharge. Its experimental dependence on the discharge current agrees very well with the expected dependence obtained from an analysis of the circuit and the experimental data on the equivalent circuit elements. The agreement confirms the validity of representing a laser discharge tube by its ac equivalent circuit in analyzing the striation phenomenon and other low frequency noises. Data have also been obtained for the variation of the striation frequency with an externally-applied longitudinal magnetic field and the increase in frequency has been attributed to a decrease in the equivalent inductance of the laser discharge.

TABLE OF CONTENTS

CHAPTER ONE

INTRODUCTION

A laser is a low noise oscillator whose output is character-
ized by an extremely monochromatic radiation around the optical region
of the frequency spectrum. The outputs from gas lasers have especially
narrow spectral widths which are of the order of megahertz. Gas lasers
have a definite advantage over other lasers in areas where spectral
purity is desired. However, their performance is worsened when noises
are present. Therefore it is important to study the noises in a laser,
and to understand their causes and their effects on the laser output.
The excess photon noise, the noise in the laser output which is over
and above the shot noise, has been measured and calculated by many
authors (1-3).

A good portion of laser noises comes from the laser dis-
charge. Prescott and Van der Ziel (4) have found a strong correlation
between the laser light noise and the discharge current noise in a
helium-neon laser. Moving striations, which are spatial fluctuations
in the electron density and the metastable atom density traveling along
the positive column of the laser discharge, often exist in a helium-
neon laser discharge. Garscadden, Bletzinger and Friar (5) have obser-
ved that the existence of moving striations in a laser discharge, in
addition to introducing noise to the laser output, also decreases its
light intensity. Moving striations have been a subject of study for

about a hundred years. A historical sketch of the work on the subject
will be given in the introductory section of Chapter 4. From the laser
point of view, the discharge noise influences the laser operation;
it and its effect on the laser output should be studied and understood.

In the present work a theoretical study of the effect of
spatial fluctuations in the electron density, the population inversion
and the dielectric permittivity of the laser medium on the frequency
spectrum of the laser output will be presented. When the spatial fluc-
tuations are periodic and travel along the axis of the laser medium,
they correspond to moving striations in the positive column of the
laser discharge. The theoretical study will show that they influence
the resonance condition of the laser cavity and cause a shift in the
frequency of the laser output.

After having studied the effect of the discharge noise on the
laser output, the attention will be centered on the discharge noise
itself. An equivalent circuit of the laser discharge will be presented
which is a valid representation of the laser discharge in the kilohertz
range of frequency. The equivalent circuit will be discussed and
analyzed, and will be shown to be applicable to analyzing the
response of the laser discharge to an external or internal excitation.
Self-sustained oscillations in the discharge can also be obtained from
a consideration of the circuit. The equivalent circuit approach to a
laser discharge provides for an alternative to the conventional analysis
of a discharge region which involves the solutions to the particle and

energy conservation equations. In addition to having certain advantages over the conventional method (which will be discussed in Section 4.2), this approach may also give some fresh insight to the treatment of the discharge tube. The present work lays the ground work for a thorough understanding of the equivalent circuit and its elements which should give all the important characteristics of the laser discharge from the external point of view.

Experimental data on the equivalent circuit elements under various discharge conditions will be presented. Besides indicating the values of the equivalent circuit elements that are relevant for a laser discharge, the set of data also gives their dependence on various discharge parameters. The dependence should be very useful in understanding and controlling the internal noises of the discharge. A better understanding of the equivalent circuit can also be obtained from the conclusions that can be drawn from the experimental data.

Finally, moving striations in a laser discharge will be studied experimentally. The measured dependence of the striation frequency on the discharge current will be compared to its predicted dependence obtained from an analysis of the equivalent circuit and the set of experimental data on its elements. The result of this comparison gives an experimental indication of the applicability of the equivalent circuit to analyzing the internal disturbances in a laser discharge. From the laser point of view, this last consideration is very important to the usefulness of the equivalent circuit since the internal noise in a laser discharge affects strongly the laser output.

CHAPTER TWO

LASER NOISE FROM THE DISCHARGE

2.1 Introduction

The laser is a low noise oscillator that emits in the optical frequency region. Its usefulness in such areas as communication and holography depends strongly on its noise level. Therefore it is important to study the noises in the laser. There are many sources of laser noise, one of which comes from the laser discharge itself. It corresponds to spatial and temporal fluctuations in the discharge.

This chapter presents a study on the effect of the discharge noise on the laser output. An analysis of the resonance condition and the resonant frequency of a laser cavity in which the dielectric permittivity has a constant value throughout the medium will be presented in Section 2.2. The effect of the stationary and traveling fluctuations in the dielectric permittivity on the resonant frequency will be considered in Section 2.3. Their effect on the intensity of the laser output will be demonstrated by assuming that the laser operates in two longitudinal modes of successive orders, each of which produces a perfectly sinusoidal wave. In order to avoid mathematical complexity, the analysis in this chapter will only treat the one-dimensional cases which illustrate the essential features.

2.2 Resonance Condition of a Laser Cavity

Consider a bounded one-dimensional laser medium. The medium can be described by a complex dielectric permittivity. The imaginary part of the permittivity corresponds to the gain in the medium while its real part gives the resonance condition and the resonant frequency (1), which are of interest in this analysis. To obtain the resonant condition frequency, consider the wave equation

$$\frac{\partial^2 E_t(z,t)}{\partial z^2} - \mu_o \varepsilon \frac{\partial^2 E_t(z,t)}{\partial t^2} = 0 \tag{2-1}$$

and the boundary condition

$$E_t(0,t) = E_t(D,t) = 0, \tag{2-2}$$

where $E_t(z,t)$ is the transverse electric field, μ_o is the constant susceptibility of the medium, z is the longitudinal position and $z=0$ and $z=D$ are the locations of the boundaries (corresponding to the locations of the mirrors in a laser cavity). ε is a real quantity which is independent of position and time.

The solution to equation (2-1) which satisfies the boundary condition in equation (2-2) is given by

$$E_t(z,t) = \int_{p=1}^{\infty} A_p \, \sin\left(\omega_p \sqrt{\mu_o \varepsilon} \, z\right) e^{j\omega_p t} \tag{2-3}$$

with $$\omega_p = \frac{p\pi v}{D} \tag{2-4}$$

where the A_p's are arbitrary complex amplitudes, p is any integer and v is the velocity of light in the medium. The convention of describing an oscillating function by a positive exponential $e^{+j\omega_p t}$ is adopted throughout this thesis. The physical quantities are the real parts of their complex expressions.

Equation (2-4) gives the angular frequencies of the oscillations that can be sustained in the cavity without significant losses. The light output of a laser is a traveling wave consisting of one or more angular frequencies given by equation (2-4) at which the laser has net gains.

Consider a laser operating at two successive longitudinal modes of orders q and (q-1). The transverse electric field of the output of the laser is

$$E_t = e^{j\omega_q t} + e^{j\omega_{q-1} t} \tag{2-5}$$

where t is chosen in such a way that at t=0, E_t has its maximum amplitude. The transverse electric fields of both modes have unit amplitudes. The intensity I of the laser output can be expressed in terms of the electric field as:

$$I = E_t E_t^* = 2 \left(1 + \cos \frac{\pi v t}{D}\right) \tag{2-6}$$

where E_t^* denotes the complex conjugate of E_t.

This analysis gives the resonance condition and the resonant frequency of the laser cavity in which the dielectric permittivity of the medium does not have spatial variations.

2.3 Effect of the Discharge Noise on the Laser Output

The discharge noise is due to some disturbances inside the discharge region of the laser tube. Consider a periodic spatial fluctuation in the electron density along the positive column of the discharge which constitutes the laser medium. The spatial fluctuation in the electron density causes a spatial variation in the population inversion in the medium which, in turn, corresponds to a spatial fluctuation in the dielectric permittivity of the medium (1). Since it is of interest only to obtain the resonant condition and the resonant frequency, the laser medium can be described by a spatially and temporally fluctuating dielectric permittivity of real value[†]

$$\epsilon' = \epsilon + \epsilon_1 \cos\left(\frac{2\pi z}{d} - \phi(t)\right) \tag{2-7}$$

where $\phi(t)$ is in general a time varying phase term and d is a constant length. ϵ is a slowly varying function of time and space. This means that d is much larger than the optical wave length and $\frac{d\phi}{dt}$ is much smaller than the optical angular frequency.

For a constant $\phi(\phi = \phi_0)$, the dielectric permittivity of the medium expressed in equation (2.7) forms a standing pattern. This case will be considered in Section 2.3.1. When the phase $\phi(t)$ is steadily

---

[†]The sinusoidal function of the permittivity is chosen so as not to obscure its effect on the resonant frequency with an excess amount of mathematics. The analysis can be extended to the general case in which ϵ' is represented by a sum of periodic spatial functions that vary slowly with time.

increasing (that is, $\phi(t) = \omega_s t$), the permittivity is a traveling wave in the positive z direction with a phase velocity $(\omega_s d/2\pi)$. This case will be considered in section 2.3.2.

2.3.1 Stationary Fluctuation in Dielectric Permittivity of the Laser Medium

Consider again the one-dimensional laser medium of Section 2.2 with a different dielectric permittivity ε' given by

$$\varepsilon'(z) = \varepsilon + \varepsilon_1 \cos\left(\frac{2\pi z}{d} - \phi_o\right) \tag{2-8}$$

where $\varepsilon \ll \varepsilon$, d is a constant length and ϕ_o is a constant phase. The transverse electric field has to satisfy the wave equation

$$\frac{\partial^2 E_t(z,t)}{\partial z^2} - \mu_o \varepsilon'(z) \frac{\partial^2 E_t(z,t))}{\partial t^2} = 0 \tag{2.9}$$

with the boundary condition

$$E_t(0,t) = E_t(D,t) = 0 \quad . \tag{2-10}$$

Equation (2-9) can be solved by the method of separation of variables. Let

$$E_t(z,t) = f(z)g(t) \quad , \tag{2-11}$$

equation (2-9) becomes

$$\frac{1}{\mu_o \epsilon'(z)} \frac{1}{f(z)} \frac{d^2 f(z)}{dz^2} = \frac{1}{g(t)} \frac{d^2 g(t)}{dt^2} = - \omega^2 \qquad (2-12)$$

where ω is a constant which is independent of both z and t. The value of ω which satisfies equation (2-12) with the expression for ϵ' given by equation (2-8) and the boundary condition given by (2-10) is the quantity of interest in this analysis.

An expression for $g(t)$ can be readily obtained from equation (2-12)

$$g(t) = e^{j\omega t} \qquad (2-13)$$

where a unit amplitude has been assumed for $g(t)$.

The spatial part of equation (2-12) with ϵ' sinusoidal is Mathieu's equation (4):

$$\frac{d^2 f(z)}{dz^2} + \omega^2 \mu_o \epsilon'(z) f(z) = 0 \quad , \qquad (2-14)$$

with the boundary condition

$$f(0) = f(D) = 0 \quad . \qquad (2-15)$$

Since $\epsilon'(z)$ is a slowly varying spatial function as compared to $f(z)$ (that is, d is much larger than the optical wavelength), then an approximate solution to equation (2-14) can be obtained by the WKB method (2),

$$f(z) = \frac{1}{[\varepsilon'(z)]^{1/4}} \left[A\ e^{j\int_0^z \omega\sqrt{\mu_0\varepsilon'(z)}\ dz'} + B\ e^{-j\int_0^z \omega\sqrt{\mu_0\varepsilon'(z')}dz'} \right]$$

(2-16)

where A and B are arbitrary complex constants. The expression in equation (2-16) is a valid solution to equation (2-14) as long as the condition

$$\frac{d}{2\pi}\ \sqrt{\omega^2\mu_0\varepsilon} \gg \frac{|\varepsilon_1|}{2\varepsilon}$$

(2-17)

is satisfied. Equation (2-17) requires that the ratio of d to the optical wavelength be much larger than the quantity $(\varepsilon_1/\varepsilon)$. In practice, this condition is always satisfied.

The boundary condition $f(0) = 0$ requires that $A = -B = C/2j$ such that

$$f(z) = \frac{C \sin\left(\int_0^z \omega\sqrt{\mu_0\varepsilon'(z')}\ dz'\right)}{[\varepsilon'(z)]^{1/4}}\ .$$

(2-18)

The boundary condition $f(D) = 0$ requires that[†]

$$\int_0^D \omega_q'\sqrt{\mu_0\varepsilon'(z')}\ dz' = q\pi$$

(2-19)

[†] Up to this point, there has been no need to specify $\varepsilon'(z)$ except that its spatial fluctuation is very slow compared with that of an optical wave. Therefore equation (2-19) serves as a starting point when a more complicated expression than equation (2-8) is used for $\varepsilon'(z)$.

where q is any integer. ω'_q denotes the resonant angular frequency which satisfies equation (2-19). Since $\varepsilon_1 << \varepsilon$, equation (2-19) becomes

$$q\pi = \frac{\omega'_q}{v} \int_o^D \left[1 + \frac{\varepsilon_1}{2\varepsilon} \cos \left(\frac{2\pi z'}{d} - \phi_o \right) \right] dz'$$

$$= \frac{\omega'_q D}{v} \left[1 + \frac{1}{2\pi} \frac{\varepsilon_1}{\varepsilon} \frac{d}{D} \sin \left(\frac{\pi D}{d} \right) \cos \left(\frac{\pi D}{d} - \phi_o \right) \right] \quad (2-20)$$

where $v = 1/\sqrt{\mu_o \varepsilon}$. Equation (2-20) gives an expression for ω'_q:

$$\omega'_q = \omega_q [1 - \frac{1}{2\pi} \frac{\varepsilon_1}{\varepsilon} \frac{d}{D} \sin \left(\frac{\pi D}{d} \right) \cos \left(\frac{\pi D}{d} - \phi_o \right)] \quad (2-21)$$

where ω_q has been defined in equation (2-4). The resonant angular frequency ω'_q can be greater than, equal to, or less than ω_q, depending on the ratio (D/d) and the value of ϕ_o.

For the laser whose output consists of two successive longitudinal modes, equation (2-6) should be modified to be:

$$I = 2(1 + \cos [\frac{\pi v t}{D} (1 - \frac{1}{2\pi} \frac{\varepsilon_1}{\varepsilon} \frac{d}{D} \sin \left(\frac{\pi D}{d} \right) \cos \left(\frac{\pi D}{d} - \phi_o \right))]). \quad (2-22)$$

Therefore the shift of the frequency of the ac component of the light intensity also depends on the ratio (D/d) and the value of ϕ_o.

For $\phi_o = \pi$, equation (2-22) can also be obtained from the sinusoidal expansion of the Mathieu Function (4)(which is a solution to equation (2-14))of a fractional order that satisfies the boundary conditions.

2.3.2 Traveling Fluctuation in Dielectric Permittivity of the

Laser Medium

It is desirable to extend the above analysis to the case in which $\phi(t)$ is a slowly varying function of time. In this case,

$$\varepsilon' = \varepsilon + \varepsilon_1 \cos \left(\frac{2\pi z}{d} - \phi(t)\right) \tag{2-23}$$

where $\frac{d\phi}{dt} <<< \omega_q \cong \frac{1}{E_t} \frac{\partial E_t}{\partial t}$ and ω_q is an angular frequency in the optical region. The time-dependent term in the wave equation can be written as:

$$\mu_o \frac{\partial^2 \varepsilon' E_t}{\partial t^2} = \mu_o [\varepsilon' \frac{\partial^2 E_t}{\partial t^2} + 2\varepsilon_1 \frac{d\phi}{dt} \frac{\partial E_t}{\partial t} \sin \left(\frac{2\pi z}{d} - \phi(t)\right)$$

$$- \varepsilon_1 \frac{d^2 \phi}{dt^2} E_t \cos \left(\frac{2\pi z}{d} - \phi(t)\right)]$$

$$\cong \mu_o \varepsilon' \frac{\partial^2 E_t}{\partial t^2} . \tag{2-24}$$

Equation (2-24) implies that the optical wave oscillates so rapidly as compared with the variation in $\phi(t)$ that at any instant of time $\phi(t)$ can be assumed to be a constant phase. The wave equation can be solved for one instant at a time. With this in mind, the analysis is similar to that in Section 2.3.1 except that ϕ_o should be replaced by $\phi(t)$ in the result. The resonant angular frequency of the q-th longi-

tudinal mode becomes

$$\omega_q' = \omega_q [1 - \frac{1}{2\pi} \frac{\varepsilon_1}{\varepsilon} \frac{d}{D} \sin (\frac{\pi D}{d}) \cos (\phi(t) - \frac{\pi D}{d})]. \qquad (2-25)$$

For a **laser** medium in which the spatial fluctuation in the dielectric permittivity travels down the medium in the positive z direction, $\phi(t)$ in equation (2-23) should be replaced by $\omega_s t$ where ω_s is a fixed angular frequency which is much smaller than the optical angular frequency[†]. Equation (2-23) becomes

$$\varepsilon' = \varepsilon + \varepsilon_1 \cos (\omega_s t - \frac{2\pi z}{d}). \qquad (2-26)$$

The resonant angular frequency of equation (2-25) becomes

$$\omega_q' = \omega_q [1 - \frac{1}{2\pi} \frac{\varepsilon_1}{\varepsilon} \frac{d}{D} \sin (\frac{\pi D}{d}) \cos (\omega_s t - \frac{\pi D}{d})]$$

$$= \omega_q - q \, \Delta\omega \, \cos (\omega_s t - \frac{\pi D}{d}) \qquad (2-27)$$

where

$$\Delta\omega = \frac{v}{2D} \frac{\varepsilon_1}{\varepsilon} \frac{d}{D} \sin (\frac{\pi D}{d}) \quad . \qquad (2-28)$$

Equations (2-27) and (2-28) show that the laser output is frequency modulated provided that the ratio of D to d is not an exact integer. When a laser is oscillating in a single mode, the traveling wave in the dielectric permittivity causes the laser frequency to be fluctuating in

---

[†] This is the case in which moving striations, which will be described in Chapter 4, are present in the positive column of the laser discharge.

time. This constitutes noise in the laser output.

For the laser whose output consists of two successive long-itudinal modes of unit amplitudes and mode orders q and $(q - 1)$, the above analyzed effect shows up in the intensity of the light output I in the form[†]

$$I = E_t E_t^* = (e^{j\theta_q(t)} + e^{j\theta_{q-1}(t)})(e^{j\theta_q(t)} + e^{-j\theta_{q-1}(t)})$$

$$= 2[1 + \cos(\theta_q(t) - \theta_{q-1}(t))] \tag{2-29}$$

where

$$\theta_q(t) = \int_{-\infty}^{t} \omega_q'(t') \, dt'$$

$$= \omega_q t - \frac{q\Delta\omega}{\omega_s} \sin(\omega_s t - \frac{\pi D}{d}) + \theta_{oq} \tag{2-30}$$

and the constant θ_{oq} is a time-independent constant determined by equation (2-30). It may be taken to be zero by referring to an appropriate phase reference. Then equation (2-29) can be written as

$$I = 2[1 + \cos\frac{\pi v t}{D} - \frac{\Delta\omega}{\omega_s} \sin(\omega_s t - \frac{\pi D}{d})] \tag{2-31}$$

The ac component of the intensity is frequency modulated. Its fre-quency spectrum consists of side bands separated from the center

---

[†]The above treatment is for a passive cavity. An analysis of an active laser cavity involves other factors. The FM effect in I is small since $(\varepsilon_1/\varepsilon)$ is of the order of 10^{-8}.

frequency $(v/2D)$ by $(n\omega_s/2\pi)$ where $n = + 1, + 2, \ldots$ Their
magnitudes are given by $J_{|n|}(\Delta\omega/\omega_s)$ (3).

2.4 Conclusion

The above analyses show the spectra of the transverse electric
field and the intensity of the laser output when the laser medium has
a spatial fluctuation in its dielectric permittivity which may or may
not be changing slowly with time. A simple sinusoidal fluctuation is
assumed, although the analyses may be extended to more complicated
spatial variations in the dielectric permittivity of the medium. The
discharge noise causes the frequency of the laser output to shift from
its value obtained when the laser medium does not have spatial varia-
tions. The effect of the noise on the laser output can be seen through
the expressions for the resonant angular frequencies. Its effect on
the intensity of the laser output is included in the analyses because
it corresponds to the experimental display on the laser noise. Typically
the laser output is measured by a photodetector or a photomultiplier
which is sensitive to the intensity of the light beam. Therefore a
spectral display of the output of the device corresponds to the fre-
quency spectrum of the intensity of the laser output.

The objective of the rest of the thesis is to obtain an under-
standing of the noise which exists in the discharge region and may be
excited externally or internally. Section 2.3.2 shows that the laser
output is greatly affected by the discharge noise. However, the laser
noise can be suppressed or controlled only by understanding and con-

trolling the noise in the laser discharge. Since the noise is inher-

ent in the discharge, it is also manifested in the discharge current,

the discharge voltage and the other discharge parameters. Hence it is

preferable to study the discharge noise from a laser discharge without

the end mirrors so as to differentiate it from other noises (such as

the cavity noise and the noise due to mirror vibrations) which are

present only in a laser oscillator. After showing the importance of

the discharge noise to laser oscillators in this chapter, the next two

chapters will study the noise in laser discharges.

CHAPTER THREE

AC EQUIVALENT CIRCUIT FOR LASER DISCHARGES

3.1 Introduction

A good portion of the laser noise comes from the discharge
tube which forms the active medium in a laser cavity (1). As shown in
Chapter 2, the discharge noise causes fluctuations in the frequency of
the light output of a laser oscillator. Since the noise is inherent in
the discharge tube, it exists even when the laser is operating as an
amplifier (i.e., when the mirrors have been removed from a laser
oscillator). The discharge noise shows up as fluctuations in the
intensity of the side light emission from the discharge, the discharge
current and the discharge voltage.

A typical frequency spectrum of the discharge current noise (2)
shows that the noise intensity decreases as the frequency increases. It
often happens that at a certain frequency the noise spectrum displays
a local maximum (a spike). For helium-neon lasers this frequency varies
from about 20 kilohertz to a few hundred kilohertz from laser to laser.
The qualitative explanation is that the laser discharge is resonant at
that particular frequency. A laser discharge can be represented by an
equivalent circuit which contains source elements. The sources cover
a large frequency range in the kilohertz region and corresponds to the
generating mechanisms for the low frequency noises in the discharge.
At the resonant frequency of the equivalent circuit the noise shows a

local maximum in its intensity. If the equivalent circuit contains a
negative resistor it is possible that the noise at the resonant
frequency would cause oscillations within the discharge.   This self-
oscillation phenomena will be considered in a later chapter. In this
chapter an ac equivalent circuit representing a laser amplifier is
presented. It is valid in the frequency range from a few kilohertz
to a few hundred kilohertz.

3.2 Equivalent Circuit of a Laser Discharge

A laser discharge can be represented by an equivalent circuit
with an equivalent internal noise source. When the discharge tube is
not self-oscillating, an external ac voltage source of a few volts in
the kilocycles frequency range causes disturbance in the discharge
that is many orders of magnitude greater in amplitude than the noise
generated by the discharge itself at that frequency. In this case
the noise source within the discharge can be neglected (it can be
assumed to be short-circuited) and the equivalent circuit can be treated
as a passive circuit. If the external ac voltage source is allowed to
vary in its oscillation frequency while its amplitude is kept constant,
the ac current through the discharge tube is plotted against the oscilla-
tion frequency in Fig. 3-1 (the experimental data points). The experi-
mental setup and the apparatus with which the data points have been
obtained will be described in a later section. It suffices to note
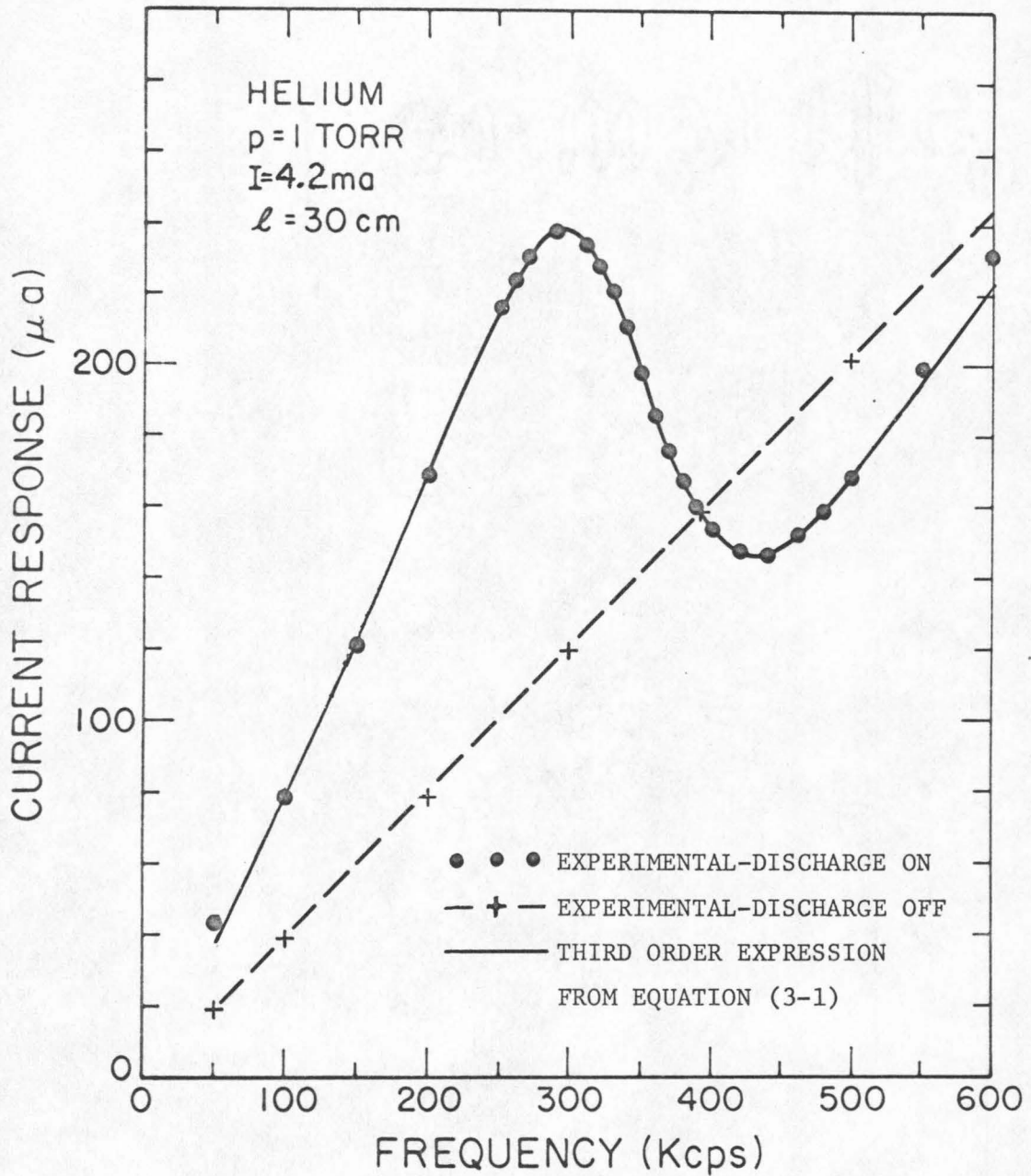
FIGURE 3-1   FREQUENCY SPECTRUM OF THE DISCHARGE
             CURRENT

that the experimental points in Fig. 3-1 show the ac current response
to a constant voltage across a laser discharge. If the values of the
data points are divided by the constant amplitude ac voltage, they
are just the values of the admittance of the laser discharge at differ-
ent frequencies. The experimental points trace out a smooth curve
which has a local maximum and a local minimum. Otherwise, it varies
linearly with frequency. These characteristics suggest that the admit-
tance function has a third order polynomial as its numerator and a second
order polynomial as its denominator. The numerator of the admittance
function goes to zero as the frequency approaches zero while the deno-
minator is a constant at zero frequency.

Fig. 3-2 shows an equivalent circuit whose admittance function
is given by

$$Y(s) = sC' + \frac{s}{L}\frac{1}{s^2 + \frac{\rho}{L}s + \frac{1}{LC}}$$

$$= sC'\left[\frac{s^2 + \frac{\rho}{L}s + \frac{1}{L}\left(\frac{1}{C} + \frac{1}{C'}\right)}{s^2 + \frac{\rho}{L}s + \frac{1}{LC}}\right] \tag{3-1}$$

where $s=j\omega$ and ω is the angular frequency variable.

Equation (3-1) can be fitted to the experimental data points
of Fig. 3-1. The solid curve in the figure shows the best fit between
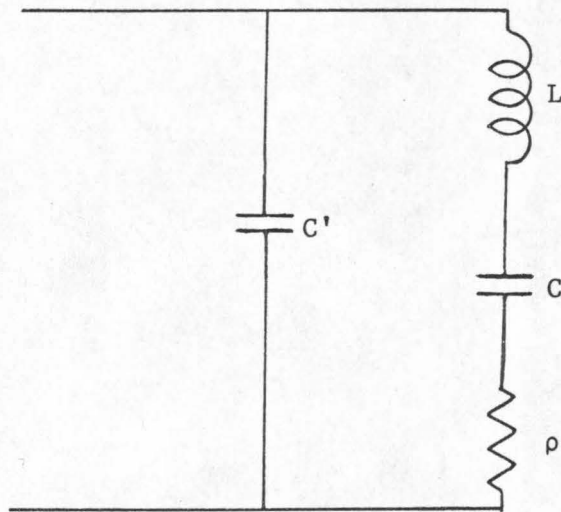
FIG. 3-2 AC EQUIVALENT CIRCUIT FOR A LASER
          AMPLIFIER

the data points and the expression in equation (3-1). It has been

obtained with the following set of values for the equivalent circuit

elements: C' = 17.7 picofarads, L = 22.6 millihenries, C = 10.6 pico-

farads and ρ = 26.7 kilohms. The values agree approximately[†] with

the experimental values to be given in later sections and with the

data of other authors (3,4). The excellent agreement between the

solid curve and the experimental points in Fig. 3-1 shows that the

admittance function of a laser discharge tube can definitely be

described by the expression in equation (3-1) in the frequency range

of the figure.

The curve drawn with the dashed line in Fig. 3-1 describes

the current response to the same external constant voltage after the

discharge has been extinguished. It is a straight line and coincides

asymptotically with the solid curve. The slope of the dashed curve

gives approximately the value of the parallel capacitance C'[††]. This

suggests strongly that the parallel capacitance represents the tube

without the discharge. It corresponds mainly to the capacitance between

the stray wiring. The series ρLC circuit represents the discharge

region. It becomes open circuited when the discharge is extinguished.

[†]The values of L and C do not agree exactly with the values in later
sections because they drift over a long time period during which the
experimental data are obtained.

[††]The slope of the dashed line gives a value of C' that is 17% smaller
than what is mentioned in the previous paragraph which gives the best
fit between the expression of equation (3-1) and the experimental
points of Fig. 3-1.

An analysis of the equivalent circuit is given in Appendix 1.

3.3 Experimental Procedures

It is the intent of the experimental work to show the depend-
ence of the reactive circuit elements on the various discharge para-
meters; in particular, the elements L and C. The parallel capacit-
ance C' exists independently of the discharge regions and will not
be considered.   Appendix 1 shows that the reactive elements determine
the resonant frequency and the self-oscillation frequency when proper
internal source and gain are present. It is of practical importance to
know the dependence so that one can maneuver the discharge parameters
in case the resonant frequency falls in an undersirable range. The set
of data that are presented in this chapter are obtained under conditions
that are exactly or close to laser operating conditions.

The experimental tube (shown in the photograph of Fig. 3-3 and
the sketch of Fig. 3-4) has a nickel disc as its cold cathode and four
kovars as its anodes. The kovers are placed at 15 cm intervals, along
a Pyrex glass tubing of about 67 cm long and 5.5 mm ID with the first
kovar located at 15 cm from the start of the Pyrex tube. Electrical
leads are connected to all the kovars so that any one of them can be
used as the anode of the discharge tube. The nickel disc cathode is
housed in a 3.4 cm ID Pyrex section of about 16 cm long with the sur-
face of the disc located at 3.3 cm from the start of the 5.5 mm ID
Pyrex tubing.

The experimental tube is stationed on a vacuum system and is
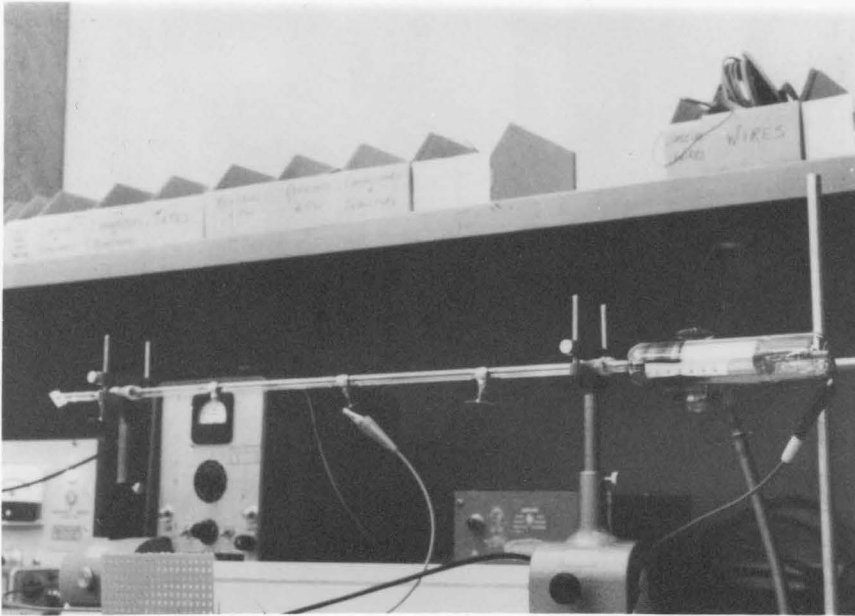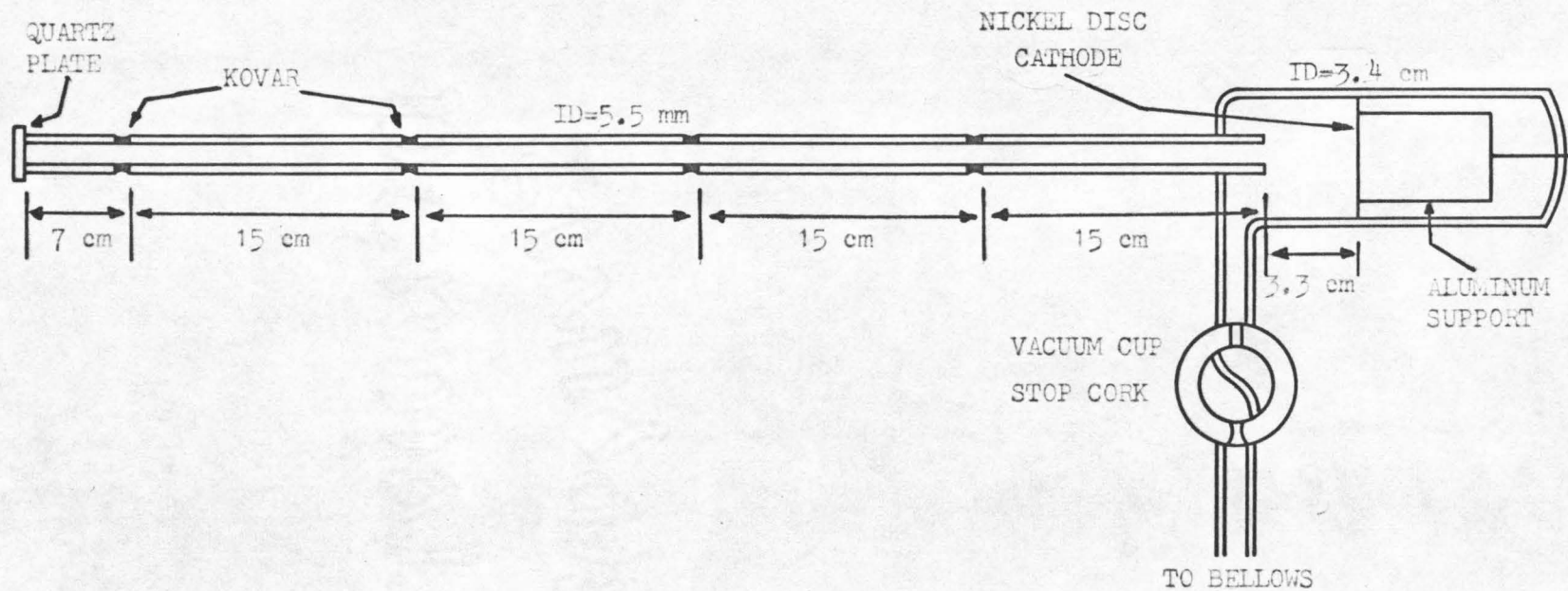
(a)   THE EXPERIMENTAL TUBE

(b)   THE EXPERIMENTAL SETUP

FIGURE 3-3 PHOTOGRAPHIC DISPLAYS OF THE EXPERIMENTAL SYSTEM

QUARTZ PLATE

KOVAR

ID=5.5 mm

NICKEL DISC CATHODE

ID=3.4 cm

7 cm

15 cm

15 cm

15 cm

15 cm

3.3 cm

ALUMINUM SUPPORT

VACUUM CUP STOP CORK

TO BELLOWS

NOT DRAWN TO SCALE

-25-

FIGURE 3-4 EXPERIMENTAL TUBE

connected to it through a steel bellow, as shown in Fig. 3-5. The diffusion pump of the vacuum system is capable of pumping the entire system to below 5×10^{-6} mm of mercury. Bottles of helium, neon and xenon are connected to the system through Granville leak valves so that the discharge tube can be filled to any pressure with any of these gases and their mixtures. The pressure gauge is located in the manifold. Since this is a non-flowing system, however, the pressure in the manifold corresponds exactly to that in the discharge tube provided that enough time is allowed for the gas to reach its equilibrium condition.

The electrical apparatus and their connections are shown in Fig. 3-6. The dc circuit loop consists of the discharge tube connected to a laser power supply through two current-limiting resistors in a series configuration, each of which is a 40 kilohms noninductive resistor with 50 watts rating. The laser power supply is capable of a current of 15 ma at about 3500 volts. An ac disturbance is coupled through a 2000 pf (3750 WVDC rating) capacitor into the dc circuit in between the two resistors. A 2800 pf (2KV) capacitor is connected in parallel with the 40 kilohms resistor that is closer to the discharge tube to provide an ac bypass so that the resonance effect in the discharge current is maximized. The noise and oscillations in the discharge current are detected by a current probe (Tektronix P6019), amplified by an amplifier (Tektronix Type 134) and shown on a wave analyzer (Hewlett-Packard 312A). The wave analyzer is connected to a tracking oscillator (Hewlett-Packard 313A) which generates an ac signal. This signal is then amplified (by a Hewlett-Packard 450A Amplifier) and coupled into the discharge

FIGURE 3-5 VACUUM SYSTEM

2800 pf

40K

40K

2000 pf

CURRENT-
REGULATED
LASER POWER
SUPPLY

AC
SOURCE

TEKTRONIX P6019
CURRENT PROBE

A

C

DISCHARGE
TUBE

TRIPLETT 630-A
DC AMMETER

AC
SOURCE

TEKTRONIX
TYPE 134
AMPLIFIER

HEWLETT-PACKARD
312A
WAVE ANALYZER

HEWLETT-PACKARD
450A
AMPLIFIER

HEWLETT-PACKARD
313A
TRACKING OSCILLATOR
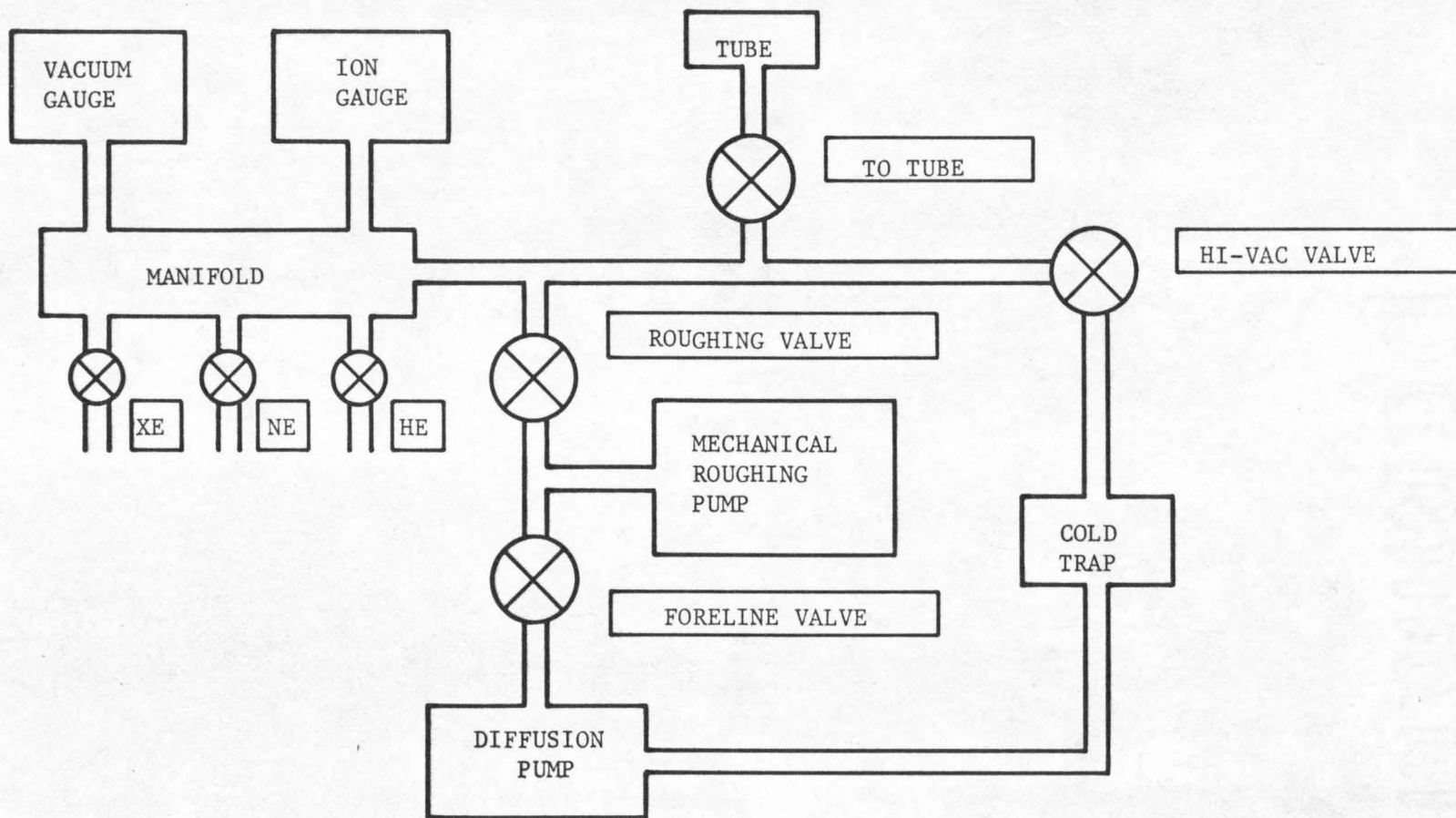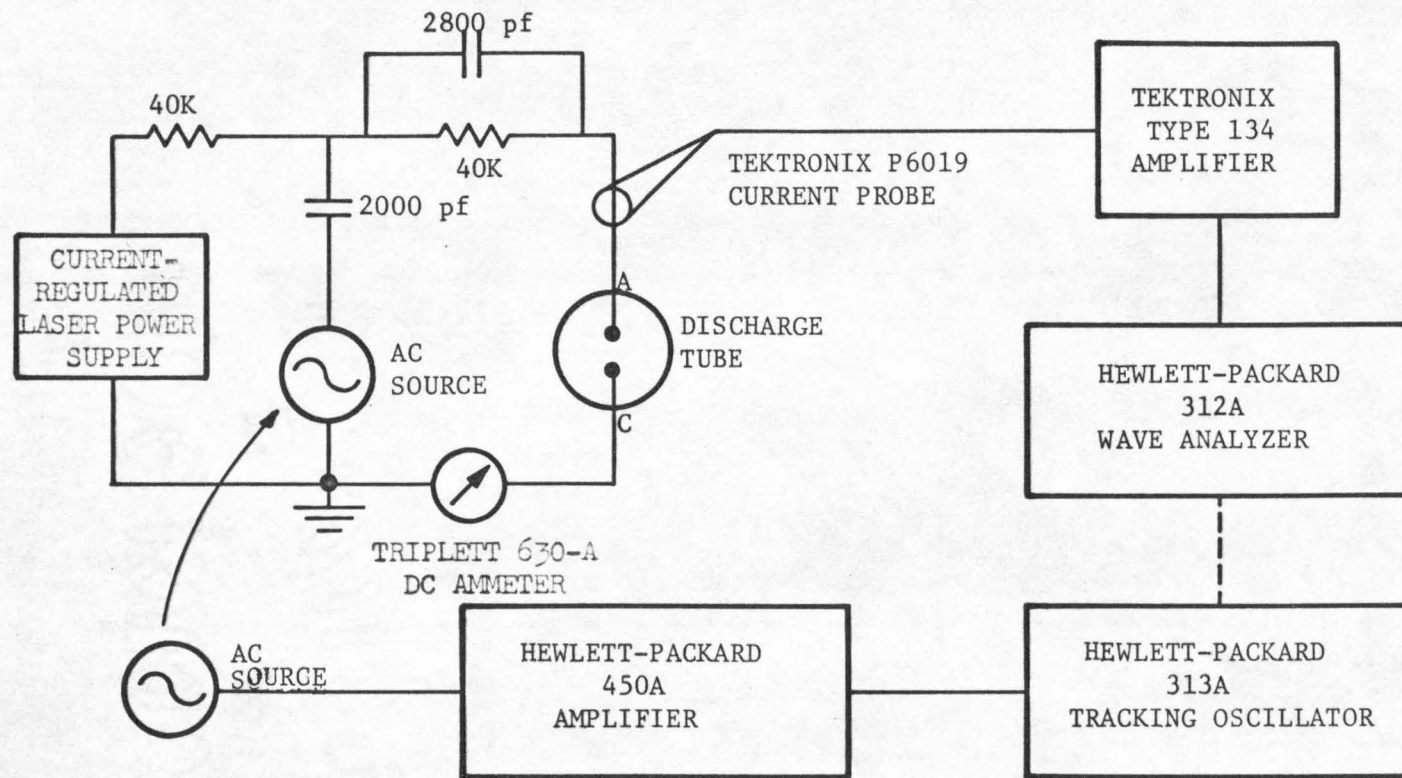
FIGURE 3-6 EXPERIMENTAL SETUP

tube circuitry as the ac disturbance. The wave analyzer and the track-
ing oscillator operate as a unit such that the frequency of the signal
generated by the tracking oscillator follows exactly the center freq-
uency of the narrow bandpass filter of the wave analyzer as it scans
over a wide range of frequency. The ac disturbance has a fairly con-
stant amplitude over a wide range of frequency*. Thus this unit of wave
analyzer and tracking oscillator provides a very convenient means of
measuring the gain and bandwidth factors of a system.

Appendix 1 shows that for an external ac voltage source across
the discharge tube the discharge current has a resonant frequency at
$(1/2\pi\sqrt{LC})$. The effect of the parallel capacitance C' is to give
the current response an asymptotic slope and a local minimum at a fre-
quency which depends on L and C as well as on C'. Fig. 3-6 shows
that in the experimental setup the ac voltage is essentially across a
series circuit consisting of two large bypass capacitors (with values
of 2000 pf and 2800 pf) and the discharge tube. Since the values of
these capacitors are much larger than that of the equivalent capacitance
of the discharge, they can be neglected in the analysis. Thus the
current response to the ac voltage still has a resonance at the fre-
quency $(1/2\pi\sqrt{LC})$.

When an external inductance L' of known value is connected
in series with the discharge tube the resonant frequency is decreased
to the value $(1/2\pi\sqrt{(L+L')C})$. Let $f = (1/2\pi\sqrt{LC})$ and $f' = (1/2\pi\sqrt{(L+L')C})$;

---

*The voltage amplitude varies by less than 5% over the frequency range
100 kHz to 400 kHz. It varies by less than 15% over the range 50 kHz
to 600 kHz

then the equivalent inductance L of the discharge can be expressed as

$$L = L' \left[\left(\frac{f}{f'} \right)^2 - 1 \right]^{-1} \tag{3-2}$$

where L' is the external inductor of known value, f and f' are the resonant frequencies of the current response to a voltage disturbance across the discharge tube with and without the external series inductor L', respectively. Since f and f' can be experimentally measured with the apparatus and the setup shown in Fig. 3-6, equation (3-2) permits the calculation of the values of L from known quantities.

Once the equivalent inductance L is known, the equivalent capacitance C of the discharge can be readily expressed in terms of L and the resonant frequency f,

$$C = \frac{1}{4\pi^2 f^2 L} \ . \tag{3-3}$$

It will be shown in the next section that L and C are not constant over variations in the dc discharge current, they depend non-linearly on the current. When an external ac voltage is connected a-cross the discharge tube the current response may contain oscillations at the fundamental frequency of the ac voltage and its harmonics. Os-cilloscope display of the current response of the discharge tube to a 6V voltage disturbance shows that it is periodic but nonsinusoidal. However the wave analyzer that measures the amplitude of the cur-

rent response has a very narrow bandpass filter (the smallest bandwidth
is 200 Hertz) which is centered at the fundamental oscillation frequency.
This filter eliminates all the harmonic components in the current re-
sponse before the response is measured. Thus the solid curve of Fig. 3-1
actually displays the fundamental component of the current response of
a laser discharge to an external ac voltage. Increasing the amplitude
of the external ac voltage merely amplifies the current response curve
of Fig. 3-1 without shifting the resonant frequency. Therefore the
resonant frequency depends on the values of L and C at the dc dis-
charge current.

3.4 Experimental Results on the Equivalent Inductance

This section presents the experimental measurements on the
equivalent inductance of various discharges. The experimental setup
and the method of measurement have been discussed in the previous sec-
tion. In this section the dependence of the equivalent inductance L
on the length of the positive column, the discharge current and the gas
pressure is presented for discharge in helium, neon and xenon. The
dependence of L on the average electron density in the positive col-
umn of the discharge is also discussed.

The emphasis of these two sections is on presenting the proper
dependence of the equivalent inductance L and capacitance C on the
parameters mentioned above, rather than on presenting the exact quan-
titative values of L and C. The quantitative values of L and C
are only applicable exactly to the experimental tube that is used to

collect this set of data. For other discharge tubes with different dimensions, tube structures, electrode materials and configurations, they merely have order of magnitude significance. Furthermore, the values of the circuit elements may change over a period of time since the emissive property of the cathode surface deteriorates because of the sputtering of the cathode surface material. Hence the quantitative values of L and C are meant only to give an indication of their orders of magnitude. However their dependence on discharge parameters are applicable to other discharges.

3.4.1 Dependence of L on the Length of the Positive Column ℓ

In this set of measurements, the kovars located along the discharge tube of Fig. 3-4 are used, one at a time, as the anodes. Thus the length of the positive column of the discharge tube varies from approximately 15 cm to 60 cm in increments of 15 cm. The equivalent inductance L for various lengths of the positive column is measured in the manner described in Section 3.3.

A reasonable way to predict the dependence of the equivalent inductance L on the length of the positive column ℓ is to express it as a sum of two quantities:

$$L = L_o + L_1 \ell \tag{3-4}$$

where $(L_1 \ell)$ is the portion of the equivalent inductance that is
contributed by the positive column and L_o is the contribution to the
equivalent inductance from discharge regions other than the positive
column. Since the various regions in a discharge (including regions of
the cathode fall, the negative glow, the positive column and the anode
fall) are in a series configuration, the equivalent inductance of the
whole discharge tube is the sum of the contributions from all these
regions. When the length of the positive column is decreased to zero
(i.e., the discharge does not have any positive column) while keeping
the discharge parameters constant, the equivalent inductance of the
discharge should approach a positive value L_o. Therefore a plot of
L versus ℓ should display a straight line with a positive slope L_1
which intercepts the L-axis at L_o.

Figs. 3-7(a) and (b)* show the dependence of the equivalent
inductance on the length of the positive column for discharges with
pure helium, neon and xenon under discharge conditions that are spec-
ified on the plots. They are fairly linear curves and this is in
agreement with equation (3-4). The value of L compares favorably in
order of magnitude with published data on equivalent inductances of dis-
charges (3,4). It should again be emphasized that exact numerical

---

*The curves in Figs.3-7(a) and (b) have been corrected to compensate
for the fact that the positive column begins at about 1.5 cm from the
start of the 5.5 mm ID Pyrex tubing. Therefore the first section (the
section that is closest to the cathode fall region) of the positive
column is 13.5 cm instead of 15 cm long. The reader should also be aware
of the drift of the values of the equivalent inductance and capacitance
over the time period during which the experimental curves of this chap-
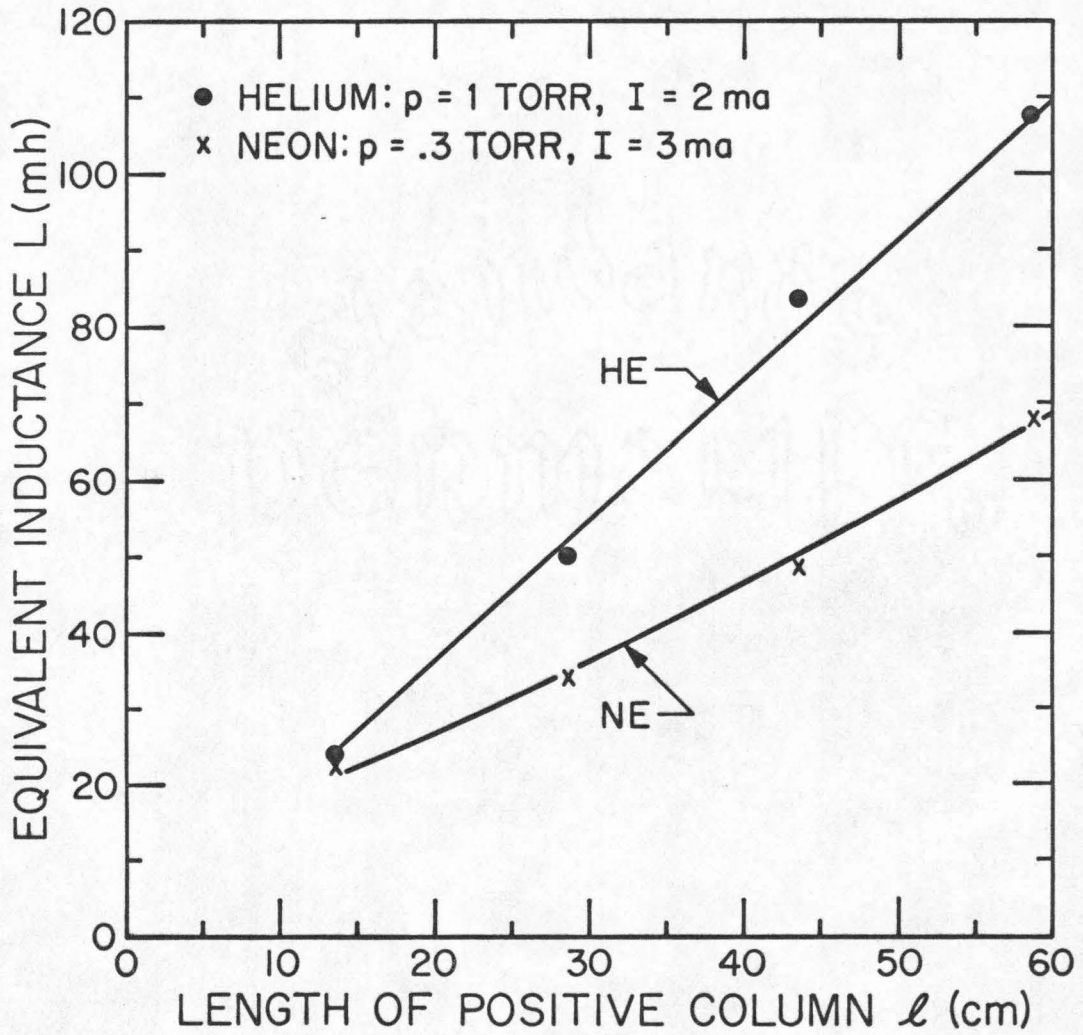ter are obtained.

FIGURE 3-7(a)   EQUIVALENT INDUCTANCE FOR VARIOUS
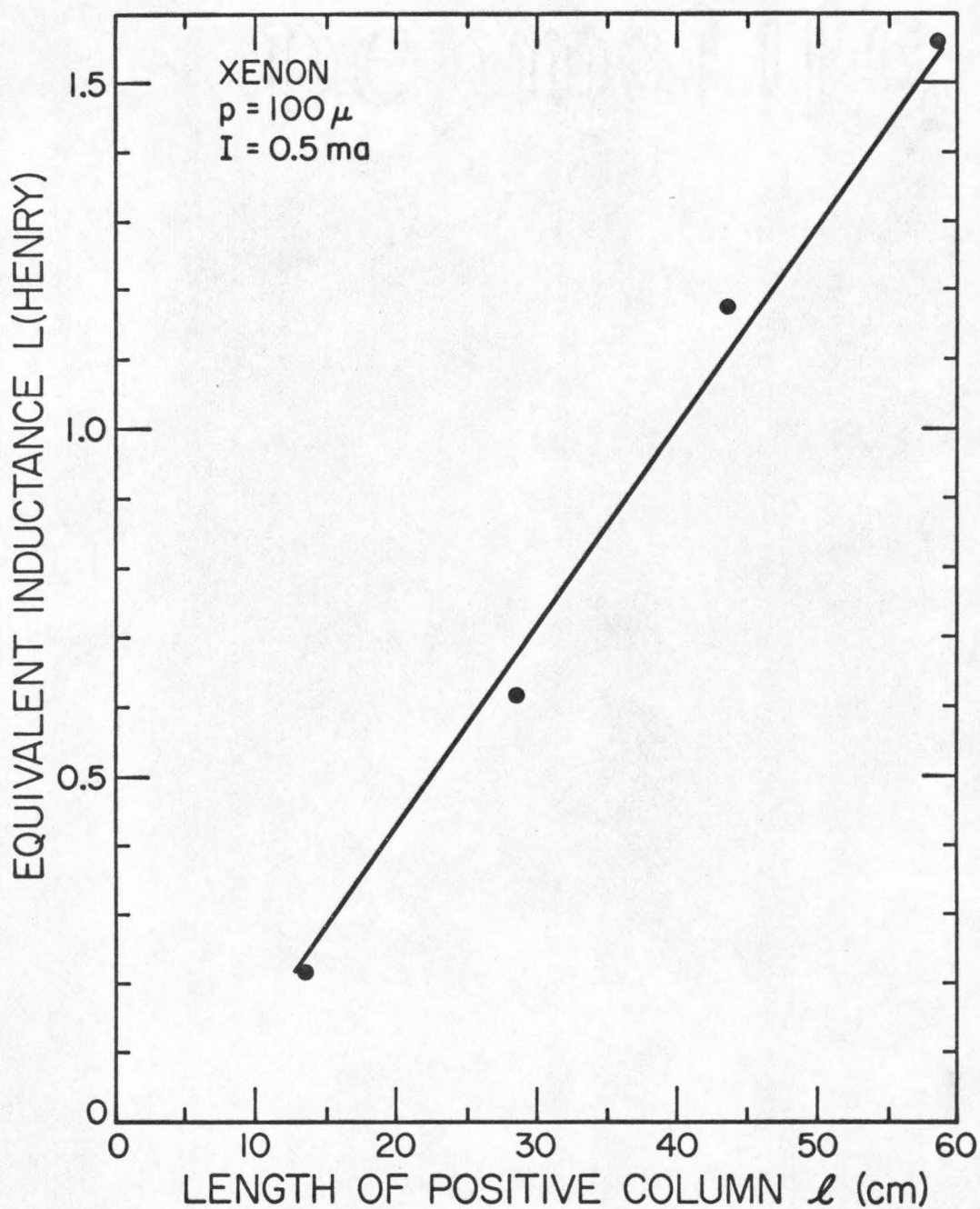   LENGTHS OF THE POSITIVE COLUMN

FIGURE 3-7(b) EQUIVALENT INDUCTANCE FOR VARIOUS
LENGTHS OF THE POSITIVE COLUMN

agreement is not being sought here, but rather the consistent dependence of the equivalent inductance on various parameters.

The linearity of the curves in Figs. 3-7(a) and (b) demonstrates that each additional section of the positive column produces an incremental amount of equivalent inductance. It should also be noted that approximately extrapolations of the curves pass through the origin. This suggests that the value of L_o in equation (3-4) is much smaller than the value of $(L_1 \ell)$ for any reasonable length of the positive column. In other words, the major portion of the equivalent inductance of a laser discharge is due to the inductance of the positive column. The other regions in the discharge contribute insignificantly to its equivalent inductance.

The above effect can be qualitatively justified as follows. Consider a cylindrical metallic wire which carries a current. The inductance of the wire depends on its length and the radius of its cross-sectional area. Approximately, it varies linearly with the length and logarithmly with the inverse of the radius (5). If a long and thin wire is connected to a short and bulky wire in a series configuration, the inductance of the two wires is dominantly due to that of the long and thin wire. In other words, the removal of the short and bulky wire does not reduce the inductance significantly. These two wires in series are somewhat analogous to the discharge tube that is sketched in Fig. 3-4. The long and thin positive column is connected to a short and bulky section which corresponds to the cathode fall region and the negative glow region. The discharge current flows

through one section and then the other. Hence it is quite justifiable
that almost all of the equivalent inductance of the laser discharge
comes from the positive column of the discharge.

3.4.2 Dependence of L on the Discharge Current I and the Average
Electron Density n_e in the Positive Column

An important discharge parameter which influences the equi-
valent inductance is the discharge current. It can easily be varied by
changing the voltage across the discharge tube and the large current
regulating resistor. The dependence of the equivalent inductance L
on the discharge current I is shown in Figs. 3-8(a) and (b) for dis-
charges in helium, neon and xenon. The discharge conditions are
specified on the plots. The curves show that the equivalent inductance
in general decreases for increasing discharge current. In particular
the equivalent inductance of a helium discharge depends inversely on
the current while that of neon discharge decreases a little slower than
(1/I) for increasing current.

Figs. 3-8(a) and (b) also show the dependence of the equi-
valent inductance on the average electron density in the positive col-
umn of the discharge, since it can be shown that the average electron
density is proportional to the discharge current under laser operating
conditions. Assume that most of the discharge current is carried by
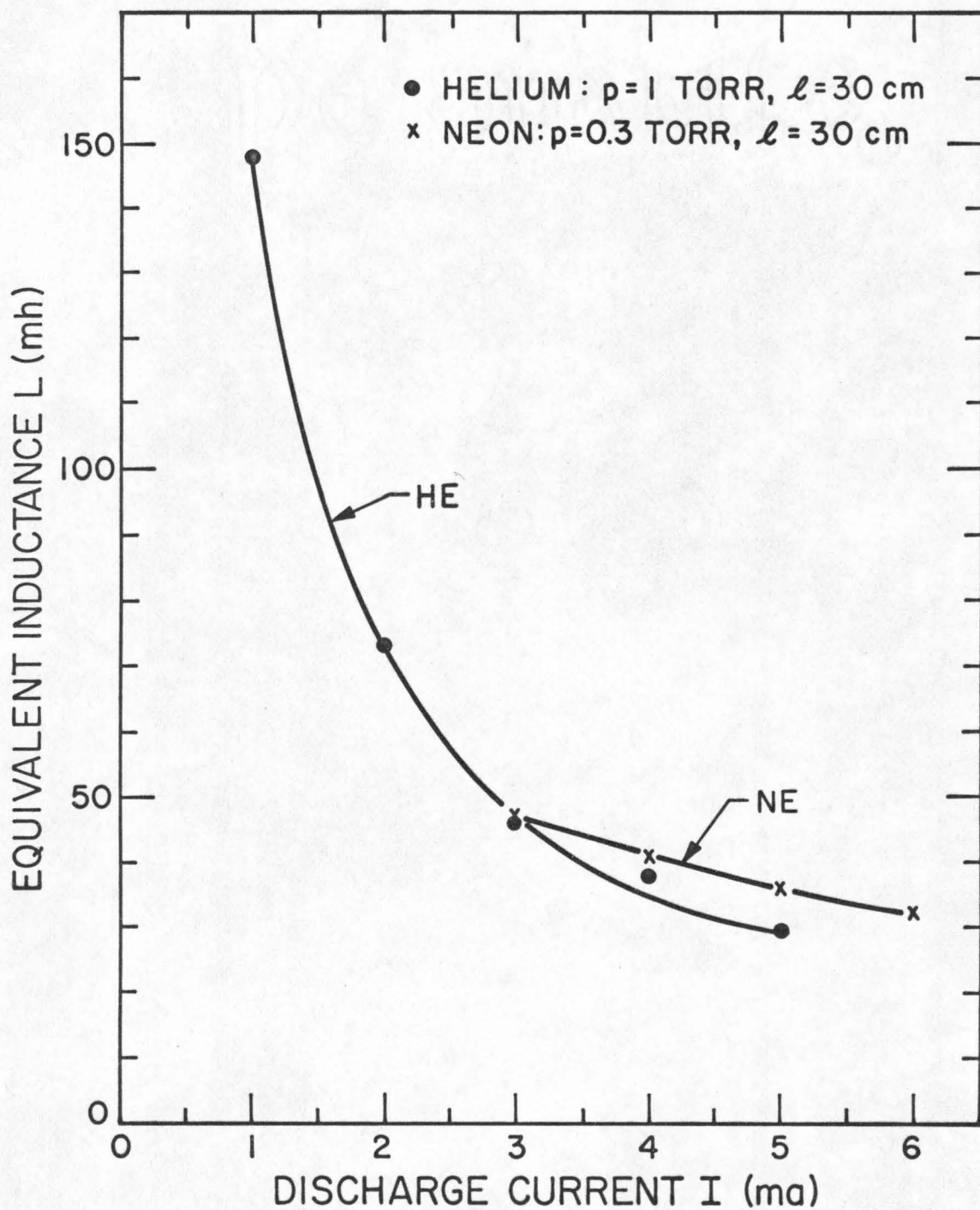the electrons in the positive column. Then the current I can be ex-

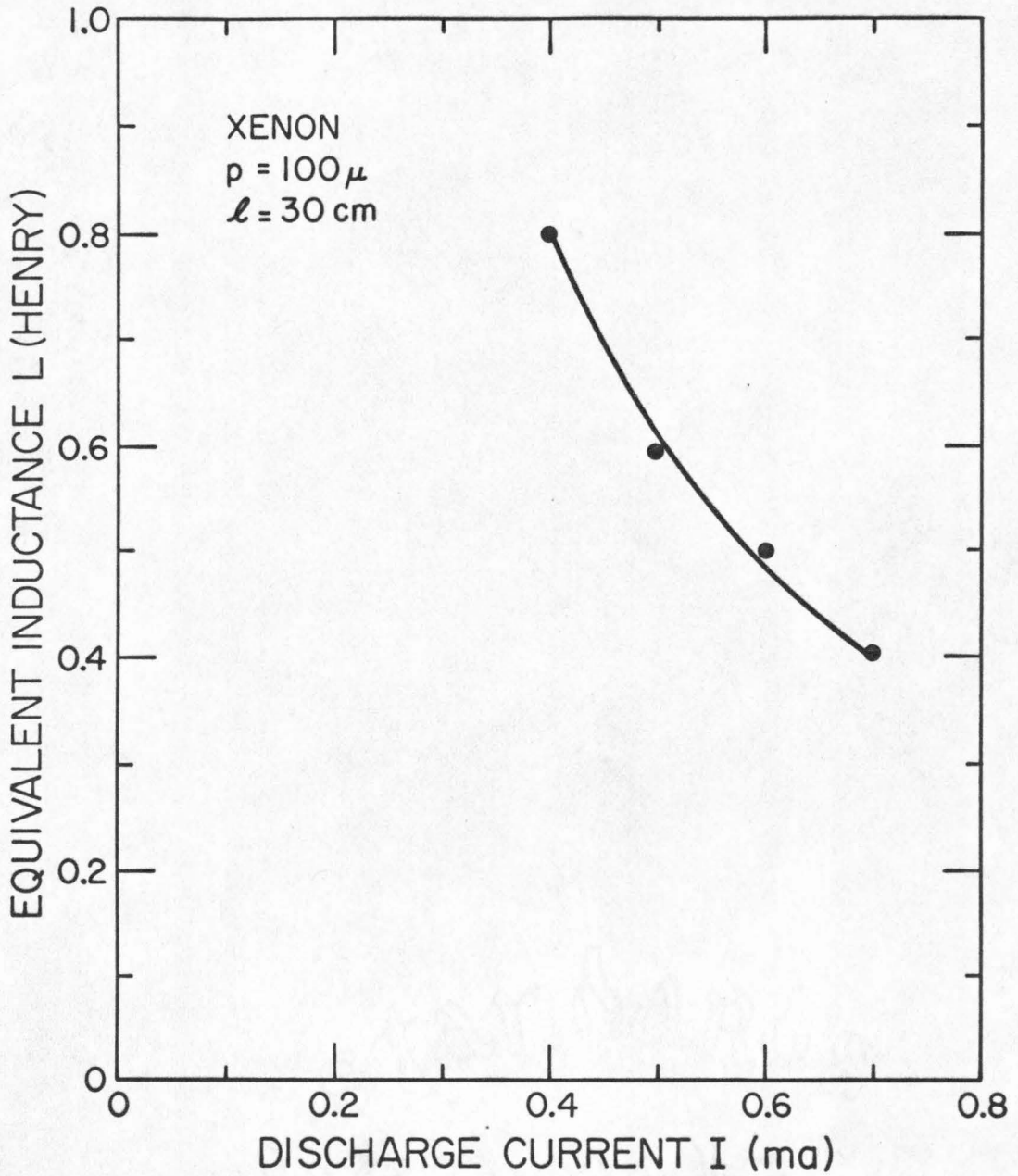FIGURE 3-8(a) EQUIVALENT INDUCTANCE FOR VARIOUS
DISCHARGE CURRENTS

FIGURE 3-8(b) EQUIVALENT INDUCTANCE FOR VARIOUS
DISCHARGE CURRENTS

pressed as

$$I = -n_e \, Ae \, \bar{v}_{de} \tag{3-5}$$

where A, $\bar{v}_{de}$ and n_e are the cross-sectional areas, the average electron drift velocity and the average electron density in the positive column, respectively, and e is the charge of the electron. In a weakly ionized discharge such as a laser discharge, the average density of the electrons is much smaller than that of the neutral atoms. Thus the average neutral atom density is approximately constant over variations in the discharge current. The collision rate between electrons and neutral atoms remains constant. Since $\bar{v}_{de}$ in the weakly ionized laser discharge is determined primarily by the collision rate between electrons and neutral atoms and the longitudinal electric field in the positive column which is also constant over variations in the discharge current, it is independent of the discharge current. With this in mind, equation (3-5) shows I to be proportional to n_e. The proportionality between I and n_e has been experimentally measured by Labuda and Gordon (6) for helium - neon laser discharges.

Since the average electron density in the positive column is proportional to the discharge current, the horizontal coordinates in Figs. 3-8(a) and (b) may just as well be the electron density, allowing for the proper conversion factor. Hence the curves in these figures also display the dependence of the equivalent inductance on the average electron density in the positive column. The experimental results can be summarized approximately by the following equation:

$$L \propto (I + I_L)^{-1} \propto (n_e + n_{eL})^{-1} \tag{3-6}$$

where I_L and n_{eL} are constants of such values as to fit equation (3-6) to the curves in Figs. 3-8(a) and (b). For the helium discharge, both quantities are zero. They may be negative, as in the case of a xenon discharge.

3.4.3 Dependence of L on the Gas Pressure p

As shown in Fig. 3-5, the experimental tube is connected to a vacuum system and bottles of various gases such that the tube can be filled with any gas at any pressure. Fig. 3-9(a) shows the dependence of the equivalent inductance on the gas pressure for a helium discharge at discharge currents of 2 ma and 4 ma. The experimental curves show approximately linear dependencies on the gas pressure p; i.e.,

$$L = L_2 + L_3 p , \tag{3-7}$$

where L_2 and L_3 are constants which depend on the discharge current, the length of the positive column and the general tube configuration.

Fig. 3-9(b) gives the dependence of the equivalent inductance of a helium-xenon discharge on the helium pressure. The xenon pressure is fixed at 100 microns. The equivalent inductance is normalized to its value when the helium is absent from the discharge. The experimental curve shows that the equivalent inductance increases significantly when the helium pressure exceeds that of the xenon. The
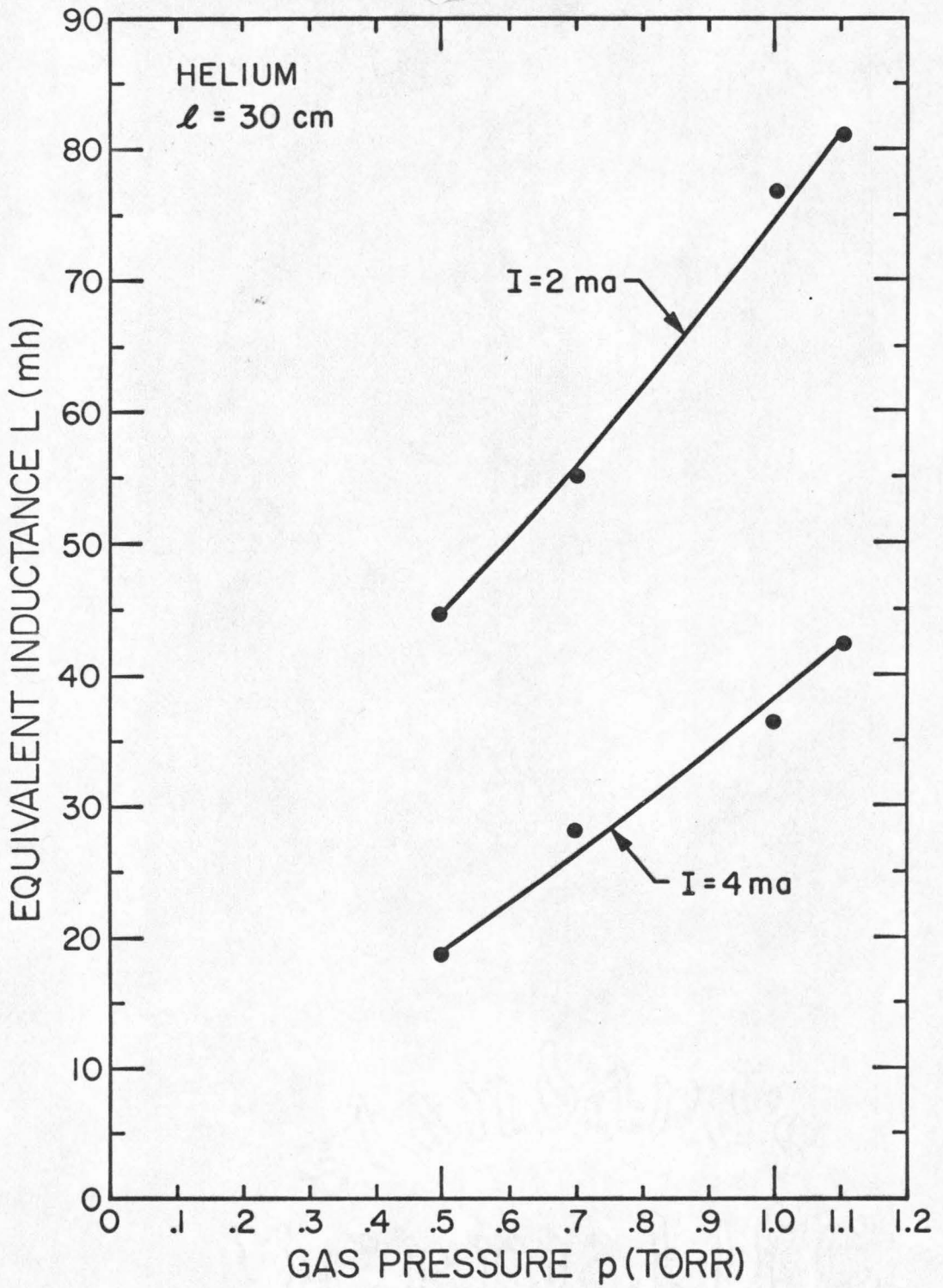
EQUIVALENT INDUCTANCE FOR VARIOUS
HELIUM GAS PRESSURES

FIGURE 4-10(b)   NORMALIZED EQUIVALENT INDUCTANCE FOR VARIOUS
HELIUM PRESSURES AT A FIXED XENON PRESSURE

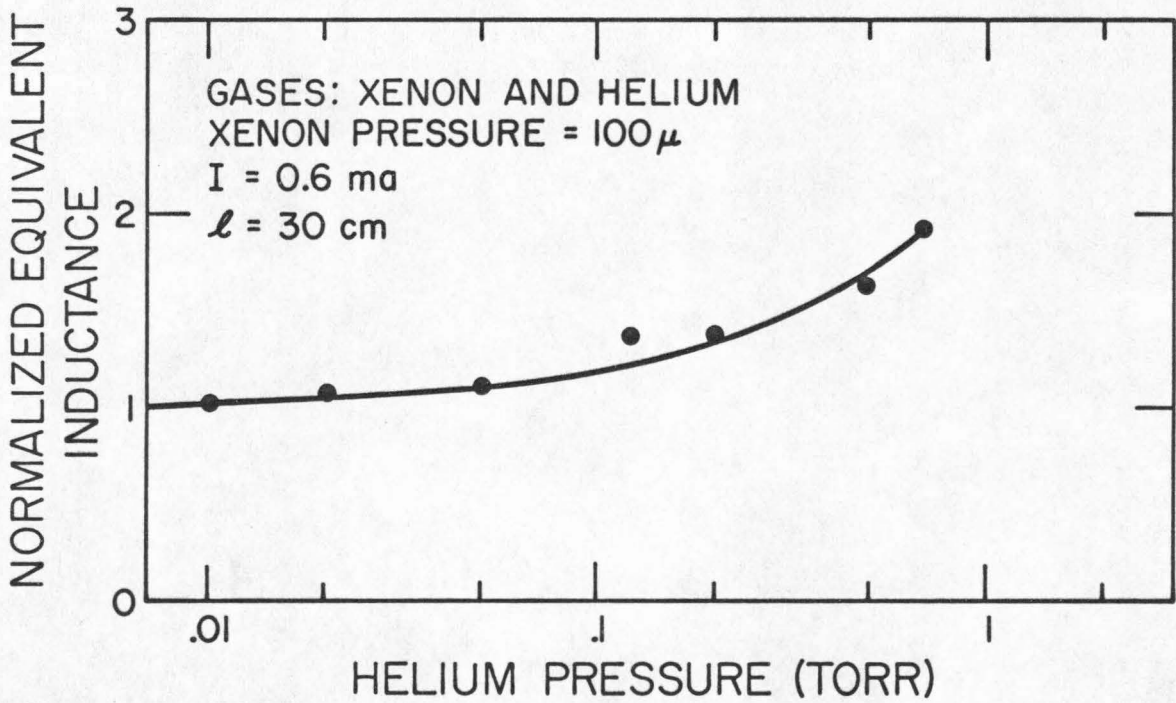curves in Figs. 3-9(a) and (b) demonstrate that the value of the equiva-
lent inductance increases with the pressure even if the increase in the
gas pressure is due to the addition of another gas.

3.5 Experimental Results on the Equivalent Capacitance

The curves in Figs. 3-10, 3-11 and 3-12 present the experi-
mental data on the equivalent capacitance C of a discharge. They are
obtained in the manner described in Section 3.3. The discharge para-
meters are indicated on the plots. Fig. 3-10 describes the dependence
of the equivalent capacitance of a helium discharge on the length of the
positive column. It shows that the value of C is approximately in-
dependent of the length of the column. Each incremental increase in
the length of the positive column does not cause any significant change
in the equivalent capacitance. In other words, the positive column of
a discharge contributes negligibly to its equivalent capacitance. The
capacitance is mainly due to the other regions in the discharge; name-
ly, the cathode fall, the negative glow and the anode fall regions.

The dependence of the equivalent capacitance of the discharge
current is shown in Fig. 3-11.* The equivalent capacitance decreases for
increasing current. The curve in Fig. 3-11 can be approximately ex-
pressed as

---

*
The last three data points in Fig. 3-11 have been calculated using
the extrapolated values of the equivalent inductance from Fig.
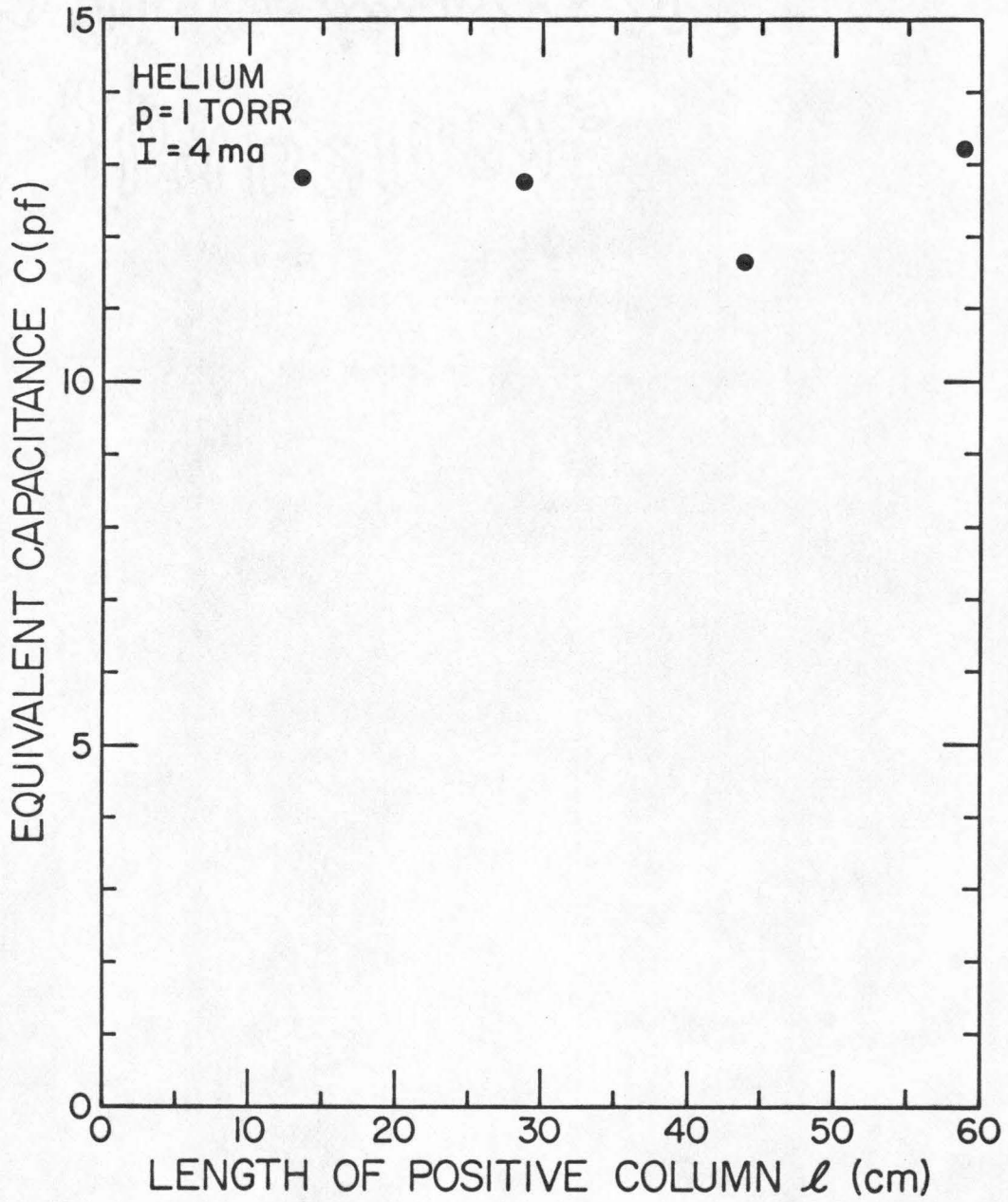3-8(a).

FIGURE 3-10 EQUIVALENT CAPACITANCE FOR VARIOUS
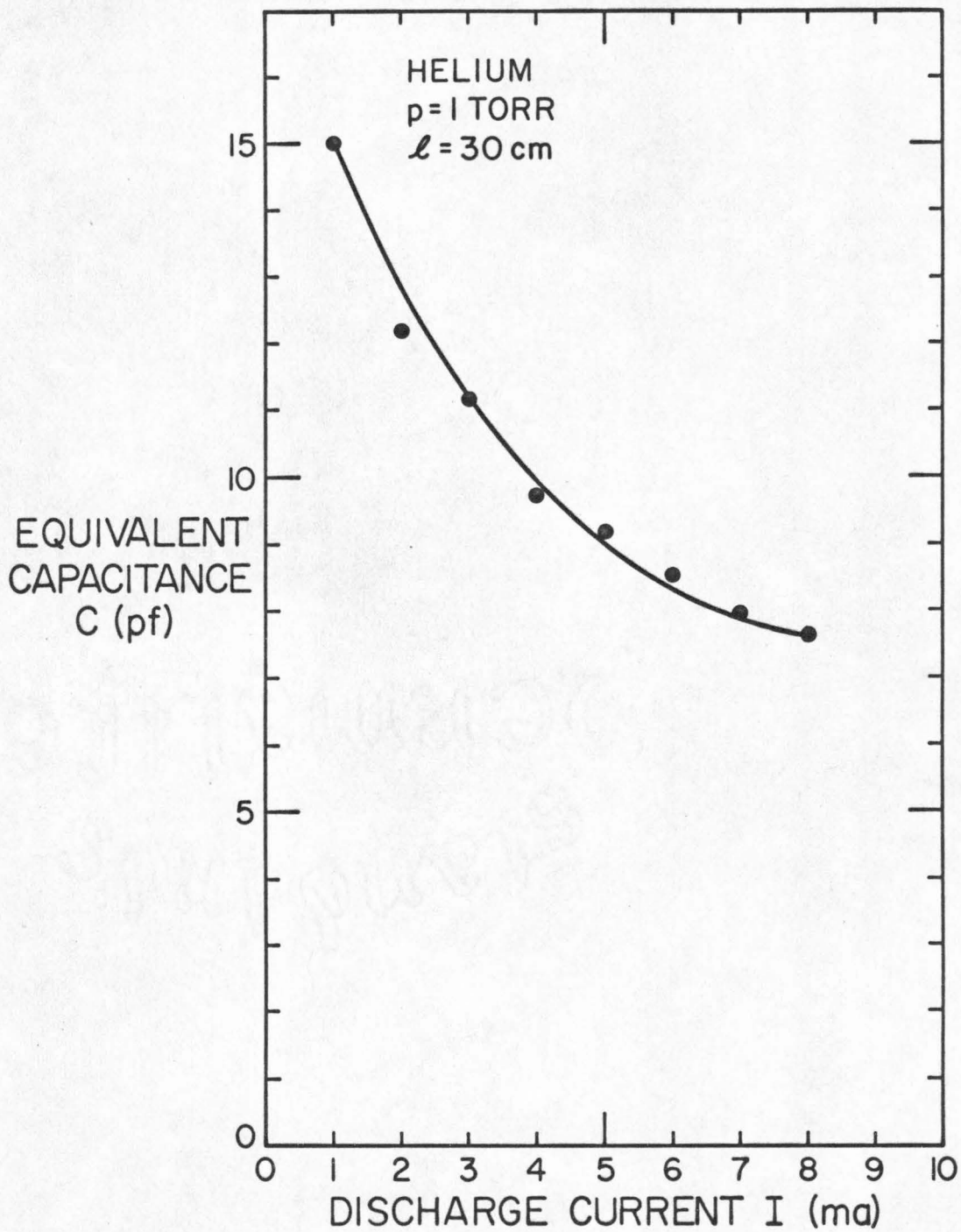LENGTHS OF THE POSITIVE COLUMN

FIGURE 3-11 EQUIVALENT CAPACITANCE FOR VARIOUS DISCHARGE CURRENTS
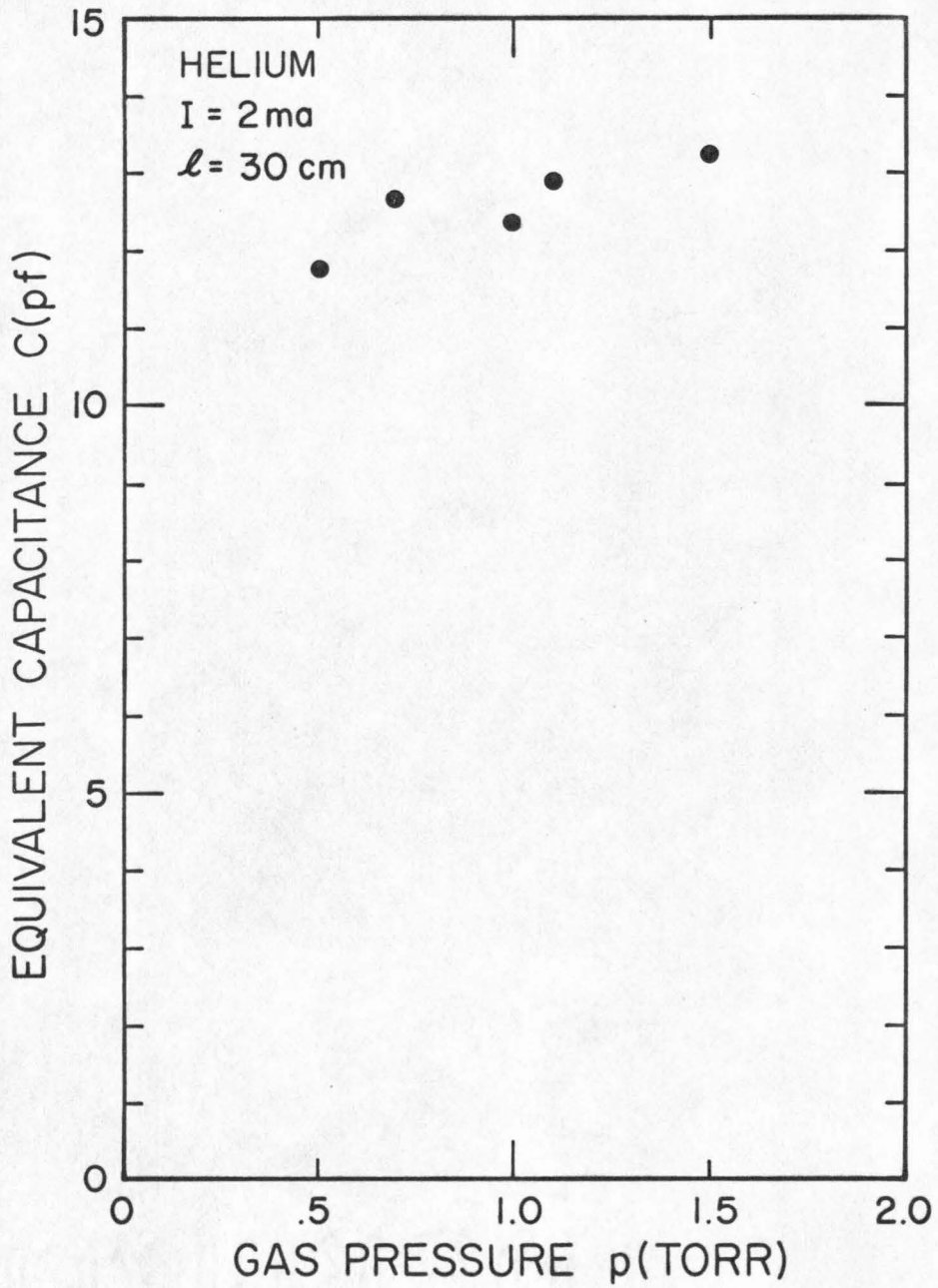
FIGURE 3-12 EQUIVALENT CAPACITANCE FOR
VARIOUS GAS PRESSURES

$$C \propto (I + I_C)^{-1} \qquad\qquad (3-8)$$

where I_C is a quantity chosen to fit equation (3-8) to the experimental curve. I_C is approximately 6 ma for the helium discharge.

Fig. 3-12 shows the dependence of the equivalent capacitance of a helium discharge on the gas pressure. It remains approximately constant over the pressure range of 0.5 torr to 1.5 torr. For a three-fold increase in gas pressure, the capacitance increases by only 11%. Hence for all practical purposes the equivalent capacitance can be assumed to be constant over variations in the gas pressure. A possible explanation of this relationship of independence between the equivalent capacitance and the gas pressure will be given in the next section.

3.6 Summary and Discussion

This chapter presents an ac equivalent circuit which represents the laser discharge tube over a frequency range in the kilohertz region. It consists of a capacitance C', which comes from the capacitance between the electrodes and between the stray wiring, in parallel with a series ρLC circuit, which is due to the discharge region (Fig. 3-2). Within the frequency range for which the ac equivalent circuit is a valid representation of the discharge, the response of the discharge tube to an ac disturbance source can be obtained through an analysis of the equivalent circuit with the source element. This chapter considers an external source element. However, if the disturbance comes from within the discharge region, the source element is

located in the series ρLC circuit. When the equivalent circuit elements have such values and the discharge is coupled to the external circuitry in such a way that a disturbance at a certain frequency grows in time, the discharge tube would oscillate by itself at that resonant frequency. This case will be considered in the next chapter.

The two sections prior to this have been devoted to presenting experimental data on the dependence of the reactive elements of the equivalent circuit on various discharge parameters. The parallel capacitance C' has been omitted from consideration. It is the capacitance of the discharge tube with the discharge extinguished. Its value depends only on the tube dimensions and the electrode configuration, and is independent of the discharge parameters.

The experimental results on the equivalent inductance L and capacitance C of the circuit have been presented and discussed in Sections 3.4 and 3.5. However, it is fitting here to recall and extend two of the interesting consequences of the experimental data. Both L and C are strongly dependent on the discharge current (Figs. 3-8(a), 3-8(b) and 3-11). Consequently the resonant frequency of the equivalent circuit should depend strongly on the discharge current too. The dependence of L and C on the current also introduces nonlinearity into a discharge, as shown in Appendix 2. It explains the experimental observation that the current response of the discharge to an external sinusoidal voltage disturbance can be quite nonsinusoidal. It also explains the nonsinusoidal behavior of the current waveform due to moving striations in a laser discharge which will be presented in the

next chapter.

The experimental dependence of L and C on the length of the positive column (Figs. 3-7(a), 3-7(b) and 3-10) suggests that the equivalent inductance of a laser discharge comes mainly from its positive column while the equivalent capacitance is due to the cathode fall, the anode fall and the negative glow regions. The cathode fall and the anode fall regions are characterized by groups of space charges adjacent to groups of opposite charges in the electrodes. Two groups of opposite and equal charges which are located next to each other form a capacitance. It is quite likely that the equivalent capacitance C of the discharge is mainly the capacitances of the cathode fall and anode fall regions. Since a capacitance depends on the charged particle density rather than the neutral atom density, the above concept of C helps to explain the independence of C from variations in gas pressure. The main effect of changing gas pressure (while keeping the discharge current constant) is to change the neutral atom density.

CHAPTER FOUR

MOVING STRIATIONS IN A LASER DISCHARGE

4.1 Introduction

One of the low frequency oscillations which occur quite frequently in direct current inert gas discharges is associated with the moving striations in the positive column. The frequency of such oscillations lies in the kHz range. Although a striated positive column may appear quite homogeneous visually, photographs taken with the aid of rotating mirrors and image converters have shown (1-3) that the light intensity emitted from the side of the positive column fluctuates periodically, though not usually sinusoidally, along its axis. This fluctuation in light intensity is caused by fluctuations in the electron density and temperature which are, in turn, caused by a spatial variation in the potential along the positive column. All these fluctuating waves in the light intensity, the electron density, the electron temperature and the potential travel from one electrode to the other. The waves that travel from the anode to the cathode are due to the positive moving striations while those that move in the opposite direction are caused by the negative moving striations. The positive moving striations occur more frequently than the negative moving striations which are often not observed experimentally (21).

Striations were first observed by Abria (4) as early as 1843. The most prominent and extensive work in the early years was done by Pupp (5,6) who measured the fluctuations in the electron density, the

electron temperature, the potential and the light intensity along a striated positive column. Sixteen years later, Donahue and Dieke (7) published extensive experimental data on the positive and negative moving striations in an argon discharge and found that they were present over large ranges of discharge conditions. In the 1950's, a few theoretical studies on moving striations were made. Watanabe and Oleson (8) gave a theoretical treatment of the traveling density waves in the positive column; Robertson (9) showed that a spatially uniform positive column was unstable; Pekarek and Krejci (10-12) studied the generation and sustaining mechanisms of moving striations while Wojaczek (13,14) used the diffusion theory to obtain a dispersion relation for the moving striations which predicted a spatially growing wave for certain frequency range. Wojaczek and Pekarek and Krejci all used a set of linearized expressions for the ion density, the electron density, the electric field and the electron temperature in their number and energy conservation equations. It is strictly valid only for small perturbations and may not be adequate since the observed spatial variations in these parameters have large amplitudes and non-sinusoidal shapes. Their linear theories also neglected the metastable atom density in the positive column which, as implied by Hakeem and Robertson (15), plays an important role in the analysis of moving striations in noble gas discharges. In addition to their theories, Wojaczek (16) and Pekarek and Krejci (17-19) also carried out some experiments on the externally-excited "waves of stratification" (using Pekarek's terminology) traveling in the positive column.

Due to the development of better instruments and the advent of new fields involving gas discharges, the interest in this area has increased recently. Lee, Bletzinger and Garscadden (2) proposed a theory which gave the oscillating modes and the stability criterion for moving striations. Gentle (20,21) included the metastable atom density and the Boltzmann Function for the distribution of electrons in analyzing the positive column and found growing waves propagating from the anode to the cathode under certain discharge conditions; and good agreement between experimental and analytical results was reported. His experimental work involved the novel idea of making measurements on striations which were made stationary by flowing the argon gas through the positive column at a velocity which was equal and opposite to the phase velocity of the moving striations. Alexeff and Jones (22) observed the striation velocity to be approximately equal to the ionic sound wave velocity of Tonks and Langmuir (23) at low gas pressures. This approximate equality suggests the possibility that moving striations are associated with corresponding ionic sound waves. The topic was also of considerable interest to Garscadden and Lee (24) who suggested the possible existence of transition and coupling between moving striations and ionic sound waves. Despite all the papers that have been written on the moving striations, the subject is still not clearly understood.

After the first direct current helium-neon laser was constructed, it was natural to look for moving striations in helium-neon lasers. Among those who work in the field, Garscadden (25) has obtained rotating mirror photographs of moving striations in a helium-neon laser. Moving

striations exist in lasers over a wide range of discharge parameters. They influence the laser light output. Garscadden, Bletzinger and Friar (26) observed that, in addition to being modulated at the striation frequency, the laser output decreased in power when waves of stratification were generated in the positive column of the laser discharge by exciting an external coupling loop with a high voltage pulse. The latter effect has also been implied by George (27). Hence, it is important to study moving striations from the laser standpoint.

The theoretical treatments of moving striations have been limited to linear theories so far. A good nonlinear theory for the propagation of moving striations, which considers all the important elements in the discharges, is still lacking. In addition, the generating mechanisms for moving striations are also unknown. Pekarek and Krejci (18, 28) claimed that moving striations were waves of stratification originating in the cathode region. Coulter, Armstrong and Emeleus (29) visualized moving striations as oscillating anode spots stripping off from the anode. Morgan (30) suggested that moving striations might have started from the head of the positive column where the electron density might be time-varying. However, Robertson's analysis (9) indicates that moving striations naturally exist in the positive column under some circumstances and that they need not originate from the electrodes or any other region in the discharge. A recent experimental paper by Cooper (3) discounts the relation between anode oscillations and moving striations. However, the picture concerning the generation of moving striations in gas discharges remains unclear.

Even though there have been much experimental data on moving striations in gas discharges (especially in argon discharges), the comparison among them is quite difficult. This is so mainly because the tube and electrode configurations and the discharge conditions are not standardized. Consequently, no two experiments yield the same result and the relation between them is not obvious.

There has been so much published work on moving striations in gas discharges that it is impractical, if not impossible, to give a complete list of papers on the subject. An attempt has been made in this section to trace the research development chronologically, to describe the major works and to discuss some of the problems and uncertainties that still remain in this area. Interested readers are referred to an extensive bibliography compiled by Palmer and Garscadden (31) on moving striations in gas discharges.

It is the intent of this chapter to describe the moving striations that exist naturally in laser discharge and to show that the equivalent circuit of Chapter 3 is applicable to understanding the striations. These objectives are achieved through qualitative discussions and the presentation of the experimental data on a laser discharge. The effect of an external longitudinal magnetic field on the striations frequency is also presented and discussed.

4.2 Equivalent Circuit Approach to Moving Striations in a Laser Discharge

Moving striations are initiated by disturbances in the ionization process. The ionization rate is uniform along the axis of the posi-

tive column in the absence of any disturbance. Consider that, at an
instant, there is a local disturbance in the ionization rate somewhere
along the positive column such that the number of pairs of electrons and
ions in the region exceeds its normal value. Because of their great mob-
ility, many of the electrons diffuse out of the region very readily,
leaving the region with a net positive charge for that instant of time.
In the positive column the current is dominantly carried by the elec-
trons. As the electrons approach this positively charged region from
the cathode side, they experience, in addition to the normal electric
field that exists in the positive column, an extra electric field due
to the net positive charge. The electrons become more energetic when
they reach the region. These energetic electrons cause a greater-than-
average amount of ionization and excitation. The extra excitation
causes the region to be brighter than the rest of the positive column.
The extra ionization reinforces the initial disturbance in the ioniza-
tion process and sustains the net positive charge in the region. How-
ever, as the electrons leave the region to drift toward the anode, the
condition is reversed. They experience an electric field which tends to
pull them back into the region. This electric field is superposed on-
to and opposite in direction to the longitudinal electric field which
exists in the positive column. The effect is that the electrons on the
anode side of the region of net positive charge are less energetic than
they would have been had the region of net positive charge not been
there. This results in a local minimum in the excitation and ionization
rates; i.e., a local minimum in the number of the excited atoms and the

number of the pairs of electrons and ions. The region is considerably
darker than its adjacent region on the cathode side. Because of their
mobility, the electrons from outside the region diffuse into the region,
leaving it with a net negative charge. Following this line of reason-
ing, bright regions with net positive charges and dark regions with net
negative charges are alternately established on the anode side of the
original distrubance. Since these regions are characterized by greater-
than-average and less-than-average amounts of positive ions, they travel
toward the cathode with a phase velocity that is approximately equal to
the average drift velocity of the ions. This is a very qualitative
picture of the sustainment and the propagation of the positive moving
striations; but it does demonstrate how a disturbance in the discharge
region can develop into moving striations.

The above paragraph presents a simplified explanation for the
existence of moving striations in a discharge. The exact analysis of
the striation phenomenon involves the knowledge of the generating mech-
anism and the solution of some nonlinear equations. As indicated in
Section 4.1, both of these aspects are not thoroughly uunderstood. How-
ever, an alternate approach to understanding moving striations is by
applying the equivalent circuit of Chapter 3 (with the proper internal
source element) to a laser discharge. The equivalent circuit of Fig. 3-2
is applicalbe to representing the striation phenomenon for several rea-
sons. The striation frequency lies in the range of frequency for which
the equivalent circuit is a valid representation of the laser discharge.
The response of the discharge to any external or internal disturbance
within the frequency range can be obtained by analyzing the equivalent

circuit with the source element properly located. In other words, the major difference between the equivalent circuits which represent the laser discharge with ac voltage modulation and with self-excited moving striations lies in the location of the source elements in the circuits. Rotating-mirror photographs of the positive column of a discharge with ac modulation show side light intensity waves traveling toward the cathode which are similar to those emitted from a positive column with self-excited moving striations. This method of obtaining induced striations through ac modulation is often used (2,25) to study the striation phenomenon in the discharge region when the self-excited moving striations are not present. Since the equivalent circuit is constructed from the current response of the laser discharge to an ac voltage modulation, it should be valid for the self-excited moving striations. The final justification for the application of the equivalent circuit to representing the laser discharge in understanding the striation phenomenon comes from the fact that it is a resonance effect. In the electrical analogy, the striation phenomenon should correspond to the resonance effect of a tank circuit which includes an inductance and a capacitance and is quite similar to the equivalent circuit of a laser discharge shown in Fig. 3-2.

Fig. 4-1 shows the ac equivalent circuit of a laser discharge with internal disturbances. The dc power supply for the laser discharge is a regulated current source and is therefore open circuited in the ac equivalent circuit. The source element which corresponds to the internal disturbances in the discharge is in series with the ρLC circuit and should cover a large frequency range. This series voltage source is a generalized representation of the internal disturbances in a discharge
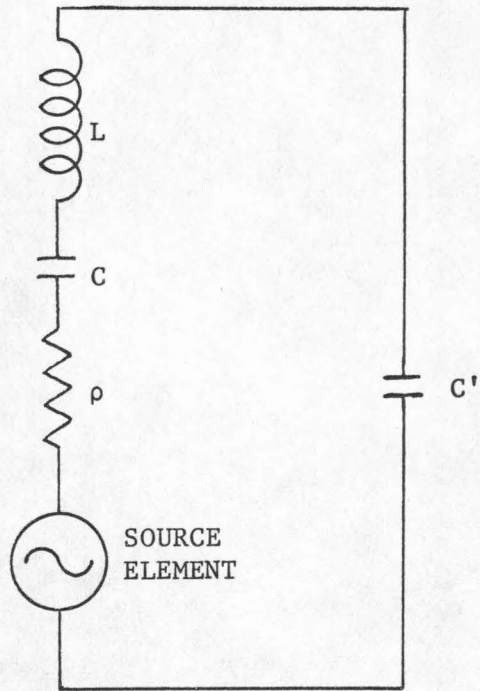
FIGURE 4-1   AC EQUIVALENT CIRCUIT OF A LASER

DISCHARGE WITH INTERNAL DISTURBANCES

since, according to Thevenin's Theorem, any two port linear circuit containing current and voltage sources is equivalent to the circuit without the sources in series with an equivalent voltage source. When ρ is negative the frequency component of the source element which is at the resonant frequency of the circuit is amplified and constitutes the moving striations. The other frequency components of the source element are attenuated.

The above concept of the resonance effect can be illuminated by considering the response of the discharge to a voltage pulse applied at the cathode. When a discharge does not have self-excited moving striations, a voltage pulse is often applied (2,18) at the cathode to study the striation phenomenon. As the pulse travels in the positive column, it gradually becomes a wave packet with the group velocity in the direction of the anode and the phase velocity in the direction of the cathode. This is the backward wave nature (2) of the positive moving striations. By the time the wave packet approaches the anode, it becomes quite sinusoidal with a characteristic frequency. This phenomenon can be explained by the equivalent circuit described in the previous paragraph. A pulse consists of frequency components from a wide spectrum of frequency. Since natural striations do not exist in the discharge, the resistor in the equivalent circuit is positive and all the frequency components of the pulse experience attenuation as they travel through the positive column. However, the component at the resonant frequency of the equivalent circuit experiences the least amount of attenuation. It becomes the only frequency component of the pulse that arrives at the anode without suffering a significant loss in its ampli-

tude. Hence a voltage pulse at the cathode becomes a sinusoidal wave

packet by the time it arrives at the anode. An external measurement of the

discharge current response to a voltage pulse disturbance would only

measure the component at the resonant frequency. The generation of stri-

ations from a pulse disturbance is similar to the self-excited moving

striations in that in both cases the source provides for disturbances

over a wide range of frequency while the equivalent circuit decides the

amplification and attenuation of the frequency components. The equi-

valent circuit approach gives no account of how the moving striations

travel in the positive column, but it does give the response of the

whole discharge region, as the external circuitry "sees" it.

The equivalent circuit approach to understanding moving stri-

ations has certain advantages over the conventional approach of solving

the particle and energy conservation equations whose limitations have

been discussed in Section 4.1. The limitations concern the location and

mechanism of the generating source, and the solution to nonlinear equa-

tions. Since the voltage source element in the equivalent circuit is in

series with the ρLC circuit which represents the discharge region, it

is unimportant to the analysis of the circuit as to where the source is

located. The mechanism by which the generating source operates is also

unimportant in the equivalent circuit approach since, as discussed pre-

viously, the series voltage source is a generalized representation of

all internal disturbances of the discharge. The important concept con-

cerning the source element in the equivalent circuit is that the dis-

turbances should cover a large frequency range in the kilohertz region.

The nonlinearity in the current and voltage waveforms of a discharge due to moving striations can be readily explained in the equivalent circuit approach. It is due to the fact that the values of the equivalent circuit elements depend on the discharge current. When the amplitude of the current fluctuation is large such that it is no longer negligible compared to the dc discharge current, the nonlinearity of the equivalent circuit elements causes the waveform to have components at the harmonics of the resonant frequency. As shown in Appendix 2, the amplitudes of these components are proportional to the amplitude of the component at the resonant frequency and cannot be attenuated. Hence the two major limitations of the conventional approach to understanding the moving striations are somewhat compensated by the equivalent circuit represent- ation of the laser discharge.

4.3 Time Display of Moving Striations in a Laser Discharge

The measurements presented in this chapter are made on a reg- ular laser discharge tube with a heated cathode. A photograph of the tube is shown in Fig. 4-2. The bulky section of the discharge tube at the left hand portion of the photograph contains the heated cathode while the kovar at the right is the anode. The tube is 80 cm long with an interelectrode distance of 63 cm. The positive column is contained in a Pyrex tubing of 60 cm long and 4 mm ID. The heated cathode is housed in a Pyrex section of 4.5 cm long and about 5 cm ID. The cathode itself is a spiralling tungsten filament forming a semicircle which occupies an area of about 5 sq. cm and carries a dc current of 4.1
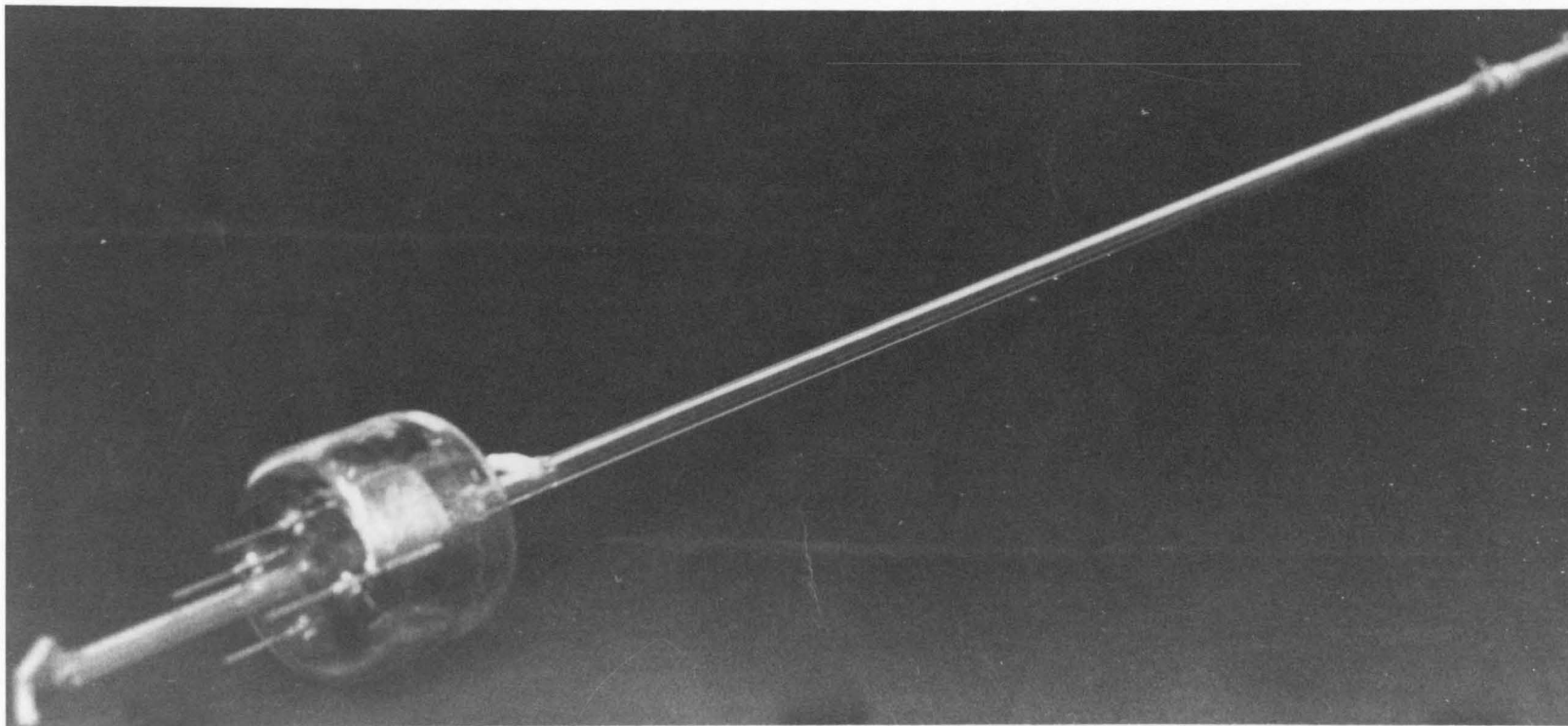
FIGURE 4-2   THE LASER AMPLIFIER DISCHARGE TUBE

amperes (corresponding to a filament temperature of about 850°C). The tube is sealed after being filled to a total pressure of 1.5 torr at a five to one ratio of helium to neon pressures.

Fig. 4-3 shows the electrical connections for displaying the current and voltage waveforms of a laser discharge. The anode of the laser tube is connected to a current-regulated laser power supply through a 60 kilohms noninductive current-limiting resistor with 60 watts power rating. Its cathode is connected to the ground through a 220 ohms carbon resistor. The waveform of the discharge current is taken directly from the voltage drop across the 220 ohms resistor while the waveform of the discharge voltage is taken from the anode of the tube through an ac bypass capacitor. The impedance of the capacitor at the striation frequency should be small compared with the input impedance of the oscilloscope which displays the discharge voltage and current waveforms simultaneously.

Fig. 4-4 shows the discharge voltage and current waveforms for the laser discharge tube described above. The voltage waveforms are the upper traces in all the photographs while the current waveforms are the lower traces. All of the four photographs in Fig. 4-4 have the same time scale, lower and upper trace sensitivities. Fig. 5-3(a) shows the waveforms at a dc discharge current of 5.2 ma. At that current the moving striations do not have enough gain to oscillate yet. However, as shown in Fig. 5-3(b), they begin to set in when the discharge current is increased beyond 5.5 ma. Note that the waveforms are quite sinusoidal (i.e., they have weak components at multiples of the fundamental striat-
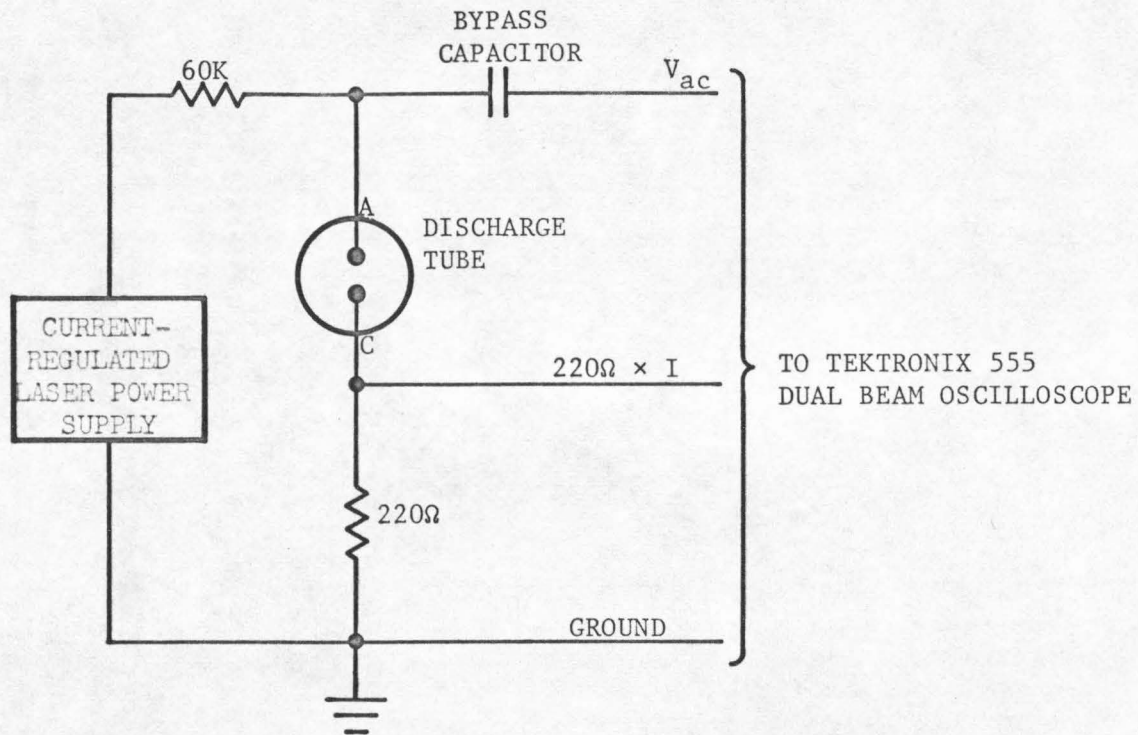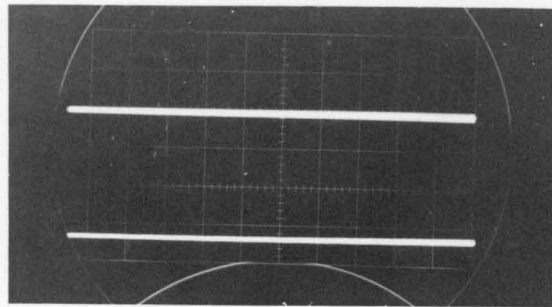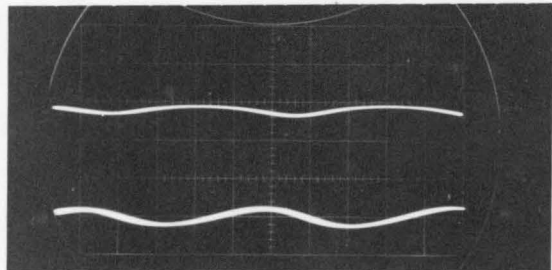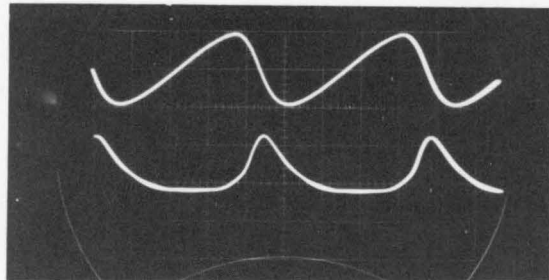
FIGURE 4-3   EXPERIMENTAL SETUP FOR THE TIME DISPLAY OF THE CURRENT

AND VOLTAGE WAVEFORMS OF A LASER DISCHARGE

(a) I = 5·2 ma.

(b) I = 5·5 ma.

(c) I = 10·5 ma.
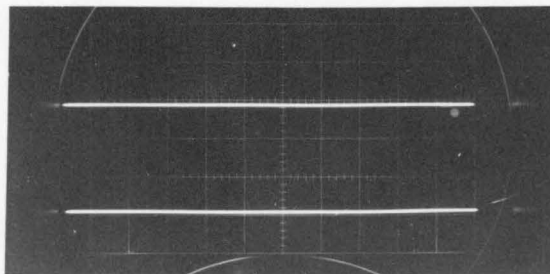
(d) I = 12 ma.

FIGURE 4-4 VOLTAGE AND CURRENT WAVEFORMS OF
MOVING STRIATIONS IN A LASER AMPLIFIER
UPPER TRACE: VOLTAGE WAVEFORM AT 40V/cm
LOWER TRACE: CURRENT WAVEFORM AT 4·5 ma/cm
HORIZONTAL TIME BASE: 2μs/cm.

ion frequency) at this stage. When the discharge current is increased

further, Fig. 4-4(c) shows that the current waveform increases in amp-

litude and nonlinearity. This means that the amplitude of the oscillat-

ion in the discharge current is large such that the values of the equi-

valent circuit elements fluctuate in time and cause significant non-

linearity in the waveforms. However, at a discharge current greater

than 12 ma, the waveforms disappear again as Fig. 4-4(d) shows.

4.4 Frequency Display of Moving Striations in a Laser Discharge

Fig. 4-5 shows the experimental setup used to make the meas-

urements on the striation frequency that will be presented in later

sections of this chapter. The laser tube of Fig. 4-1 is connected to a

current-regulated laser power supply through a 60 kilohms noninductive

current-limiting resistor with 60 watts power rating. The heated cath-

ode carries a current of 4.1 amperes (corresponding to a filament temp-

erature of about 850°C) from a dc filament supply. The discharge current

of the laser discharge in the presence of moving striations is detected

by a current probe (Tektronix P6019). The ac signal is amplified twice

(Tektronix Type 134 and 1121 Amplifiers) before it is fed into a wave

analyzer (Hewlett-Packard 310A). As the narrow bandpass filter of the

wave analyzer is scanned over a wide frequency range, the striation fre-

quency is the frequency at which the ac amplitude has a maximum (i.e.,

an amplitude spike). Alternately, the output from the wave analyzer

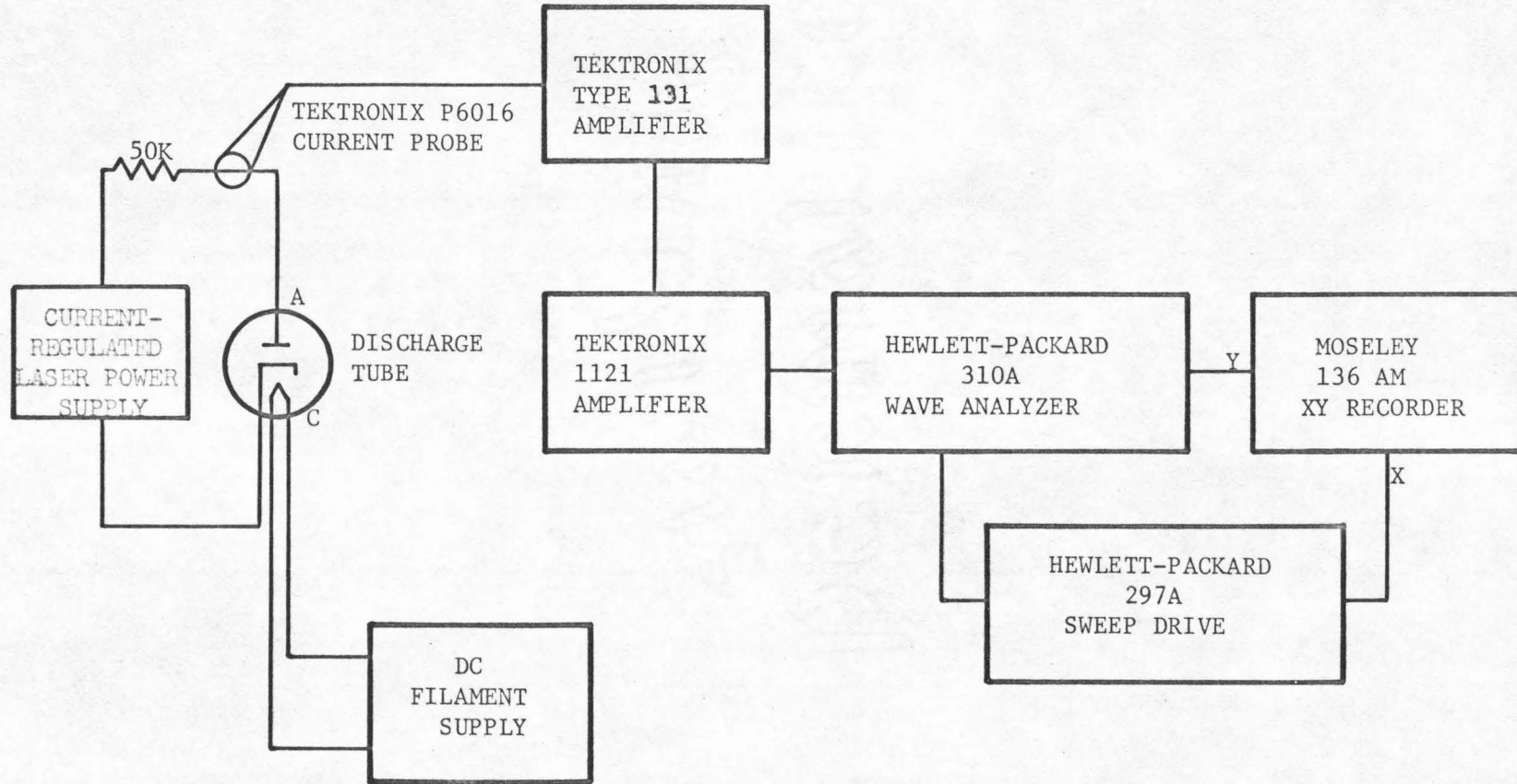can be connected to the input of an x-y recorder (Moseley 136 AM). With

FIGURE 4-5 EXPERIMENTAL SETUP FOR THE FREQUENCY DISPLAY OF THE DISCHARGE
CURRENT OF A LASER DISCHARGE

the aid of a sweep drive (Hewlett-Packard 297A), the frequency spectrum

of moving striations can be plotted on the x-y recorder. A typical dis-

play of the frequency spectrum is given in Fig. 4-6. The amplitude

spikes at the striation frequency and its harmonics are very narrow.

Hence, the striation frequency can be obtained quite accurately. How-

ever, it is observed to shift within a short duration after the laser

discharge has been turned on. This shift in the striation frequency

occurs because the internal parameters of a discharge are changing to

their equilibrium conditions when the tube is warming up. During this

warmup period (of the order of two minutes), no measurement on the

striation frequency should be made.

4.5 Dependence of the Striation Frequency on the Discharge Current

One of the objectives of this chapter is to show that the

equivalent circuit of Chapter 3 (which is redrawn in Fig. 4-1 for in-

ternal disturbances) is a valid representation of a laser discharge

in understanding the moving striations when they are present in the

positive column. Due to its particular tube structure and electrode

configuration, the discharge tube which has been used to obtain the

experimental data on the equivalent circuit elements in Chapter 3 does

not have self-excited moving striations under laser operating condi-

tions. Hence it is necessary to obtain measurements on the moving

striations from a different discharge tube: the laser discharge tube

described in Section 4.3. Since the two tubes are quite different in

their structures, configurations and electrodes, it cannot be expect-
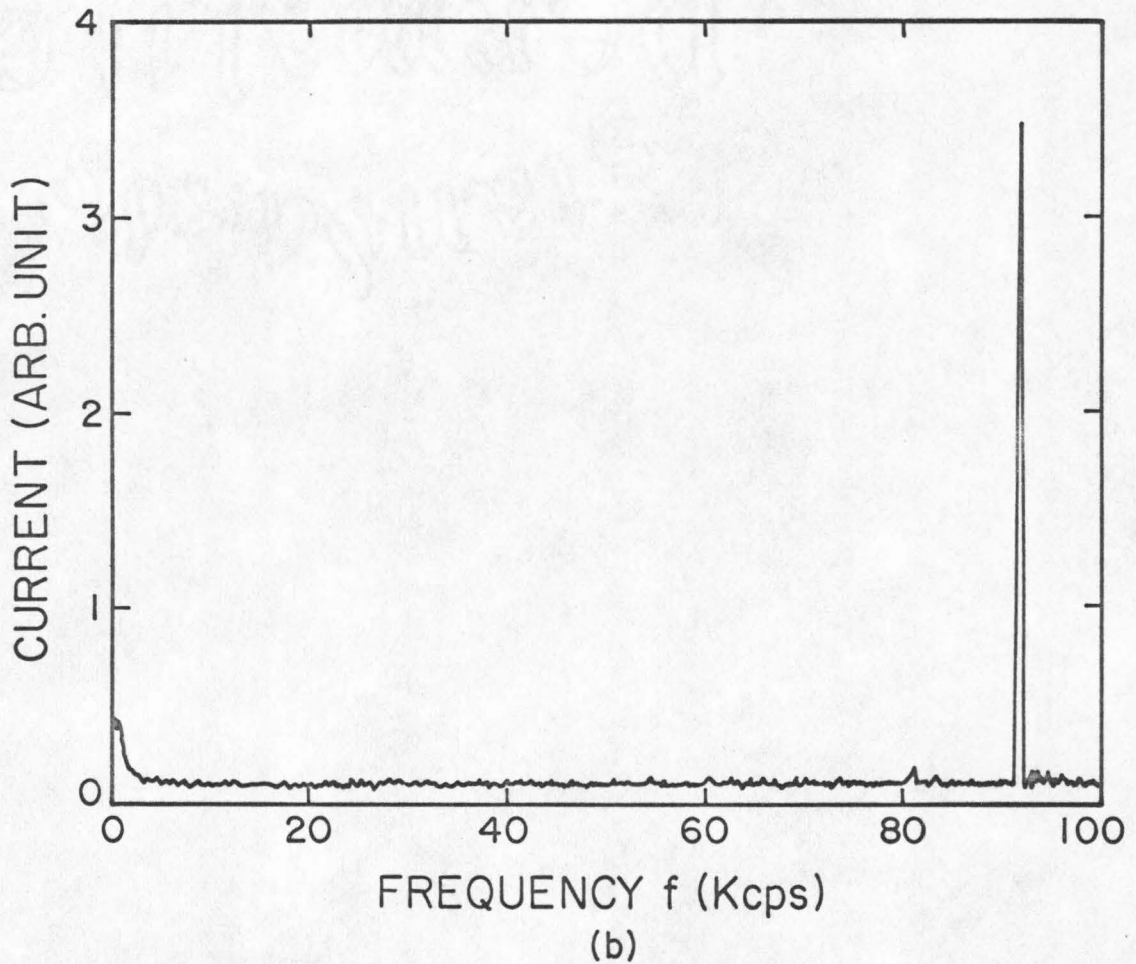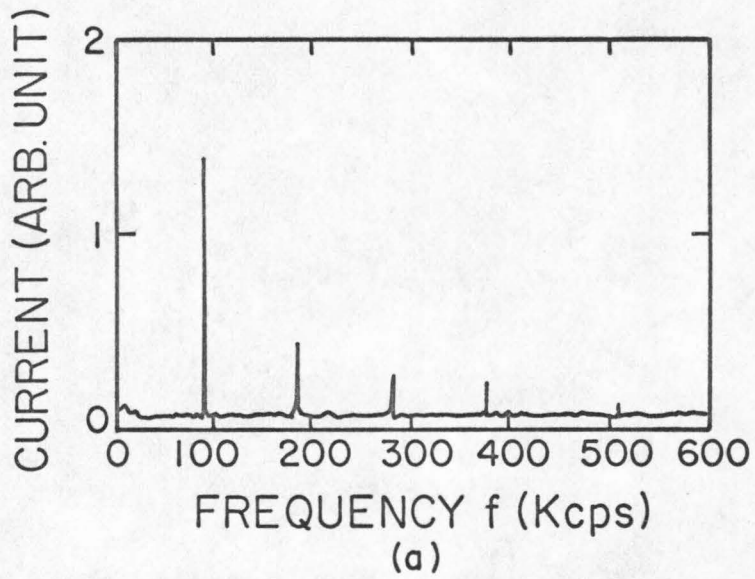
FIGURE 4-6 TYPICAL DISPLAYS OF THE FREQUENCY SPECTRUM
OF THE DISCHARGE CURRENT WHEN MOVING
STRIATIONS EXIST IN A LASER AMPLIFIER

ed that the values of the equivalent circuit elements presented in
Chapter 3 should yield the exact quantitative value of the striation
frequency. The striation frequency can be estimated only in its order
of magnitude. However, as stated in Chapter 3, the dependence of the
equivalent circuit elements on various discharge parameters should be
adaptable to most discharges. Hence a good indication on how well the
equivalent circuit is applicable to understanding the striation phe-
nomenon in a laser discharge can be obtained by predicting the depend-
ence of the striation frequency on a discharge parameter (using the
experimental data of Chapter 3) and comparing it to the experimental
measurements on the striation frequency. The discharge current is
chosen to be the discharge parameter for the above comparison since the
values of both the equivalent inductance and the equivalent capacitance
are strongly dependent on it.

Sections 3.4.2 and 3.5 show that the equivalent inductance
L and the equivalent capacitance C of a laser discharge at a dc
discharge current I can be written approximately as

$$L = \frac{L_o \, I_o}{I}$$

$$C = \frac{C_o (I_o + I_C)}{I + I_C} \tag{4-1}$$

where L_o and C_o are the values of the equivalent inductance and
capacitance at a fixed discharge current I_o, and I_C is a constant
current. Using these expressions of L and C, the resonant frequency

f   of the equivalent circuit of Fig. 4-1 can be expressed as

$$f = f_o \sqrt{\left[1 + \frac{(I - I_o)C'}{(C_o + C')(I_o + I_C)}\right]\left(\frac{I}{I_o}\right)} \qquad (4\text{-}2)$$

where f_o is the resonant frequency of the equivalent circuit at the
discharge current I_o and C' is the parallel capacitance in the cir-
cuit whose value is independent of the discharge current. Equation (4-2)
gives the expected dependence of the striation frequency on the dis-
charge current.

The experimental curve of Fig. 4-7 describes the measured
striation frequency as a function of the discharge current. The mea-
surements are made in the manner described in Section 4.4. The theo-
rectical curve of Fig. 4-7 is obtained from equation (4-2) with a rea-
sonable set of parameters: $C' = 1.2\ C_o$, $I_o = 4.64$ ma, $I_C = 6$ ma and
$f_o = 81.8$ kHz. It should be noted that, as expected, the dependence of the
striation frequency on the discharge current does not depend on the exact
values of L_o and C_o. The good agreement between the two curves in
Fig. 4-7 shows that the increase in the striation frequency with in-
creasing discharge current can be attributed to the corresponding de-
creases in the values of the equivalent inductance and the equivalent
capacitance of the laser discharge.
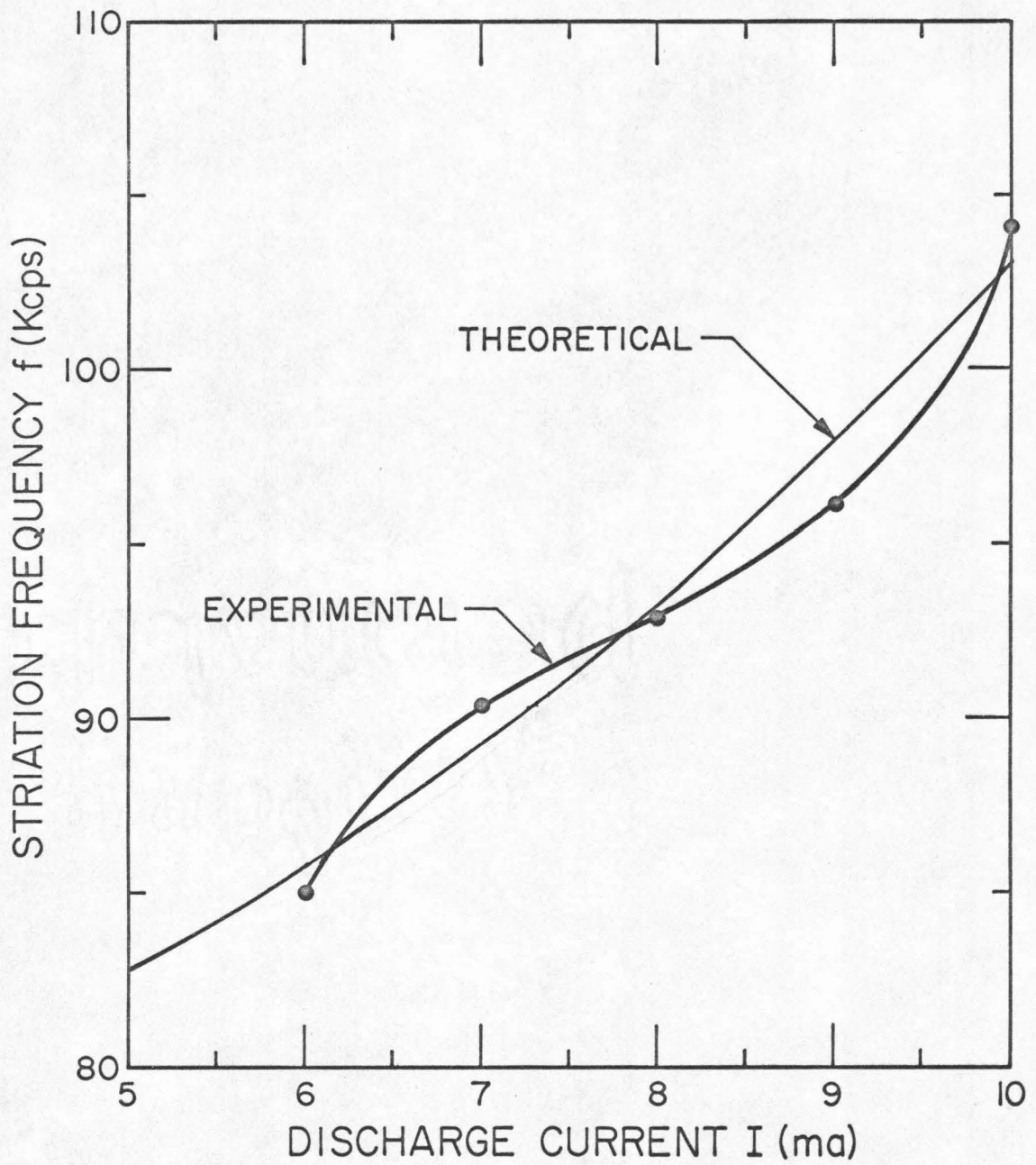
FIGURE 4-7 STRIATION FREQUENCY FOR VARIOUS DISCHARGE CURRENT

4.6 Effect of an External Longitudinal Magnetic Field on the Striation

     Frequency and the Equivalent Inductance

     A longitudinal magnetic field is applied to a portion of
the positive column of the discharge. This is accomplished by connecting
two solenoidal magnets in such a way that their magnetic fluxes flow in
the same direction (see Fig. 4-8). The magnet is made by rolling an
aluminum sheet interwovenly with a teflon sheet which is used for in-
sulation purposes. Each solenoid is 15.2 cm long and has an inner dia-
meter of 3.2 cm. A longitudinal magnetic field exists inside the sole-
noid when a dc current flows through the aluminum sheet. The direction
of the magnetic field can be reversed by reversing the current flow
through the aluminum sheet. A magnetic field of 391 gauss is measured
at the center of a solenoid when a dc current of 10 amperes passes
through the aluminum sheet. The magnetic field is quite uniform over
the cross-sectional area of the inner tube; its intensity varies by
about one per cent over the area. Hence it is not necessary that the
laser discharge tube and the solenoidal magnet are exactly coaxial.
There is, however, considerable drop in the intensity of the magnetic
field near the edges and outside of the magnet. Its value is at
a maximum in the center of the solenoid and decreases to half of the
maximum value at the edge. The center of the two solenoids connected
in series is approximately equidistant from the anode and the cathode.
Thus both electrodes are about 16 cm from the edges of the magnet. From
the discussion of the previous paragraph it can be seen that the long-
itudinal magnetic field in this experiment only effects the positive
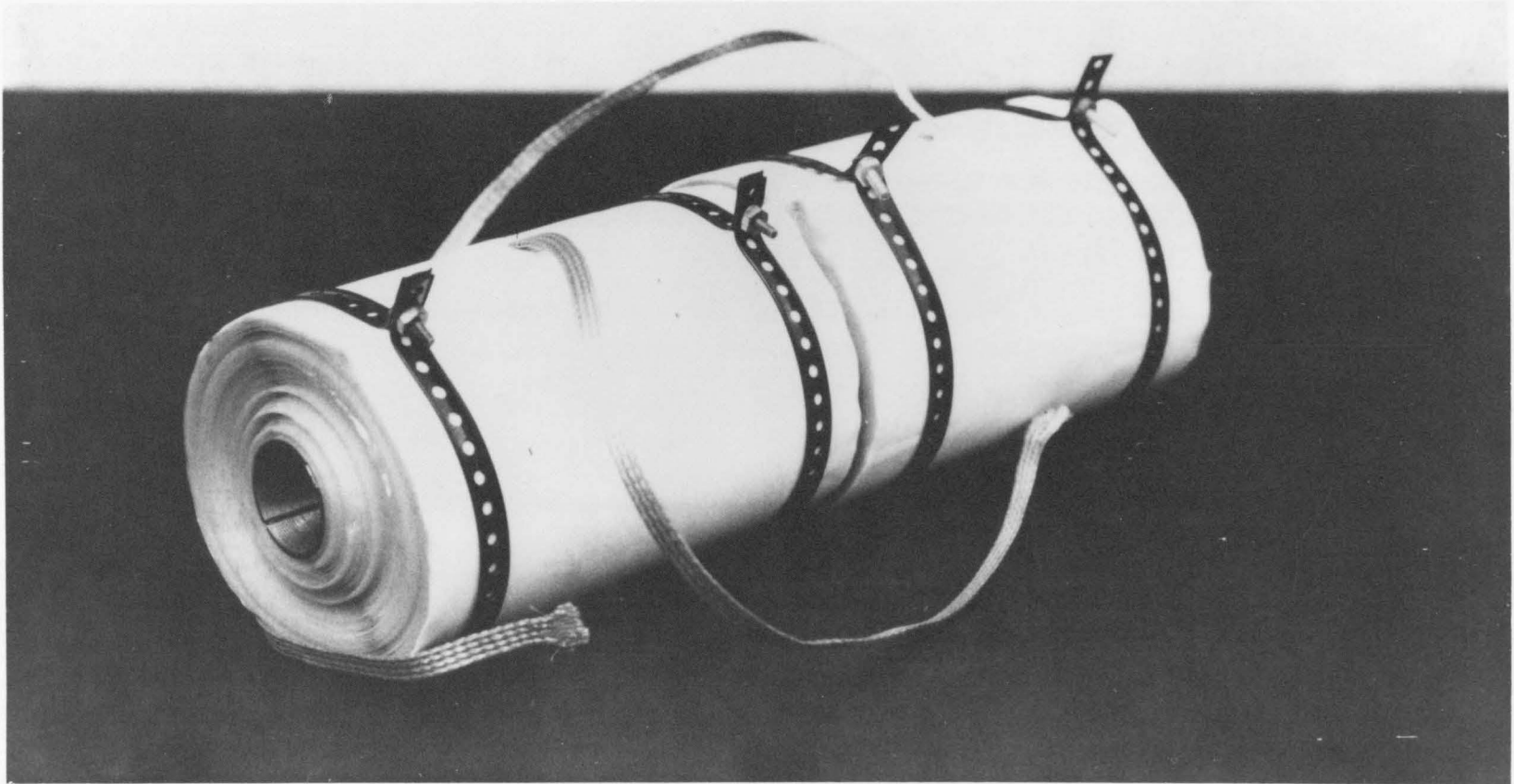
FIGURE 4-8   SOLENOIDAL MAGNET

column; it has negligible effect on the other regions of the laser dis-
charge. The experimental data of Chapter 3 suggest that the equivalent

inductance of a discharge is predominantly due to the positive column

while the equivalent capacitance comes mainly from the other regions

in the discharge (see the discussion in Section 3.6). Hence, it can be

expected that the longitudinal magnetic field in this experiment only

influences the equivalent inductance of the laser discharge, and not

its equivalent capacitance.

Fig. 4-9 shows the experimental values of the striation fre-

quency for various intensities of the longitudinal magnetic field at

four different discharge currents. The striation is again measured in

the manner described in Section 4.4. B_o is the maximum value of the

intensity of the longitudinal magnetic field along the axis of the

solenoids. The direction of B_o does not effect the striation fre-

quency. In other words, curves similar to the ones in Fig. 4-9 would

have been obtained had the direction of the longitudinal mangetic field

been reversed. Fig. 4-9 shows that the striation frequency generally

increases for increasing magnetic field. It increases by approximately

1.1 per cent for an incremental increase in B_o of 100 gauss. Since

the equivalent capacitance of the laser discharge is not effected by

the magnetic field in this experiment, the increase in the striation

frequency implies that the equivalent inductance decreases by about

2.2 per cent for the same amount of increase in B_o It should again be

emphasized that the quantities only have order of magnitude significance.

The intent of this section is to show the behaviors of the striations
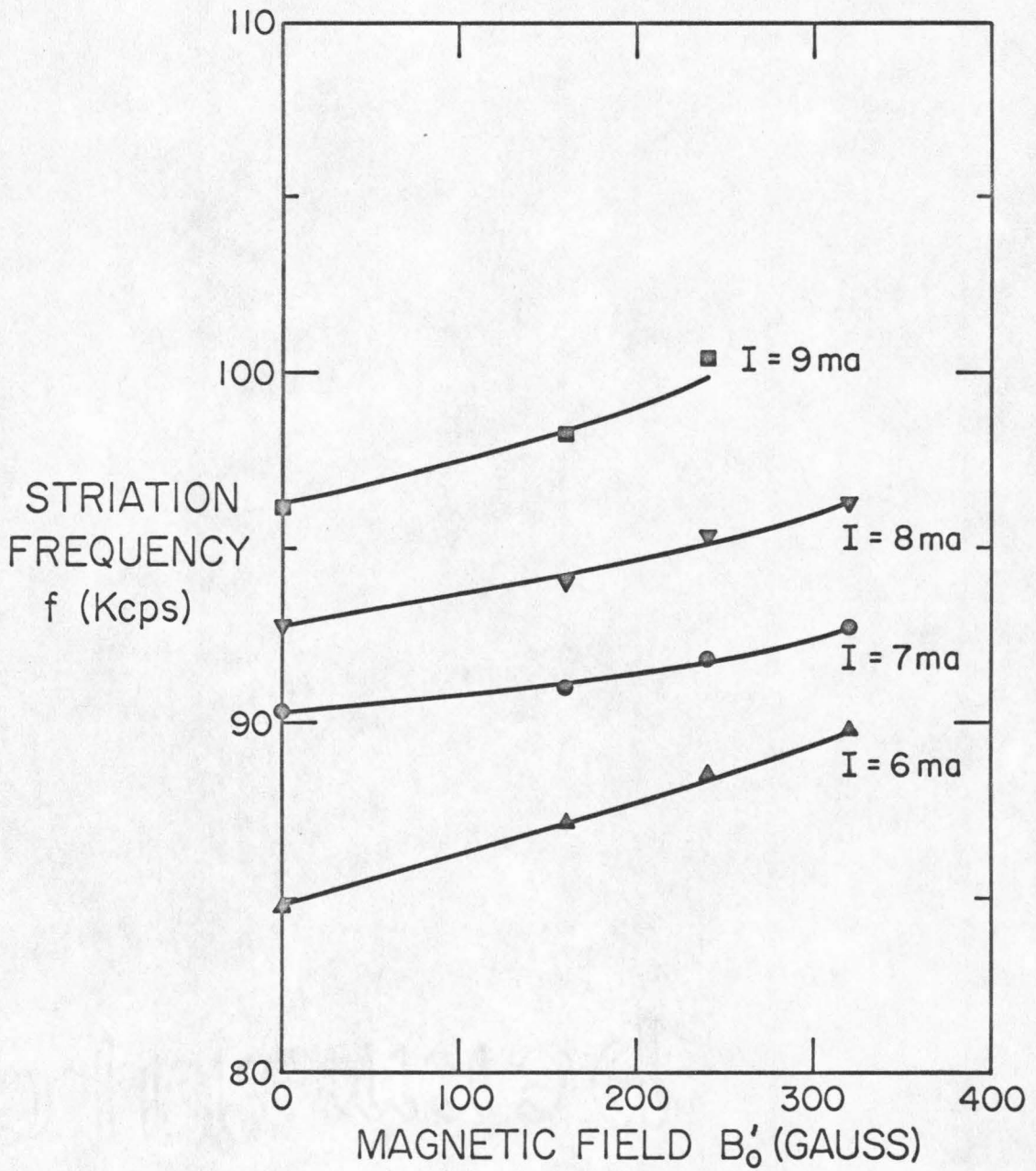
FIGURE 4-9 STRIATION FREQUENCY FOR VARIOUS
MAGNETIC FIELD STRENGTHS

frequency and the equivalent inductance of a laser discharge in the
presence of a longitudinal magnetic field. The magnetic field causes
an increase in the striation frequency and a corresponding decrease in
the equivalent inductance. The exact quantities are only applicable to
the particular laser discharge and magnetic field described in this
chapter.

4.7 Summary and Discussion

This chapter presents the experimental work on the moving
striations that exist naturally in laser discharges. It describes the
voltage and current waveforms due to moving striations and presents
measurements on the striation frequency. The discharge current is
chosen to be the discharge parameter to demonstrate the applicability
of the equivalent circuit of Chapter 3 to understanding the striation
phenomenon. The experimental results of Chapter 3 are used to predict
successfully the dependence of the striation frequency on the discharge.
The validity of the circuit can be shown through other discharge para-
meters as well. Weber (32) has shown that the striation frequency
decreases for decreasing gas pressure. This behavior of the striation
frequency can be predicted from the experimental data of Chapter 3 which
show that the equivalent inductance increases for increasing gas
pressure while the equivalent capacitance remains constant. Finally the
experimental effect of a longitudinal magnetic field on the striation
frequency is presented. The magnetic field covers a portion of the
positive column. It increases the striation frequency. This suggests

that the equivalent inductance of a laser discharge is decreased

when a longitudinal magnetic field is present.

CHAPTER FIVE

SUMMARY AND CONCLUSION

5.1 Summary

The light output from a laser oscillator contains noise from the discharge. Since gas lasers are characterized by an extreme monochromaticity, it is important to study the discharge noise and its effect on the laser light output. Chapter 2 considers a spatially fluctuating wave in the dielectric permittivity of the laser medium which travels along the axis of the medium. It causes the frequency of the laser output to be modulated at the frequency of the fluctuations. A frequency spectrum of the laser output shows a FM spectrum centered at the optical frequency. When the output of the laser consists of two optical frequencies, the intensity of the light output also shows a FM spectrum centered at the difference frequency between the two optical frequencies. In practice, the spatial fluctuation in the dielectric permittivity of the laser medium can be traced to a spatial variation in the population inversion which, in turn, corresponds to a fluctuation in the electron density of the medium. Since moving striations can be characterized by a traveling wave in the electron density along the positive column of the laser discharge, the analysis in Section 2.3.2 corresponds to the case in which moving striations are present in the laser discharge.

One approach to understanding the internal oscillations in

a laser discharge such as moving striations comes from analyzing its
equivalent circuit. An appropriate ac equivalent circuit of a laser
discharge tube has been presented and discussed in Chapter 3. It
has been obtained from the current response of the laser discharge to
an external ac voltage modulation and is a valid representation of the
discharge tube over the frequency range from a few kilihertz to a few
hundred kilihertz. It consists of a capacitance C' in parallel with
a series ρLC circuit. From a consideration of the current response
of the discharge tube to the same ac voltage modulation with the
discharge extinguished, it has been concluded that the parallel capaci-
tance C' is the capacitance between the electrodes of the discharge tube
and between the stray wirings while the series ρLC circuit represents
the discharge region.

Experimental data on the equivalent inductance and capacitance
have been presented in Chapter 3 for discharges in helium, neon, xenon and
helium-xenon. Measurements have been made of the striation frequency,
from which the values of L and C have been calculated (see Section 3.3),
including current, pressure and length of positive column variations.
The length of the positive column varies from about 15 to 60 cm. The
discharge current varies from 1 to 5 ma for helium, 3 to 6 ma for neon
and 0.4 to 0.7 ma for xenon. The helium gas pressure varies from 0.5
to 1.1 torr. The resulting equivalent inductance ranges from 25 to
150 mh for helium, 20 to 70 mh for neon and 0.2 to 1.5 henries for
xenon. The equivalent capacitance for a helium discharge varies over
the range from 7.5 to 15 pf. Of particular interest are the experimental

data on the equivalent inductance and capacitance for various lengths of the positive column (Figs. 3-7 and 3-10). These data show that the equivalent inductance comes mainly from the positive column of the laser discharge while the equivalent capacitance is due to the discharge regions other than the positive column (such as the negative glow, the cathode fall and the anode fall regions).

Naturally- existing moving striations in a laser discharge have been described in Chapter 4. The striation frequency has been experimentally measured. From an analysis of the equivalent circuit (Appendix 2) and the experimental data on the equivalent circuit elements (Chapter 3), the dependence of the striation frequency on the discharge current has been predicted. This predicted dependence agrees very well with the experimental data (Fig. 4-7). The agreement demonstrates the applicability of the equivalent circuit to analyzing moving striations and other internal noises in the laser discharge. Finally, the striation frequency has been measured in the presence of a longitudinal magnetic field which covers a part of the positive column. The increase in the striation frequency is attributed to a decrease in the equivalent inductance when the magnetic field is present.

5.2 Conclusion

The above findings lay the ground work to a good understanding of a laser discharge through its equivalent circuit. The equivalent circuit is simple enough so that its elements can be readily measured. However, it is an adequate representation of the laser dis-

charge in the frequency region of interest. Appendices 1 and 2 show analytically that it can be used to analyze the response of the laser discharge to both external and internal disturbances. Sections 3.2 and 4.5 lend experimental support to the above concept. The equivalent circuit approach to internal noises in a laser discharge is successful in solving some of the problems that have hindered the conventional approach. It successfully explains the nonlinear waveform of the discharge current due to moving striations and adequately represents any internal disturbance by a series voltage element regardless of the source mechanism. Further work on the equivalent circuit should give the relevant properties of the laser discharge that can be obtained from treating the laser discharge as a black box. The equivalent circuit can be applied for practical uses. Full knowledge of the equivalent circuit elements should help in designing laser tubes and electrode configurations such that moving striations and other discharge noises are diminished or absent under laser operating conditions. The equivalent circuit can also be used in the ac analysis of a system in which the laser discharge is a component.

The experimental conclusion of Chapter 3 that the positive column of a laser discharge is predominantly inductive rather than capacitive may have a special significance. It implies that the positive column can be expressed by the following equation:

$$L \frac{d(I-I_o)}{dt} + R(I-I_o) = V \qquad (5-1)$$

where R is the ac resistance of the positive column and V is the
voltage source corresponding to the internal disturbances. From the
discussion in Section 3.4.2, the discharge current is proportional to
the electron density of the positive column in a weakly-ionized low
pressure laser discharge. Therefore the quantity $(I-I_o)$ in equation
(5-1) corresponds to the perturbation of the electron density in the
positive column from its equilibrium value. With further work it
may be possible to link equation (5-1) to the conservation equation
for the electron density. This should be a very significant step
since it would link the equivalent circuit to the particle and energy
conservation equations and make possible the expression of the equiva-
lent circuit elements in terms of the discharge parameters such as the
ionization rate, the recombination rate and the electron-neutral atom
collision rate on which much work has already been done. However, even
without the two approaches being linked, they complement each other
by providing different insights to the problem. Each approach may be
preferred over the other in understanding certain aspects of the laser
discharge.

APPENDIX ONE

ANALYSIS OF THE AC EQUIVALENT CIRCUIT OF A LASER DISCHARGE

I. EXTERNAL SOURCE

This appendix presents a derivation of the resonant frequency
of the equivalent circuit of a laser discharge tube with an external ac
voltage source. It shows that the resonant frequency deviates from the
quantity $(1/2\pi\sqrt{LC})$ by a few percentages, where L and C are the
equivalent inductance and capacitance of the discharge. This deviation
constitutes an error in the values of the equivalent circuit elements
in Chapter 3 which are calculated from the measured values of the re-
sonant frequencies of the laser discharge tube under various discharge
conditions. However, this error is relatively unimportant since, as
stated in Chapter 3, the exact quantitative values of the circuit ele-
ments only have order of magnitude significance. The result of this
appendix is checked against and agrees with that from a computer cal-
culation.

A1.1 Resonant Frequency of the Series ρLC Circuit
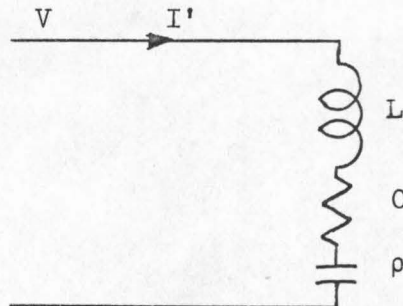
FIGURE A1-1 SERIES ρLC CIRCUIT

As the first step, consider the circuit of Fig. A1-1 which is the equivalent circuit of a laser discharge tube (Fig. 3-2) without the parallel capacitance C'. The circuit represents the discharge region of the laser discharge tube. Its resonant frequency can be found exactly.

Consider that the circuit in Fig. A1-1 is modulated by an ac voltage source of constant amplitude and varying frequency. As discussed in Section 3.2, the current response of the circuit, as a function of frequency, is directly proportional to the admittance function of the circuit given by

$$Y'(j\omega) = \frac{1}{\rho + j(\omega L - \frac{1}{\omega C})} \qquad (A1-1)$$

where ω is the angular frequency. The magnitude of the admittance function is

$$|Y'(j\omega)| = \frac{1}{\sqrt{\rho^2 + (\omega L - \frac{1}{\omega C})^2}} . \qquad (A1-2)$$

The amplitude of the current response is different from the expression in equation (A1-2) only by a constant multiplier. Thus both the amplitude of the current response and the magnitude of the admittance function have local maxima at the resonant angular frequency ω_o which is con-

tained in the condition

$$\frac{d|Y'(j\omega)|}{d\omega}\Bigg|_{\omega = \omega_o} = 0 \qquad\qquad (A1-3)$$

Substituting equation (A1-2) into equation (A1-3), an expression of ω_o can be obtained,

$$\omega_o = \frac{1}{\sqrt{LC}} . \qquad\qquad (A1-4)$$

Equation (A1-4) gives the resonant angular frequency of the series ρLC circuit of Fig. A1-1. The resonant frequency does not depend on the value of ρ, but only on the values of L and C.

A1.2 Resonant Frequency of the Equivalent Circuit
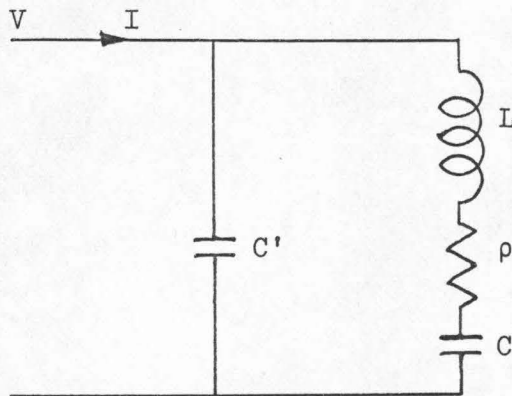
FIGURE A1-2 AC EQUIVALENT CIRCUIT OF A LASER DISCHARGE

The ac equivalent circuit of Fig. 3-2 is redrawn in Fig. A1-2. Again, since the voltage source has a constant amplitude as its frequency is varied, the current response, as a function of frequency, corresponds to the admittance function of the circuit which is given by

$$Y(j\omega) = \frac{1 + \dfrac{C'}{C} - \omega^2 LC' + j\omega C'\rho}{\rho + j\omega L \left(1 - \dfrac{1}{\omega^2 LC}\right)} \quad . \tag{A1-5}$$

Making the following substitutions, in which k, ω' and b are dimensionless quantities,

$$k = \frac{C'}{C}$$

$$\omega_o = \frac{1}{\sqrt{LC}}$$

$$\tag{A1-6}$$

$$\omega' = \frac{\omega}{\omega_o}$$

$$b = \omega_o^2 C'^2 \rho^2 \quad ,$$

the magnitude of the admittance function can be expressed as

$$|Y(j\omega)| = \sqrt{\omega_o^2 C^2 \frac{\left[1 + k(1 - \omega'^2)^2 + b\omega'^2\right]}{\frac{b}{k^2} + (\omega' - \frac{1}{\omega'})^2}} \qquad (A1-7)$$

The resonant frequency of the circuit corresponds to the frequency at which the amplitude of the current response and the magnitude of the admittance function have their local maxima. It can be obtained from the following condition

$$\left. \frac{d|Y(j\omega')|}{d\omega'} \right|_{\omega' = \omega_o'} = 0 \qquad (A1-8)$$

where ω_o' is the normalized resonant angular frequency. The resonant angular frequency is the quantity $(\omega_o \omega_o')$. Combining equations (A1-7) and (A1-8), the resonant condition of equation (A1-8) can be restated as

$$[b - 2k\{1 + k(1-\omega_o'^2)\}][\frac{b}{k^2} + \omega_o'^2(1 - \frac{1}{\omega_o'^2})^2]$$

$$-(1 - \frac{1}{\omega_o'^4})[\{1 + k(1 - \omega_o'^2)\}^2 + b\omega_o'^2] = 0 \qquad (A1-9)$$

It would be quite difficult to obtain an exact analytic expression of ω_o' from equation (A1-9). However, a computer calculation of equation

(Al-7) using the values of the equivalent circuit elements from Section 3.2 shows that the resonant angular frequency of the equivalent circuit is smaller than the quantity ω_0 by only a few percentages. In other words, ω_0' is very close to unity. With this in mind, an expression for the resonant angular frequency can be obtained from equation (Al-9) by an approximation method. Express ω_0' as

$$\omega_0' = 1 + \Delta \quad \text{with} \quad \Delta \ll 1 \tag{Al-10}$$

The quantity Δ may be positive or negative, so long as its magnitude is small compared with unity. Substituting equation (Al-10) into equation (Al-9) and neglecting the terms higher than the third order in Δ,

$$(4k + 4b + 5)\Delta^2 - 2\Delta - \frac{b}{k}(1 - \frac{b}{2k}) = 0. \tag{Al-11}$$

Equation (Al-11) gives two values of Δ; one is positive and the other is negative. An indication of the correct value of Δ can be obtained by solving equation (Al-11) for Δ to the first approximation. Neglecting the second order term in Δ, equation (Al-11) gives

$$\Delta \simeq - \frac{b}{2k}(1 - \frac{b}{2k}) . \tag{Al-12}$$

Since the quantity b is typically quite small compared with unity while k is normally greater than unity, Δ is negative. The exact

solution of equation (A1-11) is

$$\Delta = \frac{1 - \sqrt{1 + \frac{b}{k}(1 - \frac{b}{2k})(4k + 4b + 5)}}{4k + 4b + 5} \qquad (A1-13)$$

Finally the resonant angular frequency of the equivalent circuit of a laser discharge (Fig. A1-2) is $(\omega_o \omega_o')$, given by

$$\omega_o \omega_o' = \frac{1}{\sqrt{LC}} \left(1 + \frac{1 - \sqrt{1 + \frac{b}{k}(1 - \frac{b}{2k})(4k + 4b + 5)}}{4k + 4b + 5} \right) \qquad (A1-14)$$

Using the values of the equivalent circuit elements present-ed in Section 3.2 (which are appropriate for the current response curve of Fig. 3-1), Δ of $(- .1215)$ can be calculated from equation (A1-13). This is slightly larger in magnitude than the computer calculation which shows that the resonant frequency of the complete equivalent circuit of the laser discharge is about 10 per cent lower than the resonant fre-quency of the circuit without the parallel capacitance C'. However, a third order term in equation (A1-11) corrects the value of Δ to be $(- .097)$. It can be seen from equation (A1-13) that the magnitude of Δ decreases for decreasing value in b which, in turn, depends on the square of the resonant angular frequency (equation (A1-6)). The resonant frequency of about 300 kHz used in the above calculation of Δ is quite large compared with most of the resonant frequencies from

which the experimental data of Chapter 3 are obtained. Therefore the
above value of Δ is close to the maximum shift in the resonant angular
frequency (from ω_o) encountered in the experiment.

APPENDIX TWO

ANALYSIS OF THE AC EQUIVALENT CIRCUIT OF A LASER DISCHARGE

II. INTERNAL SOURCE

This appendix analyses the equivalent circuit of a laser dis-
charge tube with only its internal disturbance. The circuit (Fig. 4-1)
has been discussed qualitatively to a great extent in Section 4.2; it
is treated analytically here. This appendix contains three sections.
The first section derives the resonant angular frequency for the equi-
valent circuit. The second section shows that the laser discharge has
oscillations if there is either a strong internal source or a negative
resistance (or both). The third section shows that the dependence of the
equivalent circuit elements on the discharge current introduces non-
linearity into the current waveform. The discharge current contains
components at the fundamental resonant frequency of the equivalent cir-
cuit as well as its harmonics. The analysis in this appendix is appli-
cable to the striation phenomenon and other low frequency disturbances
in a laser discharge.

A2.1 Resonant Frequency of the Equivalent Circuit
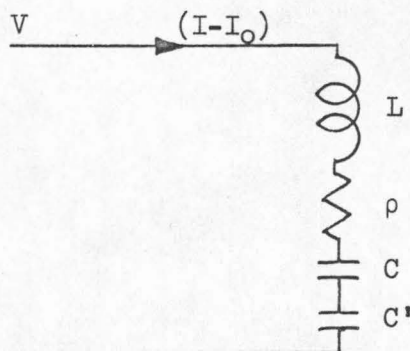
FIGURE A2-1 AC EQUIVALENT CIRCUIT OF A LASER DISCHARGE WITH AN
INTERNAL SOURCE

The equivalent circuit of Fig. 4-1 is redrawn in Fig. A2-1 and will be used throughout this appendix. The capacitance C' always has a constant value. However, L, ρ anc C only assume constant values in the linear analyses of the first two sections. They are dependent on the discharge current in the nonlinear analysis of the third section. It should be noted that I is the total discharge current while I_o is its dc component. V is the ac voltage source which represents the internal disturbances of the laser discharge. This convention will be used throughout this appendix.

The admittance function Y and its magnitude $|Y|$ of the circuit in Fig. A2-1 can be written as

$$Y(j\omega) = \frac{1}{\rho + j(\omega L - \frac{1}{\omega}(\frac{1}{C} + \frac{1}{C'}))} \tag{A2-1}$$

and

$$|Y(j\omega)| = \frac{1}{\sqrt{\rho^2 + (\omega L - \frac{1}{\omega}(\frac{1}{C} + \frac{1}{C'}))^2}} \tag{A2-2}$$

Assuming that the ac voltage contains components of equal aplitudes in a wide range of frequency, the resonant frequency of the circuit is the frequency at which the current response has the largest amplitude. Following the same line of resoning as in Appendix 1, this is also the frequency at which the magnitude of the admittance function is at a local

maximum. Hence the resonant condition can be expressed as

$$\frac{d}{d\omega}\left|Y(j\omega)\right|_{\omega=\omega_o} = 0 \tag{A2-3}$$

where ω_o is the resonant angular frequency of the equivalent circuit. Substituting the expression of $\left|Y\right|$ in equation (A2-2) into equation (A2-3), the resonant angular frequency is obtained

$$\omega_o = \sqrt{\frac{C + C'}{LCC'}} \tag{A2-4}$$

If the internal voltage source contains components in a range of frequency, the component at ω_o induces the greatest current response from the discharge tube.

A2-2 Linear Analysis

Assuming that the internal disturbance in a laser discharge contains many components over a wide range of frequency, the voltage loop of the ac equivalent circuit of Fig. A2-1 is described by the following equation:

$$L \frac{d(I-I_o)}{dt} + \rho(I-I_o) + (\frac{1}{C} + \frac{1}{C'})\int_{-\infty}^{t} (I-I_o)dt' = \sum_{n=1}^{\infty} V_n e^{j\omega_n t} \tag{A2-5}$$

where $(I-I_o)$ is the ac component of the discharge current and I_o is the dc component. The summation on the right side of equation (A2-5) re-

presents the internal source; in general, V_n's have small amplitudes.
In this linear analysis, the equivalent circuit elements L, ρ, C and C'
all have constant values. The convention of using the positive
exponential ($e^{j\omega t}$) to describe an oscillatory function will be used
throughout this appendix.

In the linear analysis, the total current response to the volt-
age source is the sum of all the current responses to each of the fre-
quency components of the voltage source. Thus the particular solution
of equation (A2-5) can be expressed as

$$(I-I_o)_p = \sum_{n=1}^{\infty} \frac{V_n}{\rho^2 + (\omega_n L - \frac{1}{\omega_n}(\frac{1}{C} + \frac{1}{C'}))^2} e^{j(\omega_n t - Tan^{-1}[\frac{1}{\rho}(\omega_n L - \frac{1}{\omega_n}(\frac{1}{C} + \frac{1}{C'}))])}$$

(A2-6)

Equation (A2-6) describes the steady state current response of the laser
discharge to an internal continuous disturbance. It shows that the
amplitude of the current response would be the largest at the resonant
angular frequency ω_o (i.e., $\omega_n = \omega_o$) which has been defined by Equa-
tion (A2-4). The amplitude at ω_o can be increased further by de-
creasing the value of ρ or by increasing the amplitude of the volt-
age source which corresponds to the continuous internal disturbances
in a laser discharge.

The homogeneous solution to equation (A2-5) can be obtained
by inserting a solution $(I-I_o) = A_1 e^{-\alpha t} e^{j\omega t}$ into the reduced equation
with no source term. Equating the real and imaginery portions of the

equation separately, the following homogeneous solution is obtained:

$$(I-I_o)_h = A_1 \, e^{-\frac{\rho}{2L} t} \, e^{j\omega_o t} \tag{A2-9}$$

where ω_o is defined by equation (A2-4). Equation (A2-9) shows a damped function when ρ has a positive value. Any instantaneous disturbance is readily damped out. However, when ρ is negative, equation (A2-7) shows a temporally growing oscillation at the resonant angular frequency. Any disturbance at ω_o which may exist only for an instant can trigger this growing oscillation.

The current response of the laser discharge is the sum of the particular and the homogeneous solutions to equation (A2-5); i.e.,

$$(I - I_o) = (I - I_o)_p + (I - I_o)_h \tag{A2-8}$$

However, one solution often dominates over the other. For positive ρ, the particular solution of equation (A2-6) predominates. Any instantaneous disturbance quickly dies out; only the response to the continuous disturbances prevails. For negative ρ, on the other hand, the homogeneous solution of equation (A2-7) predominates. Any instantaneous disturbance at ω_o can trigger a growing oscillation. The amplitude of this oscillation soon becomes much larger than that of the current response to the continuous voltage source of oscillations of generally small amplitudes (the particular solution).

The above analysis is applicable to moving striations and other

low frequency noises in the laser discharge. A laser discharge contains noise sources over a large frequency range. If ρ is positive, moving striations are absent and the only sustained oscillations in the laser discharge are due to the continuous internal disturbances. When ρ is negative, the homogeneous solution of equation (A2-7) predominates. Thus moving striations are induced at the resonant frequency of the equivalent circuit of Fig. A2-1 by any small instantaneous disturbance (which is readily available in a laser discharge). The amplitude of the moving striations increases until the gain is saturated.

A2.3 Nonlinear Analysis

Section A2.2 demonstrates that for negative ρ the discharge current has a growing oscillation at the resonant angular frequency ω_o. The experimental data of Chapter 3 show that the equivalent inductance and capacitance are strongly dependent on the discharge current. When the oscillation in the discharge current has a small amplitude, it is valid to treat the equivalent circuit elements as having constant values. However, when the amplitude of the oscillation is not negligible compared with the dc discharge current, the equivalent circuit elements must be expressed as functions of the discharge current. The following analysis shows that the current waveform becomes nonsinusoidal and contains frequency components at the harmonics of the resonant frequency. The nonlinear analysis is important since the phenomenon of moving striations is quite nonlinear. Experimental data in Chapter 4 show components of the discharge current at multiples of the striation

frequency. This nonlinearity in moving striations is due to the fact that the amplitude of the oscillation in the discharge current is so large that the equivalent circuit elements do not have constant values within the time duration of one cycle.

The simplest nonlinear case is one in which the equivalent circuit elements are linearly dependent on the discharge current. The circuit elements at a discharge current I in the vicinity of I_o can be expressed as

$$L = L_o + \frac{L_1 I}{I_o}$$

$$\rho = \rho_o + \frac{\rho_1 I}{I_o} \qquad (A2-9)$$

$$\frac{1}{C} = \frac{1}{C_o} + \frac{I}{C_o I_o}$$

where L_o, L_1, ρ_o, ρ_1, C_o and C_1 are constants with positive or negative real values. The values of L, ρ and C at the dc discharge current I_o are $(L_o + L_1)$, $(\rho_o + \rho_1)$ and $(\frac{1}{C_o} + \frac{1}{C_1})$, respectively. Thus the resonant angular frequency ω_o of equation (A2-4) becomes

$$\omega_o = \left. \sqrt{\frac{C + C'}{LCC'}} \right|_{I = I_o}$$

$$= \sqrt{\frac{\frac{1}{C_o} + \frac{1}{C_1} + \frac{1}{C'}}{L_o + L_1}} \qquad (A2-10)$$

The term I in equation (A2-9) denotes the total discharge current and can be expressed as

$$I = I_o + \sum_{n=1}^{\infty} A_n \, e^{jn\omega_o t} \qquad (A2-11)$$

where A_n is the complex amplitude of the ᴀᴄ component of the current at the angular frequency $n\omega_o$.

The circuit equation for the a.c. equivalent circuit of Fig. A2-1 can be written as

$$\left(L_o + \frac{L_1 I}{I_o}\right) \frac{d(I - I_o)}{dt} + \left(\rho_o + \frac{\rho_1 I}{I_o}\right)(I - I_o) + \left(\frac{1}{C_o} + \frac{I}{C_1 I_o} + \frac{1}{C}\right)\int_{-\infty}^{t}(I - I_o)dt' = 0 .$$

$$(A2-12)$$

Using the expression of I in equation (A2-11), equation (A2-12) becomes

$$\sum_{n=1}^{\infty} e^{jn\omega_o t} \left[\left\{ jn\omega_o(L_o + L_1) + \rho_o + \rho_1 + \frac{1}{jn\omega_o}\left(\frac{1}{C_o} + \frac{1}{C_1} + \frac{1}{C'}\right) \right\} A_n \right.$$

$$\left. + \frac{1}{I_o} \sum_{m=1}^{n-1} A_n A_{n-m} \left(jm\omega_o L_1 + \rho_1 + \frac{1}{jm\omega_o C_1} \right) \right] = 0 . \qquad (A2-13)$$

For $n \geq 2$ the amplitude A_n can be obtained from equation (A2-13)

$$A_n = \frac{1}{I_o} \frac{\sum_{m=1}^{n-1} A_m A_{n-m}\left[\rho_1^2 + \left(m\omega_o L_1 - \frac{1}{m\omega_o C_1}\right)^2\right]^{1/2} e^{i(\phi_m - \theta_n)}}{\left[\omega_o^2 \left(n - \frac{1}{n}\right)^2 (L_o + L_1)^2 + (\rho_o + \rho_1)^2\right]^{1/2}} \qquad (A2-14)$$

where

$$\phi_m = \tan^{-1}\left[\frac{1}{\rho_1}\left(m\omega_o L_1 - \frac{1}{m\omega_o C_1}\right)\right]$$

and

$$\Theta_n = \tan^{-1} \frac{\omega_o(n - \frac{1}{n})(L_o + L_1)}{\rho_o + \rho_1}$$

From equation (A2-14) the amplitudes of all the harmonic components in the discharge current I can be obtained in a successive order in terms of A_1, the amplitude of the fundamental a.c. component in I. For $n = 1$ the second term in equation (A2-13) vanishes and the equation becomes the reduced equation in the linear analysis of the last section. Hence the quantity A_1 has been analyzed in Section A2-2 and is not considered here.

This section shows that the discharge current has components at the harmonics of the resonant frequency when the dependence of the equivalent circuit elements on the current is taken into consideration. When the amplitude of oscillation in the discharge current becomes large as compared with the d.c. current (as in the case of moving striations), even the linear expressions of equation (A2-9) may not suffice. The equivalent circuit elements have quadratic or higher order dependence on the discharge current. The analysis becomes more tedious, but is essentially similar to the one presented here. The present analysis is sufficient to explain the nonlinearity in the current waveform of the laser discharge when moving striations exist in the positive column.

APPENDIX THREE

MEASUREMENTS ON LASER DISCHARGE NOISE

Experimental measurements are presented in this appendix on the discharge noise and its effect on the helium-neon laser. In addition to the wideband spectrum of the background noise which is nearly "white" (1), the narrow spikes of noise due to the striations appear in the discharge current, the spontaneous emission from the side of the discharge tube and the laser light output. By the measurements described in this appendix, we establish, experimentally, that the plasma striation phenomenon leads to the predicted modulation of the laser light. We measure the striation frequency and find that it compares within experimental error to the fine-structure frequency which appears as a modulation of the laser light.

A3.1 Experimental Setup

The experimental setup is diagrammed in Fig. A3-1 while in Fig. A3-2 photographs are shown of the setup. Fluctuations in the discharge current, the spontaneous emission and the laser output are analyzed in four frequency ranges: the optical frequency range, the radio frequency (RF) range and two low frequency (LF) ranges. The exact ranges in frequency covered in this experiment are shown in Fig. A3-1.

The discharge current fluctuations are measured by the LF wave analyzer (Hewlett Packard 310A). The output from the wave analyzer is plotted on an x-y recorder (Hewlett Packard 136AM) as the frequency of the wave analyzer is scanned over its range with the aid of a sweep drive (Hewlett Packard 297). The spontaneous emission
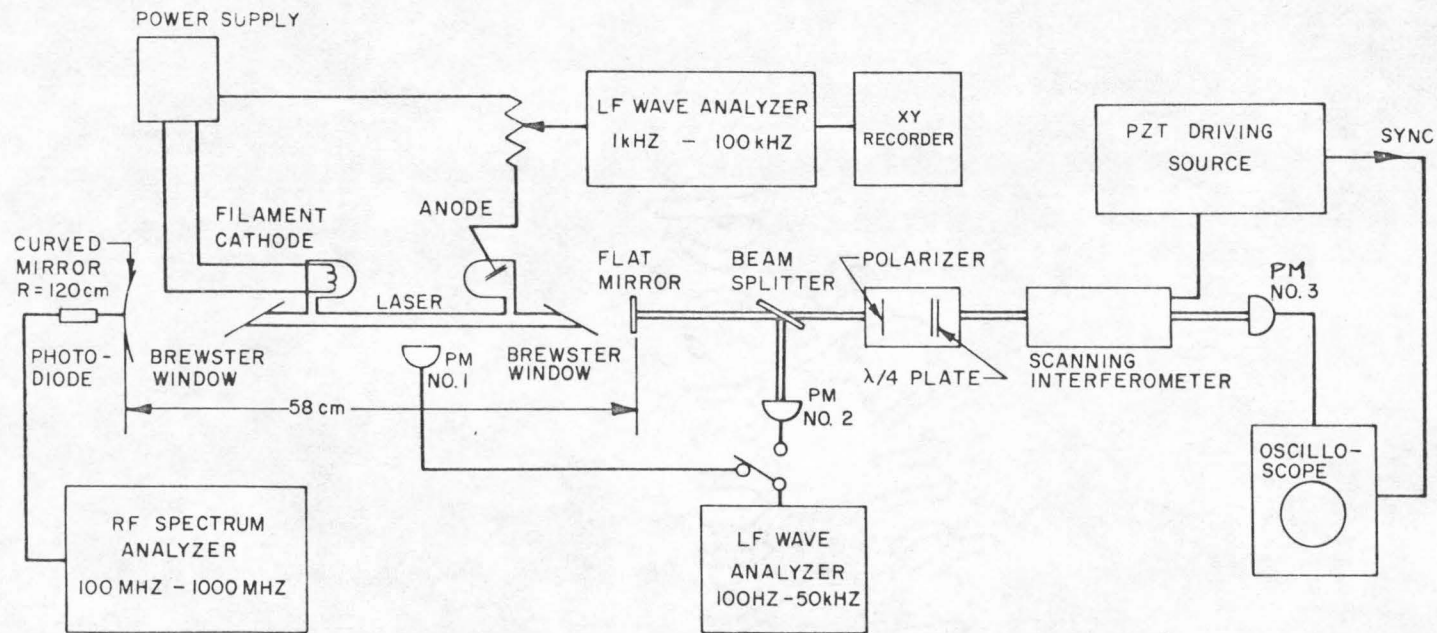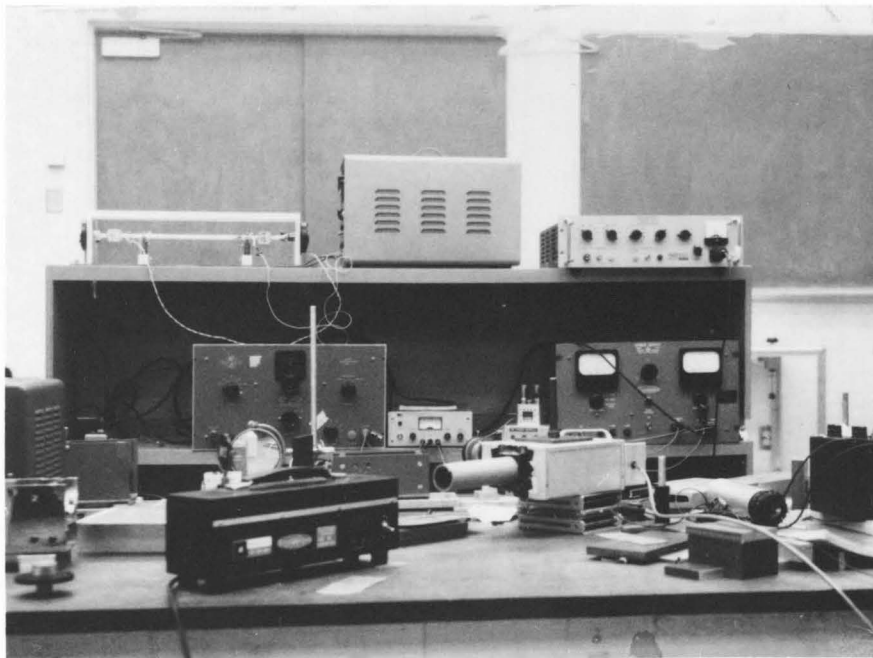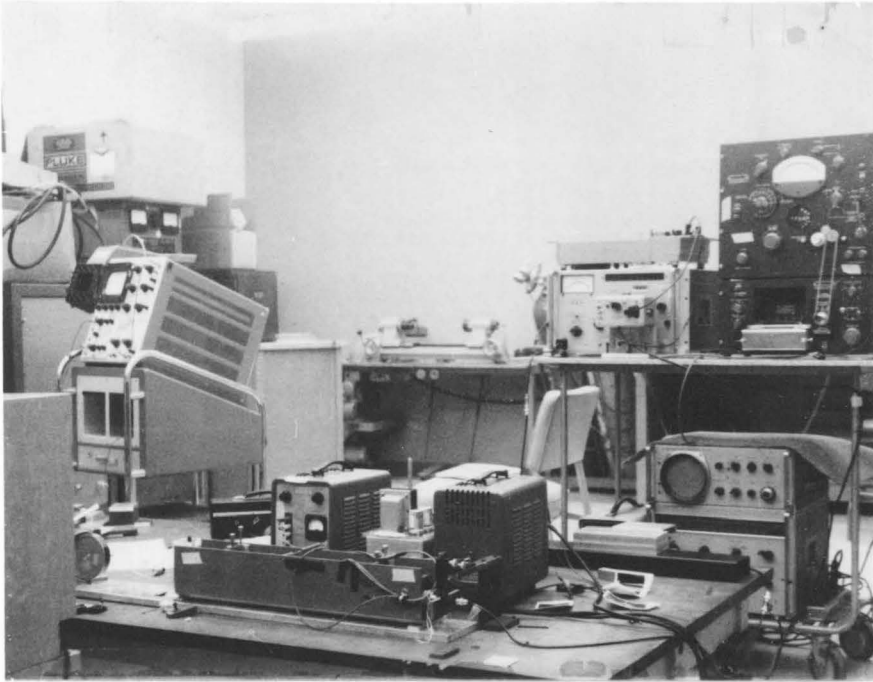
FIGURE A3-1 EXPERIMENTAL SETUP

FIGURE A3-2   EXPERIMENTAL SETUP

is detected by a photomultiplier (PM No. 1) and analyzed by the other
LF wave analyzer (General Radio 1900-A) whose output is plotted on the
strip chart recorder that accompanies it. It should be noted that all
the photomultipliers used in this experiment employ RCA 7102 photo-
multiplier tubes.

The laser output is examined in three frequency ranges. The
LF spectrum of its intensity is picked up by a photomultiplier (PM No.2)
and analyzed by the General Radio wave analyzer. The RF spectrum of
its intensity is detected by a photodiode (Philco 4502) which is
sensitive to the light output of the helium-neon laser and has a
frequency response of 4.5 gigahertz. The output of the photodiode is
fed into the RF spectrum analyzer (Hewlett Packard 851 A/8551 A) which
displays the portion of the frequency spectrum of the laser output
intensity at the difference frequency between the longitudinal modes
of the laser. Finally the optical spectrum of the laser is examined
with a scanning interferometer. The scanning interferometer is a cavity of
10 cm long with two lighly reflecting mirrors at its two ends. One of
the mirrors can be driven by a PZT crystal to oscillate back and forth,
thus constituting the scanning motion. In this setup the PZT crystal
is driven at the rate of 1 kHz by a triangular voltage wave which is
generated by a function generator (Hewlett Packard 302) and amplified.
An isolator consisting of a polarizer and a quarter wave plate is
situated in the beam path between the laser and the scanning interfero-
meter such that there is not any coupling between the two. The output
of the scanning interferometer is detected by a photomultiplier (PM No.3)

and displayed on an oscilloscope. When the triggering of the oscil-
loscope is synchronized with the driving voltage of PZT, the
oscilloscope displays the optical spectrum of the laser with the horizon-
tal axis being the frequency scale. The resolution of such a spectrum
is in excess of 10 mHz, which means that the fine details of the
spectrum cannot be resolved in the oscilloscope display.

The discharge noise is measured on a laser which is shown in
the foreground of the upper photograph in Fig. A3-2. The laser tube is
contained in a heavy and rigid steel can such that mechanical vibrations
are reduced to a minimum. The cavity is enclosed by a flat mirror and
a curved mirror of 1.2 meter radius with an interelectrode distance of
58 cm. The laser discharge tube has a length of about 52 cm and is
excited by a dc current-regulated power supply. Its cathode is heated
by passing a dc current through it. The dc filament supply is capable
of supplying 5 amperes to a load of 2 ohms. The entire setup is on the
top of a steel table which, in turn, sits on a cement block isolated
from the building.

A3.2 Experimental Results

Figs. A3-3 through A3-7 show the discharge current spectra
for various dc discharge currents. The filament setting is 55 on the
variac, corresponding to a filament current of 4.1 amperes and a
filament temperature of about 850°C. The plots show that the
oscillations do not occur until the discharge current is above 4.5 ma.
Below the critical current, the discharge is very quiet, as shown in
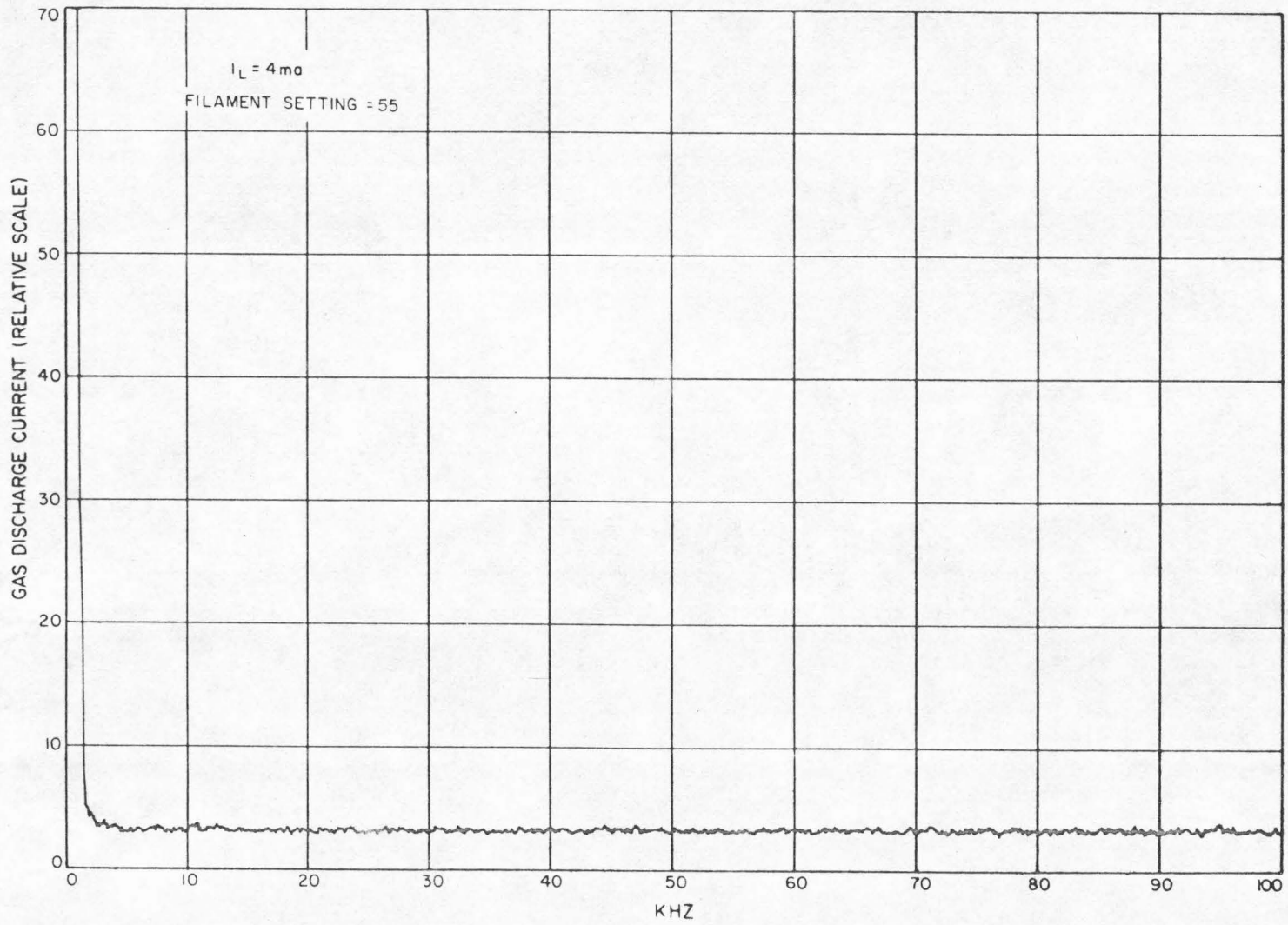
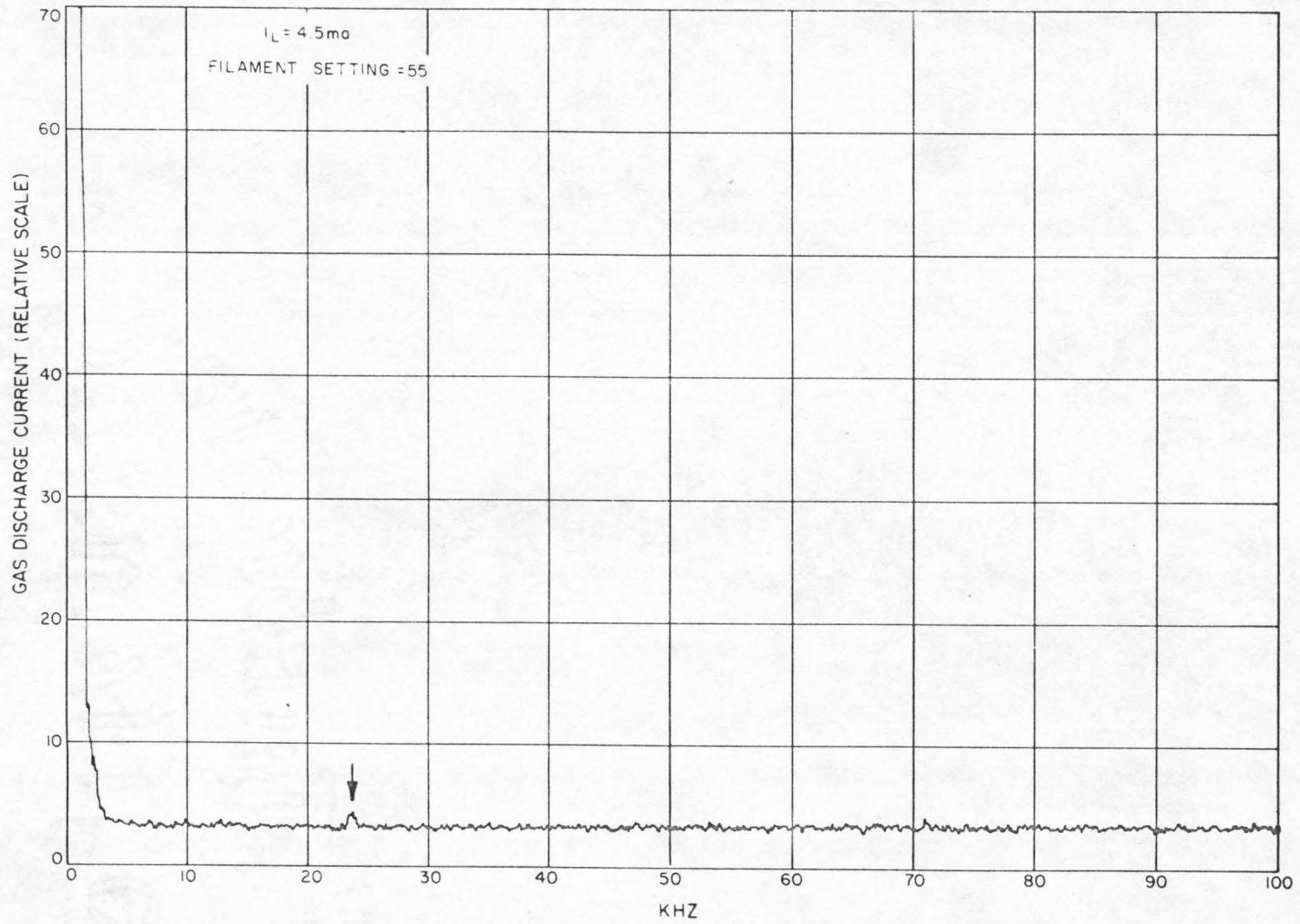FIGURE A3-3 GAS DISCHARGE CURRENT SPECTRUM
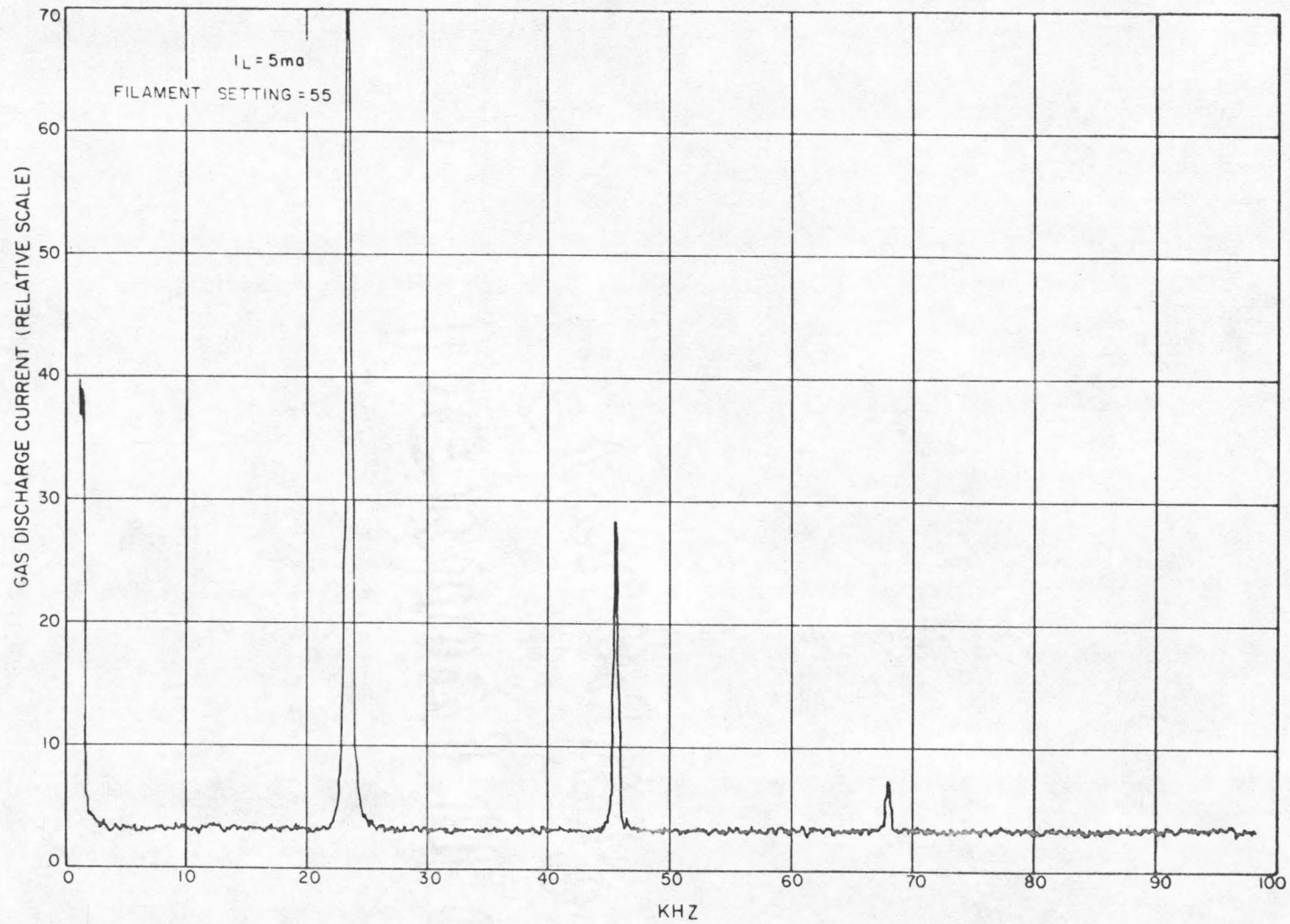
FIGURE A3-4 GAS DISCHARGE CURRENT SPECTRUM

FIGURE A3--5 GAS DISCHARGE CURRENT SPECTRUM
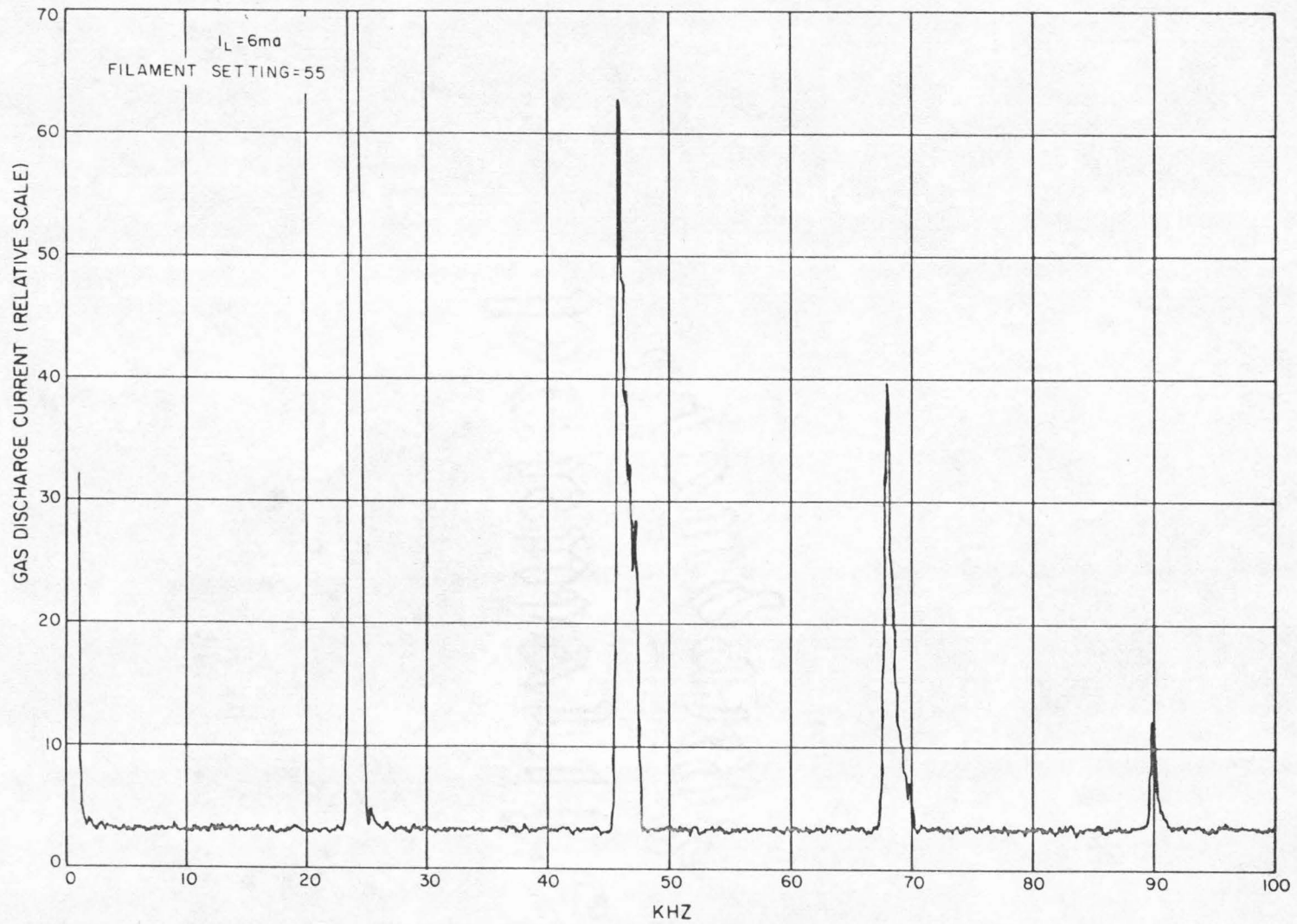
FIGURE A3-6   GAS DISCHARGE CURRENT SPECTRUM
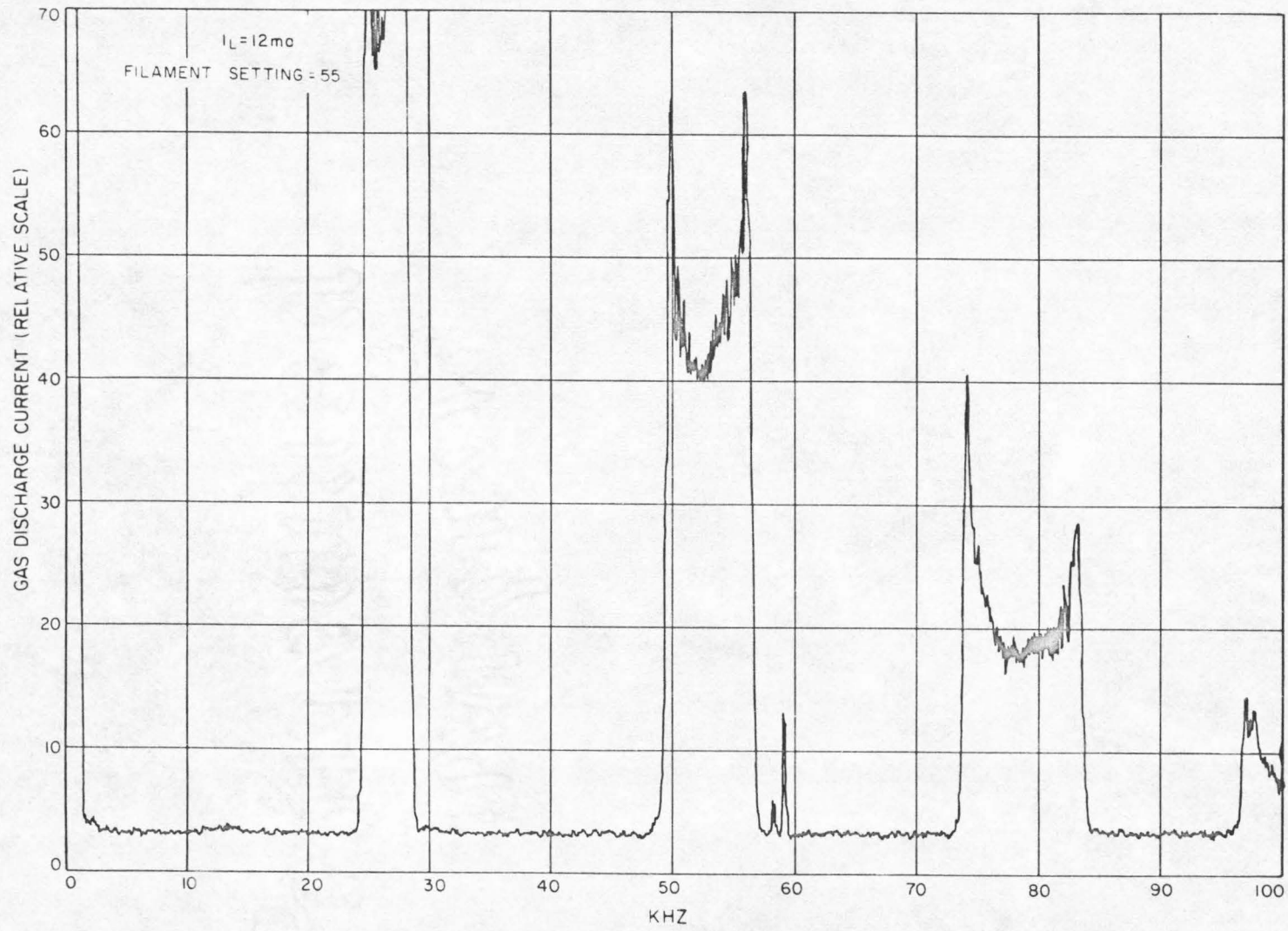
FIGURE A3-7   GAS DISCHARGE CURRENT SPECTRUM

Fig. A3-3. When the discharge current is increased beyond 4.5 ma, the striation waveform rapidly becomes nonlinear and the amplitudes of its frequency components become large. As the current increases further, the bandwidth becomes broader and the center frequency increases. At a discharge current of 12 ma, the oscillations become quite broad-banded. There does not appear any good explanation for this phenomenon. It is possible that the frequency fluctuates rapidly within the band such that the recorder pen maps out a broad-band spectrum as it slowly moves over the region of interest. It is also possible that as the discharge current increases, gain exists within a broad band of frequency such that disturbances within the frequency band are simultaneously oscillating. It should be noted that the harmonic components are broader than fundamental component by their orders, i.e., the second harmonic has a band that is twice as broad as that of the fundamental while the third harmonic has one that is three times as broad. However, this observation does not favor any one of the above possibilities over the other.

As the setting on the variac of the dc filament supply is increased to 57 corresponding to a filament current of 4.2 amperes, the onset of oscillations occurs at a larger discharge current. The discharge is quiet until the discharge current is increased to beyond 9 ma, at which time the striations occur at a frequency of 27 kHz. The spectrum at the discharge current of 9 ma is similar to that of Fig. A3-3 while the spectrum at the discharge current of 9.5 ma shows a spike whose amplitude is roughly halfway between those in Figs. A3-4

and A3-5. It is significant that striation oscillations occur at a
much larger discharge current when the filament current is raised by
0.1 amperes. If the filament current is increased further, the oscil-
lations would not occur under the laser operating conditions of this
particular laser. Of course, raising the temperature of the filament
shortens its lifetime. The optimization between the discharge noise
and the filament lifetime should be of interest to the future design
of lasers with heated cathodes.

Fig. A3-8 shows the optical spectrum of the laser light
output and the RF spectrum of its intensity. The output of the scanning
interferometer shows that the laser is operating in three successive
longitudinal modes. The mirror motion is large enough to scan through
two optical spectra such that the display shows at least one complete
spectrum of the laser output. Although the frequency scale of the
display is not linear, an idea of the scaling can be obtained by the
knowledge (from consideration of the configurations of the laser cavity
and the scanning interferometer) that the successive modes are separated
from each other by 259 mHz while the two spectra are 1500 mHz apart.

The RF spectrum from the photodiode which is sensitive to the
intensity of the laser output is shown in the photograph on the right
side of Fig. A3-8. The spectrum is centered at 259 mHz with the various
spikes at about 30 kHz apart from each other. The frequency separation
corresponds to the striation frequency. These spikes are undoubtedly
present in the optical spectrum also, but they cannot be resolved by
the scanning interferometer; in fact, displaying the beat
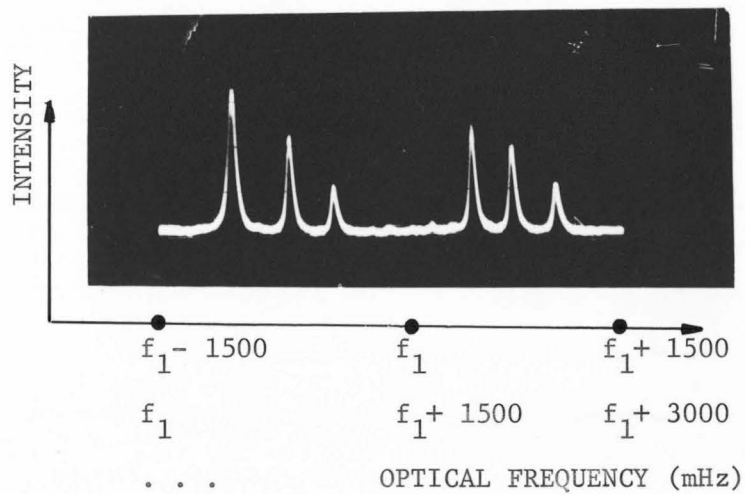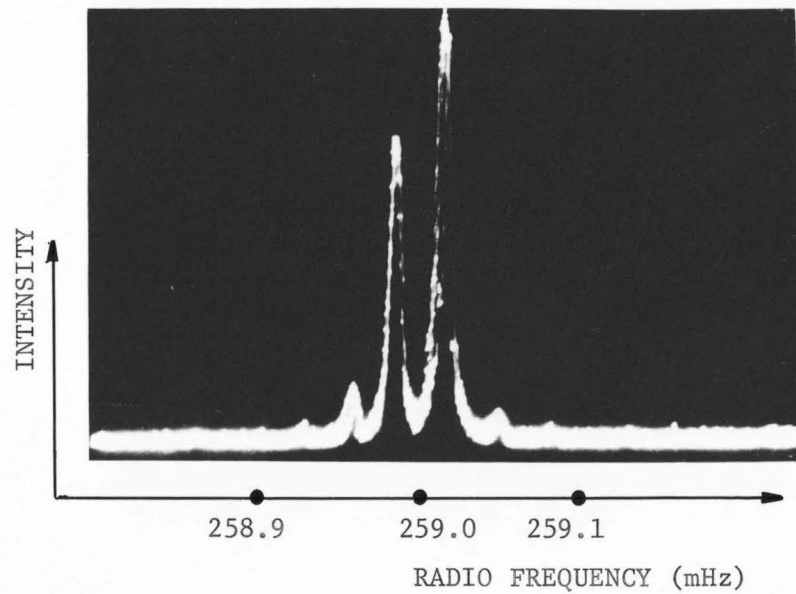
FIGURE A3-8 (a) OPTICAL SPECTRUM OF THE LASER OUTPUT SHOWING INTENSITY VERSUS FREQUENCY, AS DISPLAYED
ON PM3-CRO (SEE FIG. A3-1), OF THE SCANNING INTERFEROMETER OUTPUT;

(b) RF SPECTRUM BEAT FREQUENCY DISPLAY AT THE LONGITUDINAL MODE FREQUENCY INTERVAL,
CENTERED APPROXIMATELY AT 259 mHz, SEE PHOTODIODE MONITOR IN FIG. A3-1.

frequency spectrum is principally done as a technique for examining the

fine structure of an optical spectrum. It is relatively simple to

resolve 1 kHz in this manner. However, with a scanning interferometer

of 10 cm spacing and high reflectivity mirrors, a good practice would

be a resolution of 10 mHz. The appearance of the beat tones with a

spacing of 30 kHz on Fig. A3-8 (b) is definitive evidence in support

of the passive cavity mode analysis of Chapter 2. Either AM or FM in

the laser output would lead to an intensity spectrum as shown, how-

ever the occurrence of either is demonstration of the validity of the

theory. Briefly, in our theory we consider a passive cavity, while the

mode spectrum resulting in the oscillator configuration is signifi-

cantly more complex due to the following nonlinear effects. Saturation

effects such as hole burning and combination tone generation will tend

to couple these modes in an undetermined way; however it is clear

that the results of a linear theory would not give an adequate basis for

a quantitative prediction.

Fig. A3-9 shows the experimental measurements made on

another helium-neon laser (Perkin-Elmer 5220) with a heated cathode.

The plots are obtained with the General Radio LF Wave Analyzer.

They display the spectra of the discharge current, the light from the

spontaneous emission and the laser light output which all show a

resonance at around 19 kHz. The discharge current and the spontaneous

emitted light are about 25 db above their normal levels while the laser

light output is more than 10 db higher than its normal level. The

plots show quantitatively the influence of the striations on these

HORIZONTAL SCALE 1/5 IN./DIV

FREQUENCY SPECTRUM OF GAS DISCHARGE CURRENT
P. E. LASER 5220

GAS DISCHARGE CURRENT = 6.4 ma
ANALYSER: FULL SCALE = 10 mv
          BANDWIDTH = 10 Hz

40 db
30 db
20 db
10 db

(a)

HORIZONTAL SCALE 1/5 IN./DIV

FREQUENCY SPECTRUM OF DETECTED SPONTANEOUS EMISSION LIGHT
P. E. LASER 5220
7102 PHOTOMULTIPLIER
GAS DISCHARGE CURRENT = 6.4 ma
ANALYSER FULL SCALE = 100 mv
          BANDWIDTH = 10 Hz

40 db
30 db
20 db
10 db

(b)

HORIZONTAL SCALE 1/5 IN./DIV

FREQUENCY SPECTRUM OF DETECTED COHERENT LASER LIGHT
P. E. LASER 5220   GAS DISCHARGE CURRENT = 6.4 ma
7102 PHOTOMULTIPLIER ANALYSER FULL SCALE = 1.0 mv
                      BANDWIDTH = 10 Hz

40 db
30 db
20 db
10 db

SPONTANEOUS EMISSION STRAY LIGHT

12   13   14   15   16   17   18   19   20   21   22

FREQUENCY IN KHZ

(c)

FIGURE A3-9   LF FLUCTUATIONS SPECTRA

three spectra. The appearance of this tone on the low frequency

spectrum is a measure of AM on the optical spectrum, i.e., the tone

prediction of about 19 kHz due to the measured plasma striation

frequency causes a mode splitting which in the linear or passive system

gives rise to an FM spectrum. Experimentally, the presence of a

low frequency beat Fig. A3-9 confirms our prediction of the effects of

a striation phenomenon in the gas discharge.

APPENDIX FOUR

SUMMARY OF EXPERIMENTAL DATA

Data are presented in this appendix in a complete form of resonant frequencies in typical laser discharges for a variety of gases and discharge parameters. The equivalent inductance and capacitance, calculated from the resonant frequencies, are presented in Chapter 3; however the data in this appendix should be useful to research workers in this field. The appendix also includes a discussion of the experimental error and some typical frequency spectra of the current responses for helium discharges.

The experimental data from which the equivalent inductance and capacitance have been calculated are presented in this section. They are measurements on the resonant frequencies for discharges with various discharge parameters. The experimental setup and the method of measurement have been described in Section 3.3. The expressions for the equivalent inductance L and capacitance C are

$$L = \frac{L'}{(f/f')^2 - 1}$$

$$C = \frac{1}{4 \pi^2 L'} \left(\frac{1}{f'^2} - \frac{1}{f^2} \right)$$

where L' is an external inductor of known value (40 mh), f' and f

are the resonant frequencies of the discharge with and without the

external inductor, respectively. The other symbols used in the

presentation of data are: ℓ is the length of the positive column,

I is the dc discharge current and p is the gas pressure. The

experimental data are presented in the following sequence: the

dependencies of L on ℓ, I and p, and the dependencies of C on ℓ , I

and p. The figure numbers are included for reference.

The wave analyzer (Hewlett Packard 312A) through which

the resonant frequencies have been measured displays the value of its

center frequency with electronic lights so that the frequency value

can be exactly read. The frequency accuracy of the instrument is

± 30 Hz when the wave analyzer is operated with the 200 Hz bandwidth.

This error is negligibly small compared with the errors to be considered.

The major contributions to the random errors in the experimental values

of L and C come from the measurement of the frequency at the resonance

of the current response spectrum and the reading of the value of the dc

discharge current from the ammeter (Triplett 630A). These human errors

introduce random errors to the values of the equivalent inductance

and capacitance. Helium and xenon discharges are very quiet discharges

so that the errors can be estimated. In the case of a helium discharge,

the resonant frequency of the current response can be determined to

within 400 Hz when the resonant frequency is at 182 kHz (i.e. about

60% of the readings fall within the range). The range is proportional

L versus ℓ Helium Fig. 3-7(a)				
ℓ (cm)	15	30	45	60
f (kHz)	299.5	190.5	144	123.5
f' (kHz)	184	142	118	105.5
L (mh)	24.1	49.7	84	108

L versus ℓ Neon Fig. 3-7(a)				
First Set				
ℓ (cm)	15	30	45	60
f (kHz)	307.6	215.6	175.5	135.4
f' (kHz)	179.8	138.9	126.7	103
L (mh)	20.8	28.4	43.5	54.8
Second Set				
ℓ (cm)	15	30	45	60
f (kHz)	304.6	213.5	171.9	134.2
f' (kHz)	189.1	145.2	130.5	107.9
L (mh)	25	34.5	54.4	72.7
Third Set				
ℓ (cm)	15	30	45	60
f (kHz)	305.8	218.7	171.9	136.2
f' (kHz)	181.2	153.5	126.3	110.2
L (mh)	21.7	38.9	47.1	76.2
Average L (mh)	22.5	33.9	48.3	67.9

L versus ℓ Xenon Fig. 3-7(b)				
ℓ (cm)	15	30	45	60
f (kHz)	109	64.4	47.3	40.4
f' (kHz)	100	62.4	46.5	39.9
L (mh)	214	615	1141	1480

L versus I Helium Fig. 3-8(a)					
I (ma)	1	2	3	4	5
f (kHz)	106.8	168.3	219.6	262.3	306.4
f' (kHz)	94.9	135.5	161.5	183.3	199.3
L (mh)	148	73.7	47.1	38.1	29.4

L versus I Neon Fig. 3-8(a)				
First Set				
I (ma)	3	4	5	6
f (kHz)	201.8	232	250.7	260.0
f' (kHz)	155	174.1	177.4	182.3
L (mh)	57.9	51.2	38.9	38.9
Second Set				
I (ma)	3	4	5	6
f (kHz)	206.7	250.1	262.5	270
f' (kHz)	152.7	169.8	174.5	171.4
L (mh)	48.2	34.2	31.8	27.4

L versus I   Neon   Fig. 3-8(a)   (continued)

Third Set

I (ma)	3	4	5	6
f (kHz)	199.4	222.4	246.3	262
f' (kHz)	142.2	164.1	173.9	174.4
L (mh)	41.2	47.6	39.6	31.8

Fourth Set

I (ma)	3	4	5	6
f (kHz)	193	222.1	246.1	265.7
f' (kHz)	138.2	146.5	172	174.6
L (mh)	42.1	30.8	38.1	30.5
Average L (mh)	47.35	40.95	36.85	32.15

L versus I   Xenon   Fig. 3-8(b)

I (ma)	.4	.5	.6	.7
f (kHz)	54.7	63.9	72.1	78.1
f' (kHz)	53.4	61.9	69.3	74.5
L (mh)	800	597	500	400

L versus p   Helium   Fig. 3-9(a)   at I= 2ma

p (torr)	.5	.7	1	1.1
f (kHz)	219	190	164	155.5
f' (kHz)	159.5	145	133	127.5
L (mh)	44.9	55.5	76.8	81.6

L versus p Helium Fig. 3-9(a) at I = 4ma				
p (torr)	.5	.7	1	1.1
f (kHz)	328	186	247.5	230
f' (kHz)	181.5	183	170.5	165
L (mh)	17.6	27.75	36	42.5

L versus p Helium-xenon Fig. 3-9(b)				
p_{He} (micron)	0	10	20	50
f (kHz)	88.7	87.2	86.1	87.8
f' (kHz)	85	83.7	82.8	84.5
L (mh)	454	470	493	507
p_{He} (micron)	120	200	500	700
f (kHz)	84.4	80.6	67.3	62.5
f' (kHz)	81.8	78	65.5	61.1
L (mh)	614	614	727	888

C versus ℓ Helium Fig. 3-10				
ℓ (cm)	15	30	45	60
f (kHz)	430.5	266	211	165.5
f' (kHz)	198	171	157	132.5
C (pf)	12.8	12.73	11.6	13.2

C versus I	Helium	Fig. 3-11		
I (ma)	1	2	3	4
f (kHz)	106.8	168.3	219.6	262.3
f' (kHz)	94.9	135.5	161.5	183.3
C (pf)	15	12.13	11.16	9.69
I (ma)	5	6	7	8
f (kHz)	306.4	345.4	388.5	423
f' (kHz)	199.3			
C (pf)	9.21	8.62^*	7.95^*	7.66^*

C versus p	Helium	Fig. 3-12		
p (torr)	.5	.7	1	1.1
f (kHz)	219	190	164	155.5
f' (kHz)	159.5	145	133	127.5
C (pf)	11.8	12.7	12.3	12.9

* These values of the equivalent capacitance have been obtained
using the extrapolated values of the equivalent inductance from
Figure 3-8(a).

to the frequency. The discharge current can be measured to within

.01 ma. The random errors in the values of the equivalent induct-

ance and capacitance of the helium discharge are estimated to be

within 4%. In the case of xenon discharge, the frequency of the

resonant peak of the current response can be determined to within

150 Hz when the peak frequency is at 60 kHz. The discharge current

can be measured to within .001 ma. The estimated random error for

the equivalent inductance of xenon discharge are 7.8% for the ind-

uctance value of 400 mh, 11.3% for the value of 600 mh and 26.9%

for the value of 1480 mh (the largest value encountered in the

experiment). The neon discharges are quite noisy. The random

error of its equivalent inductance can be calculated from the exper-

imental data. For the L versus ℓ curve, the average error in the

equivalent inductance of the neon discharge is 6.26% (for a set of

three measurements). For the L versus I curve, the average error

is 7.13% (for a set of four measurements).

Typical plots of the frequency spectra of discharge cur-

rents for helium discharge are given from Figure A4-1 to Figure

A4-3. The helium discharge is at a pressure of 1 torr. The three

plots show the frequency spectra for three different discharge

currents. They show that the resonance of the current response

increases in its amplitude and frequency with the discharge current.

The spectra for discharge currents of 2 ma and 4.2 ma seem to have

good resonances. Therefore the experimental data on helium discharges

presented in Chapter 3 have been obtained from these two discharge
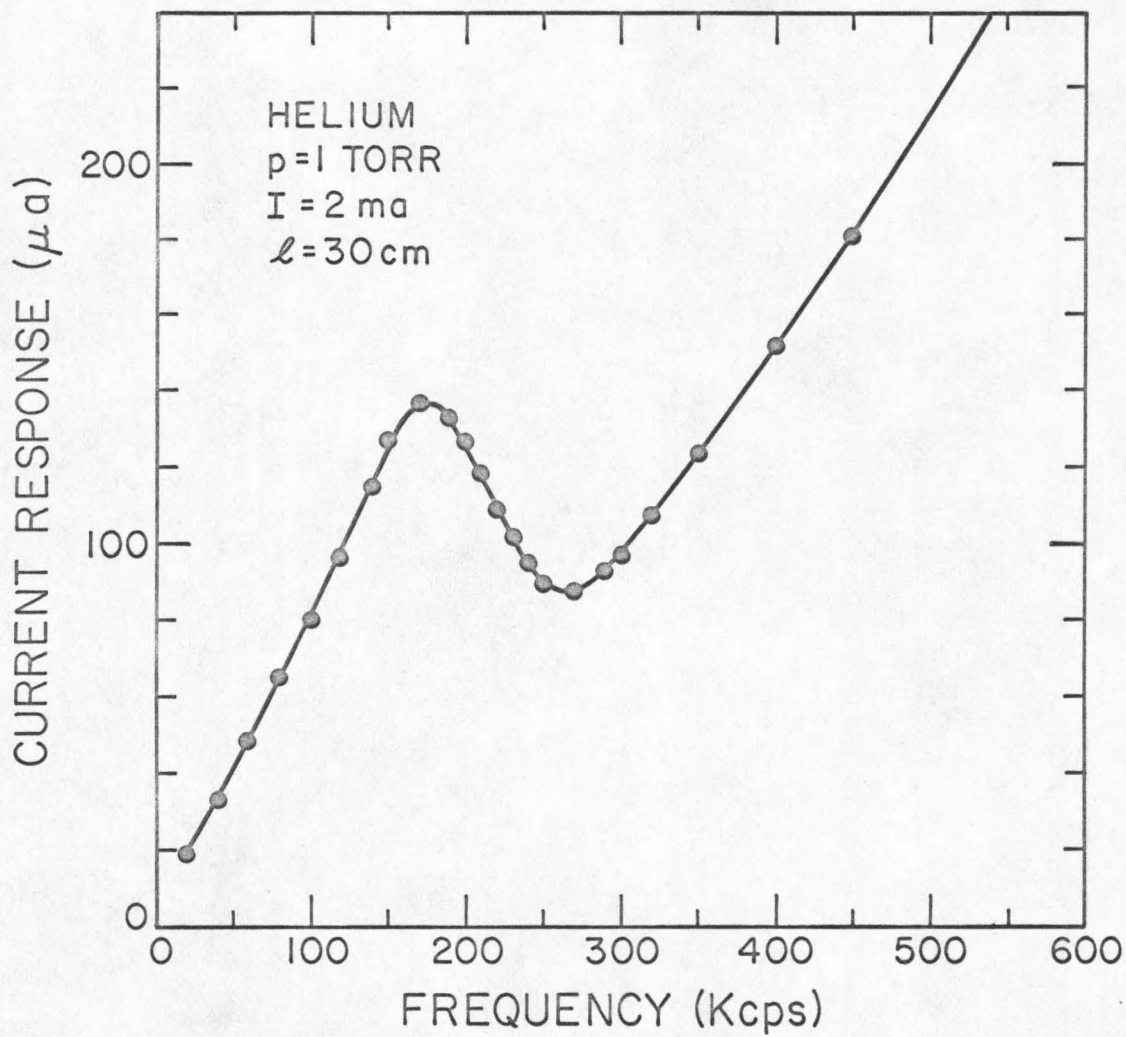
-126-

FIGURE A4-1   DISCHARGE CURRENT RESPONSE TO
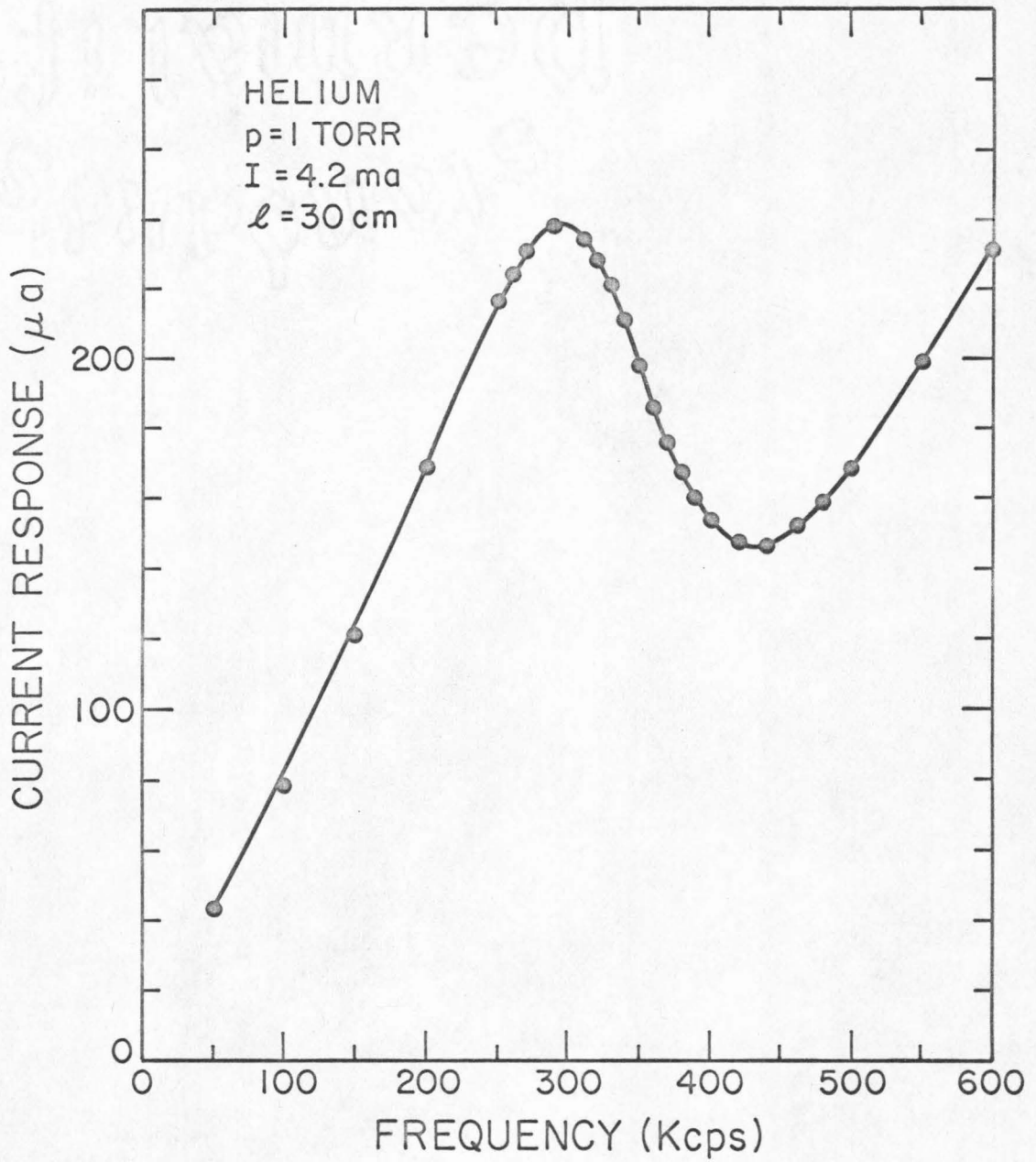AC VOLTAGE MODULATION

FIGURE A4-2   DISCHARGE CURRENT RESPONSE TO
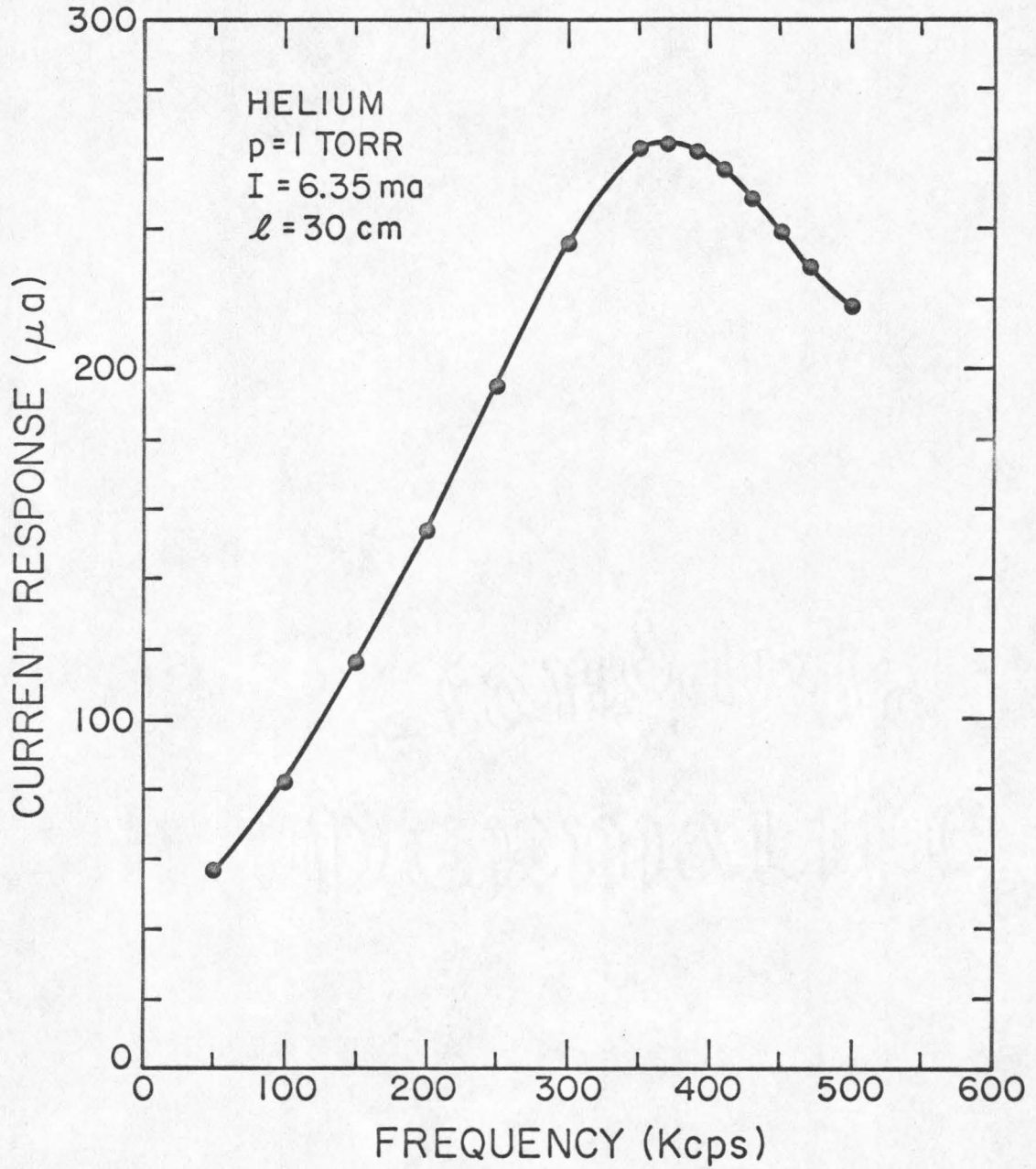AC VOLTAGE MODULATION

FIGURE A4-3 DISCHARGE CURRENT RESPONSE TO
AC VOLTAGE MODULATION

currents. These plots show the typical spectra from which the present

frequencies presented earlier in the appendix have been obtained.

REFERENCES

CHAPTER ONE

1. C. Freed and H. A. Haus, "Measurement of Amplitude Noise in Optical Cavity Masers", Appl. Phys. Letters 6, 85-87 (1965).

2. H. Hodara and N. George, "Excess Photon Noise in Multimode Lasers", J. Quantum Electronics QE-2, 337-340 (1966).

3. P. T. Bolwijn, C. Th. J. Alkemade and G. A. Boschloo, "Excess Photon Noise and Spectral Line Shape of Laser Beam", Phys. Letters 4, 59-61 (1963).

4. L. J. Prescott and A. Van der Ziel, "Gas Discharge Modulation Noise in He-Ne Lasers", J. Quantum Electronics QE-2, 173-177 (1966).

5. A. Garscadden, P. Bletzinger and E. M. Friar, "Moving Striations in a He-Ne Laser", J. Appl. Phys. 35, 3432-3433 (1964).

CHAPTER TWO

1. W. E. Lamb, "Theory of an Optical Maser", Phys. Rev. 134, A1429-A1450 (1964).

2. J. Mathews and R. L. Walker, Mathematical Methods of Physics, Benjamin, New York (1965), pp. 26-27.

3. M. Schwartz, Information Transmission, Modulation, and Noise, McGraw-Hill, New York (1959), pp. 114-132.

4. N. W. McLachlan, Theory and Application of Mathieu Functions, Dover, New York (1964).

CHAPTER THREE

1. A. Bloom, "Noise in Lasers and Laser Detectors", Spectra Physics Laser Technical Bulletin, Number 4 (1965).

2. L. J. Prescott and A. Van der Ziel, "Gas Discharge Modulation Noise in He-Ne Lasers", J. Quantum Electronics QE-2, 173-177 (1966).

3. Y. Asami and A. Akimoto, "Noise Effect due to the Internal Negative Resistor of Glow Discharges", Proc. IEE Japan (Kemki Gakkwai Zasahi) 73, 804-809 (1953).

4. F. A. Benson and M. W. Bradshaw, "Impedance/Frequency Characteristics of Glow Discharges", Proc. IEE 113, 62-72 (1966).

5. H. L. Curtis, Electrical Measurements, McGraw-Hill, New York (1939), p. 159.

6. E. F. Labuda and E. I. Gordon, "Microwave Determination of Average Electron Energy and Density in He-Ne Discharges", J. Appl. Phys. 35, 1647-1648 (1964).

CHAPTER FOUR

1. L. Pekárek, "Theory of Moving Striations", Phys. Rev. 108, 1371-
    1372 (1957).

2. D. A. Lee, P. Bletzinger and A. Garscadden, "Wave Nature of Moving
    Striations", J. Appl. Phys. 37, 377-387 (1966).

3. A. W. Cooper, "Experiments on the Origin of Moving Striations",
    J. Appl. Phys. 35, 2877-2884 (1964).

4. Abria, "Sur les Lois de L'induction des Courants par les Courants",
    Ann. de Chemie et Phys., Series 3, Vol. 7, 462-488 (1843).

5. W. Pupp, "Oszillographische Sondenmessungen an laufenden Schichten
    der positiven Säule von Edelgasen", Physik. Z. 36, 61-66 (1935).

6. W. Pupp, "Frequenz und Schichtweite laufender Schichten in der
    positiven Säule von Edelgasen", Physik. Z. 33, 257-262 (1934).

7. T. Donahue and G. H. Dieke, "Oscillatory Phenomena in Direct
    Current Glow Discharges", Phys. Rev. 81, 248-261 (1951).

8. S. Watanabe and N. L. Oleson, "Traveling Density Waves in Positive
    Columns", Phys. Rev. 99, 1701-1704 (1955).

9. H. S. Robertson, "Moving Striations in Direct Current Glow Dis-
    charges", Phys. Rev. 105, 368-377 (1957).

10. L. Pekárek and V. Krejčí, "The Mechanism of the Amplification of
    Moving Striations in a d-c Discharge", Czech. J. Phys. B12, 296-
    306 (1962).

11. L. Pekárek and V. Krejčí, "Theory of Moving Striations in Plasma
    of d-c Discharge. I. Basic Equation and its General Solution",
    Czech. J. Phys. B12, 450-461 (1962).

12. L. Pekárek and V. Krejčí, "The Theory of Moving Striations in a

d-c Discharge Plasma. II. High Current Approximation", Czech. J. Phys. B13, 881-894 (1963).

13. K. Wojaczek, "Vereinfachte Diffusionstheorie der laufenden Schichten", Ann. der Physik, Series 7, Vol. 3, 37-47 (1959).

14. K. Wojaczek, "Zur Theorie laufender Schichten kleiner Amplitude in Niederdruckentladungen", Beitr. Plasma Physik 2, 1-12 (1962).

15. M. A. Hakeem and H. S. Robertson, "Alkali Vapor Plasmas", J. Appl. Phys. 31, 2063-2064 (1960).

16. K. Wojaczek, "Über künstlich erzeugte laufende Schichten in der Argon - Niederdruckentladung", Ann. der Physik 7, 68-80 (1958).

17. L. Pekárek and V. Krejčí, "The Physical Nature of the Production of Moving Striations in a d-c Discharge Plasma", Czech. J. Phys. B11, 729-741 (1961).

18. L. Pekárek, "The Development of a Pulse-Disturbance in a d.c. Discharge Plasma", Proc. Sixth Intern. Conf. Ionization Phenomena Gases Paris 2, 133-136 (1963).

19. L. Pekárek, "Experimental Verification of the Theory of the Successive Production of Striations in a Glow Discharge", Czech. J. Phys. B9, 67-77 (1959).

20. K. W. Gentle, "Moving Striations in the Argon Positive Column. I. Theory", Phys. Fluids 9, 2203-2211 (1966).

21. K. W. Gentle, "Moving Striations in the Argon Positive Column. II. Experiments", Phys. Fluids 9, 2212-2218 (1966).

22. I. Alexeff and W. D. Jones, "Observations on the Velocity of Moving Striations", Phys. Fluids 9, 1871-1872 (1966).

23. L. Tonks and I. Langmuir, "Oscillations in Ionized Gases", Phys. Rev. 33, 196-210 (1929).

24. A. Garscadden and D. A. Lee, "Velocity of Moving Striations", Phys. Fluids 10, 2093-2095 (1967).

25. A. Garscadden, "Moving Striations and Cataphoretic Effects in a He-Ne Laser", Appl. Phys. Letters 8, 85-87 (1966).

26. A. Garscadden, P. Bletzinger and E. M. Friar, "Moving Striations In a He-Ne Laser", J. Appl. Phys. 35, 3432-3433 (1964).

27. N. George, "Improved Population Inversion in Gaseous Lasers", Proc. IEEE 51, 1152-1153 (1963).

28. L. Pekarek, "A Theory of the Successive Production of Moving Striations in the Plasma of Inert Gases", Czech. J. Phys. B7, 533-556 (1957).

29. J. R. M. Coulter, N. H. K. Armstrong and K. G. Emeleus, "Moving Striations and Anode Sopts in Neon", Proc. Phys. Soc. (London) 77, 476-482 (1961).

30. G. D. Morgan, "Origin of Striations in Discharges", Nature 172, 542 (1953).

31. R. S. Palmer and A. Garscadden, "A Bibliography of Moving Striations", USAF Report ARL 65-120 (1965).

32. R. F. Weber, "The Glow Discharge in Mixtures of He-Ne and He-Xe", Master Thesis, Air Force Institute of Technology (1966).

APPENDIX THREE

1. P. Parzen and L. Goldstein, "Current Fluctuations in D. C. Gas Dis-
    charge Plasma", Phys. Rev. 79, 190 (1950).